The University of Manitoba

BURNING VELOCITY, STRUCTURE AND KINETICS OF HYDROGEN FLAMES CONTAINING DILUENTS

by

G.W. Koroll

A Thesis submitted to the Faculty of Graduate Studies in partial fulfillment of the requirements for the Degree of Master of Science through the Department of Chemistry.

The research work was conducted at the Systems Analysis Branch, Whiteshell Nuclear Research Establishment, Pinawa, Manitoba ROE 1LO

Winnipeg, Manitoba, 1985

BURNING VELOCITY, STRUCTURE AND KINETICS OF HYDROGEN FLAMES CONTAINING DILUENTS

BY

GRANT W. KOROLL

A thesis submitted to the Faculty of Graduate Studies of the University of Manitoba in partial fulfillment of the requirements of the degree of

MASTER OF SCIENCE

I hereby declare that I am the sole author of this thesis.

I authorize the University of Manitoba to lend this thesis to other institutions or individuals for the purpose of scholarly research.

G.W. Koroll

I further authorize the University of Manitoba to reproduce this thesis by photocopying or by other means, in total or in part, at the request of other institutions or individuals for the purpose of scholarly research.

G.W. Koroll

ACKNOWLEDGEMENTS

I take this opportunity to acknowledge and offer my thanks to the following people.

Dr. D.F. Torgerson, my supervisor, for his advice and enthusiasm in this project and for an illuminating graduate course on the subject of combustion.

Dr. S.R. Mulpuru, for generously providing his fine one-dimensional flame model.

Dr. R.K. Kumar, for making available his flammability limit data and for numerous helpful discussions and willing criticism.

Dr. D.J. Clouthier, for his guidance and input in the early part of this work and for setting a fine example as a physical chemist.

Margaret Knox, for processing the manuscript and revisions with excellence and good humor.

Dr. K.N. Tennankore, G.E. Gillespie, Dr. H. Rosinger, W.C. Harrison and D.R. Greig, for their capable management of the research program and facilities and for their personal attention and support.

Dr. H. Tamm, for his encouragement and for pointing out the virtue of taking the time to learn what all the numbers mean.

D.D.S. Liu and R.M. MacFarlane, whose LDA apparatus and method was adapted to this work.

J.F. Lafortune, a fellow graduate student; together, we taught ourselves a small part of combustion.

My wife, Margaret, from whom much time was borrowed in completing the manuscript and to whom much is lovingly owed.

Also, a warm thank you to my friends and colleagues in the Containment Behaviour Section for continuing fellowship and advice.

This work was conducted at the Whiteshell Nuclear Research Establishment (WNRE) of Atomic Energy of Canada Limited (AECL), Pinawa, Manitoba. Financial support from Ontario Hydro, Hydro-Quebec, New Brunswick Electric Power Commission and AECL-CANDU Operations in a joint funding agreement with AECL-WNRE (COG-CANDEV 1984/85 number 435) is gratefully acknowledged.

Dedication

To Katherine and William Paul, born during this work

ABSTRACT

An experimental and theoretical study is made of the effect of diluents on the laminar burning velocities of hydrogen-oxygen and deuterium-oxygen flames. Burning velocities are measured by the nozzle burner/schlieren cone angle method with particle tracking by Laser Doppler Anemometry. The diluents studied reduce the burning velocity in the order $CO_2 > N_2 > Ar > H_2O > O_2 > He > H_2$.

A correlation is obtained, based on physical properties and flammability limits, which predicts the burning velocities of mixtures with chemically inert diluents within 5% of the measured values. For mixtures with non-inert diluents the correlation is used to uncouple physical effects on the burning velocity from chemical kinetic effects. The effects of non-inert diluents on reaction kinetics and flame structure are assessed through the use of a one-dimensional flame model. In this context, particular attention is given to the unique effect of steam diluent on burning velocity, structure and kinetics of H_2-O_2 flames.

With steam diluent, the reduction in burning velocity by physical mechanisms is found to be compensated by an increase in the burning velocity due to the participation of steam in the chemical mechanisms. By virtue of its high third body efficiency, steam catalyses an exothermic reaction pathway initiated by the formation of $HO_2 \cdot$ in the preheat zone of the flame, producing an increase in burning velocity of 27%.

Mechanisms of lean and rich flame propagation are examined by considering O_2 and H_2, in excess of the stoichiometric amount, as simple diluents. The effects on physical and chemical mechanisms are separately assessed.

A reduction in burning velocity when H_2 is replaced in a mixture by D_2 is quantitatively linked to differences in thermal diffusivity and H and D collision frequency.

CONTENTS

CONTENTS (continued)

CONTENTS (continued)

1. INTRODUCTION

In nature, combustion is an uncontrolled destructive process. Combustion research is motivated by a need to predict and control combustion behaviour, for safety and for the use of combustion as an energy source.

The H_2-O_2 system is fundamental to the study of combustion. The chain branching reactions in the H_2-O_2 reaction network, that produce $O^{\bullet}$, $H^{\bullet}$ and $^{\bullet}OH$, dominate the processes of more complex systems such as hydrocarbon combustion. The H_2-O_2 system is comparatively simple. Nonetheless, H_2-O_2 combustion is sufficiently complex, involving a complete chain-branching reaction network coupled with heat and fluid transport, to realistically represent fundamental problems in more complex systems.

This is a study of the mechanisms of premixed hydrogen flame propagation, as revealed by the effects of different diluents on the laminar burning velocity. The laminar burning velocity is a physical/chemical constant for a combustible mixture at a given temperature and pressure, a product of reaction kinetics and heat transport. The laminar burning velocity is an intermediate quantity from which basic physical and chemical mechanisms can be derived and which is itself useable as a fundamental input parameter in modeling many aspects of more complex combustion phenomena [2].

While this study utilizes the burning velocity data to probe flame mechanisms, the data itself are specifically required in applications not directly considered here, but which provided motivation for this study. Two such applications pertain to energy utilization and nuclear reactor safety.

In practical combustors using gaseous fuel, maximum output is attained when the fuel is reacted with oxygen in a stoichiometric mixing ratio. If the gaseous fuel is hydrogen, it is difficult to operate a combustor at a stoichiometric hydrogen-oxygen ratio because of the extremely high burning rate of hydrogen and high combustion temperature. Diluent addition provides a means of controlling the burning rate and temperature without altering the stoichiometry [3,4]. As hydrogen shows increasing promise as a future fuel, its use will require reliable knowledge of the role of diluents in controlling combustion.

From a perspective of safety, hydrogen combustion is of particular interest in the closed environments of nuclear reactor containment buildings [5]. In the event of a dual-failure accident involving loss of normal and emergency coolant to the reactor core, hydrogen is produced by the reaction of steam with the hot zirconium fuel cladding.

$$Zr + 2\ H_2O \xrightarrow{\geq 800^\circ C} H_2 + ZrO_2$$

The hydrogen thus produced, upon mixing with containment gases (air and steam), can produce a combustible mixture. The overpressure transient resulting from ignition of this mixture represents a potential threat to the integrity of the containment.

An important input parameter in models to predict combustion behavior is the laminar burning velocity. Burning velocity data for gas mixtures in a containment building environment (H_2-air-steam) are incom-

plete. In this study, mixtures relevant to the containment building atmosphere are specifically included, and analysed in the context of a broad base of self-consistent data for the general H_2-O_2-diluent system.

2. THEORY

2.1 FLAME PROPAGATION

A flame is a unique chemical system in which very high temperature gas reactions are fixed in space, without physical containment, (i.e., a "wall-less" gas phase reaction). However, a flame is a difficult system for detailed chemical study. The reaction network in a flame is strongly coupled with fluid flow, heat transport and diffusion of species. With additional factors such as turbulence and mixing of the fuel with oxidant (diffusion flames) the system becomes unmanageably complex. In this respect, the simplest flame is the premixed laminar flame. In this ideal case, the flow of premixed gases is laminar and normal to a plane combustion wave where the mixture is consumed and from which flow the hot combustion products. The flame, or combustion wave, propagates by diffusion of heat (and mass) from the highly exothermic reactions to the unburnt gas [6].

The most important experimentally accessible property of a combustible gas mixture is its laminar burning velocity. The laminar burning velocity, S_u, of an ideal flat flame is the velocity of the unburnt gas relative to and normal to the flame front [8]. The laminar burning velocity

is controlled by the rate of heat released from the chemical reactions and by the rate of heat transported to the unburnt gas, through thermal conduction and diffusion of energetic species.

The governing equations for flat-flame propagation are the conservation equations for mass, momentum and energy [7]. In the steady state, mass continuity requires that the product of density ρ and velocity v is constant through the combustion wave.

$$\rho \cdot v = \rho_i \cdot v_i \tag{1}$$

where ρ_i and v_i are the density and velocity of the unburnt gas, respectively. For a stationary flame, $v_i = S_u$.

Conservation of energy requires that,

$$\frac{d}{dx}\left(\lambda \cdot \frac{dT}{dx}\right) - \frac{d}{dx}\left(C_p \cdot T\ \rho v\right) + Q \cdot U = 0 \tag{2}$$

where x = distance in the direction normal to the flame front

T = absolute temperature

λ = thermal conductivity

Q = heat of reaction

U = reaction velocity (containing the integrated rates of all elementary reactions),

and $\lambda \frac{dT}{dx}$ is the heat current

$C_p \cdot T\ \rho v$ is the heat carried by the flow

$Q \cdot U$ is the heat released by the reaction.

Finally, from the conservation of the number of atoms

$$\frac{d}{dx}\left(D_j \cdot \frac{dn_j}{dx}\right) - \frac{d}{dx}\left(n_j \cdot v\right) - \nu_j \cdot U = 0 \qquad (3)$$

where, n_j = number of moles/cm^3 of component j

D_j = diffusion coefficient of j

ν_j = number of moles of j which disappear in the stoichiometric reaction,

and $D_j\left(\frac{dn_j}{dx}\right)$ is the diffusion current of j

$n_j u$ is the number of moles of j carried by the flow

$\nu_j u$ is the number of moles of j removed by the reaction.

The conservation equations may be used in two ways. Simplifying assumptions can be applied to produce a practical, qualitative expression for burning velocity, or the equations may be expanded and solved in detail if the relevant physical properties and chemical rates are known. Early flame theories took the former approach by necessity. These are reviewed in several books on flames and combustion [6,7,9]. Modern computing capabilities and the availability of detailed experimental data for transport and rate parameters have permitted the second approach to be applied with increasing sophistication [1,10,11]. This study employs both approaches.

First, a simple thermal theory is adopted to obtain a calculable quantity for the effect of a diluent on physical processes, and thus identify any effects of the diluent on chemical rates of reaction. Next,

kinetic effects are analysed with the use of a one-dimensional flame model [12] where the conservation equations are solved for the complete kinetic scheme with heat and mass transport. A description of the computer model is given in Appendix A. The computer model provides a means by which rate parameters can be varied and realistically integrated into the flame dynamics. In addition to the laminar burning velocity of the gas mixture, the model calculates mass fractions of each species, flame temperatures and heat release rates as a function of distance into a one-dimensional flame front.

A simple thermal approach is developed as follows [7]. Consider the temperature profile across a plane combustion wave (see Figure 1), consisting of a preheat zone, a reaction zone and a recombination zone. Between the preheat zone and the reaction zone is an arbitrary ignition temperature, T_o at x = 0. In the preheat zone, the temperature rises from T_i to T_o by conduction only ($Q \cdot U = 0$), and Equation (2) can be integrated between $x = -\infty$ and x = 0, giving,

$$C_p \cdot \rho_i \cdot v_i \ (T_o - T_i) = \lambda\left(\frac{dT}{dx}\right) \tag{4}$$

In the reaction zone, continuity requires that,

$$S_u = \int_o^{\delta_r} U \cdot dx = \bar{U} \ \delta_r \tag{5}$$

where $\bar{U}$ = average reaction rate over the reaction zone

δ_r = thickness of the reaction zone.

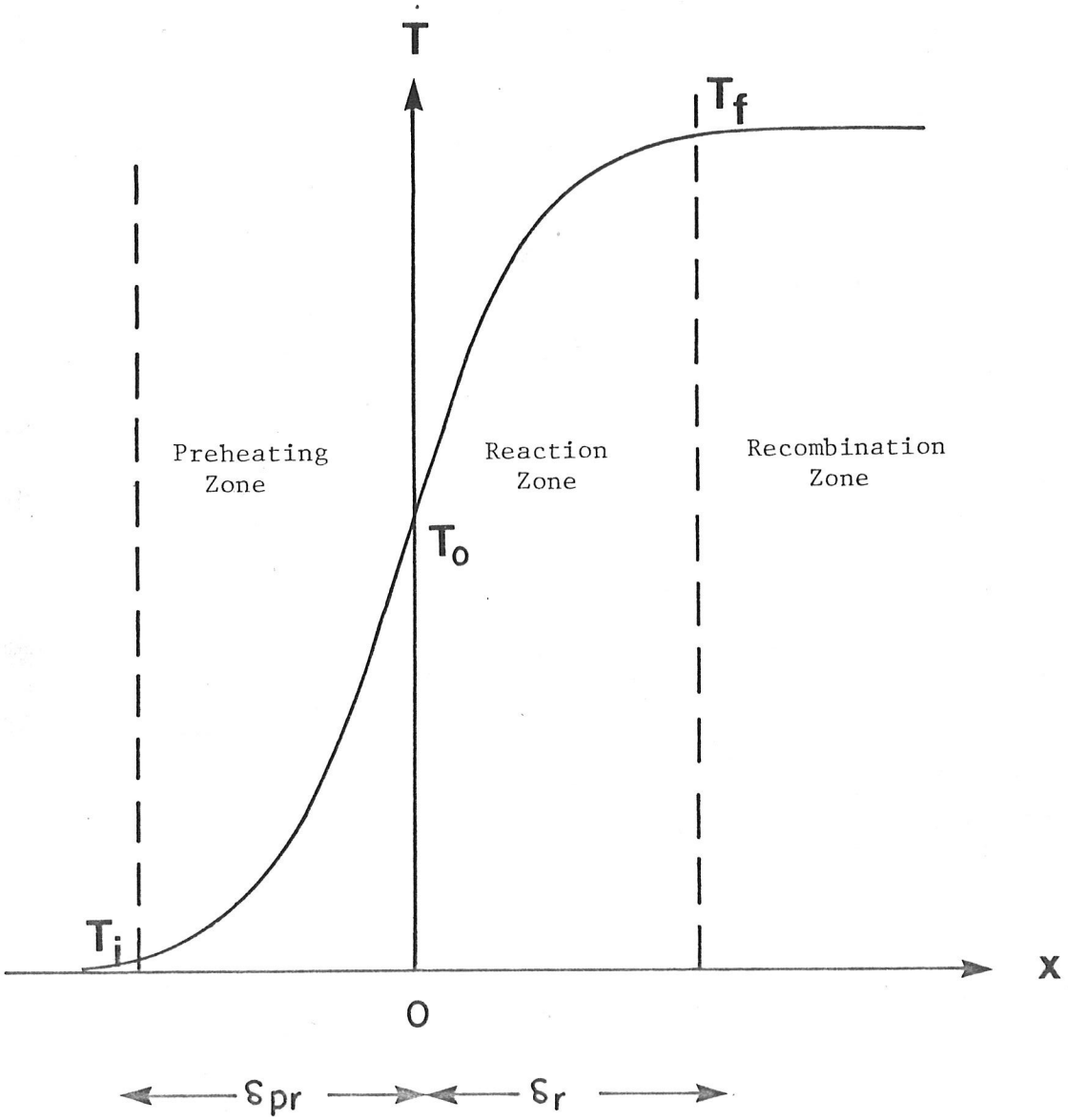

FIGURE 1: Temperature profile of an idealized flat-flame front

The temperature gradient is assumed to be approximately linear at the interface of the preheat and reaction zones.

$$\frac{dT}{dx} = \left(\frac{T_f - T_o}{\delta_r}\right)$$

From Equation 5, $\delta_r = \frac{\bar{U}}{S_u}$.

Substituting in (4) we get,

$$v_i = \frac{\lambda}{\rho_i C_p} \left(\frac{T_f - T_o}{T_o - T_i}\right) \frac{\bar{U}}{S_u}$$

and, for a stationary, one-dimensional flame, since by definition $S_u = v_i$,

$$S_u^2 = \frac{\lambda}{\rho C_p} \cdot \left(\frac{T_f - T_o}{T_o - T_i}\right) \cdot \bar{U}$$

Since the reaction zone thickness is comparable to the preheating zone thickness [13],

$\left(\frac{T_f - T_o}{T_o - T_i}\right) \sim 1$ and,

$$S_u \sim \underbrace{\left(\frac{\lambda}{\rho C_p}\right)^{\frac{1}{2}}}_{\text{transport term}} \underbrace{(\text{reaction rate})^{\frac{1}{2}}}_{\text{rate term}} \qquad (6)$$

Since no specific law for the reaction rate is included, Equation (6) is generally applicable. It expresses in general terms what is

common to most flame theories, that the burning velocity is proportional to the square root of the average reaction rate times a transport term.

The transport term is the thermal diffusivity, α.

$$\alpha = \frac{\lambda}{\rho C_p} \tag{7}$$

Table 1 lists the values for λ, ρ and C_p for the gases studied. An inert diluent is expected to influence the burning velocity by its effect on the transport properties of the combustible mixture. Thermal diffusivity is a calculable quantity so burning velocities with different diluents can be corrected for differences in thermal diffusivity of the mixture. Any remaining differences between diluents are assumed to arise in the rate term.

In reality, the rate term is not a simple term. It contains the integrated rates of a complex chain branching reaction scheme. A summary of the ways that diluents can affect the rate term is given at the end of Section 2.2.

2.2 THE H_2-O_2 REACTION SYSTEM

The H_2-O_2 reaction mechanism includes a network of as many as 80 individual reactions, which have been tabulated [14] and reviewed [15,16,17]. To reduce the number of reactions to a manageable size, Warnatz [18] offers two criteria by which reactions can be eliminated from consideration without significantly affecting the overall reaction rate or flame structure:

TABLE I

PHYSICAL PROPERTIES OF GASES

Gas	Thermal Conductivity at 300 K λ ($\times 10^{-6}$ W·m^{-1}·K^{-1})	Heat Capacity at 300 K C_p ($\times 10^{-3}$ J·kg^{-1}·K^{-1})	mol wt M ($\times 10^{-3}$ kg·mol^{-1})	Density at 273 K, 1 atm ρ (kg·m^{-3})	Viscosity at 273 K, 1 atm μ ($\times 10^{6}$ kg·m^{-1}·s^{-1})
H_2	18.7	14.3	2.0	0.089	8.42
O_2	2.68	0.92	32.0	1.43	18.09
He	15.1	5.20	4.0	0.178	18.6
Ar	1.77	0.52	40.0	1.79	21.0
N_2	2.61	1.04	28.0	1.25	16.7
CO_2	1.66	0.84	44.0	1.96	13.8
H_2O	1.78	1.84	18.0	0.804	12.5
D_2	14.0	7.29	4.0	0.178	12.5

(i) Where the concentration of a species consumed in a reaction is less than 5% of the concentration of that species consumed in all reactions occurring, that reaction is eliminated.

(ii) Subsequent reactions of by-products, comprising less than 2.5% of products are eliminated.

By these criteria, 18 reactions are identified to represent a complete mechanism for the H_2-O_2 system as it affects flame propagation. These are listed in Table 2, with the respective rate parameters as recommended by Baulch et al [15,16].

Characteristic of the H_2-O_2 reaction (see Table 2) is the existence of two parallel oxidation pathways. The first is initiated by the termolecular reaction R11 which, due to its low activation energy, proceeds readily at low temperatures. Reaction R11 is exothermic, producing $\sim$ 200 kJ/mol due to the formation of HO_2, and an additional $\sim$ 180 kJ/mol is produced in subsequent reactions R12 - R15. Table 3 contains the heats of formation for species in the H_2-O_2 system. The low temperature reactions R11-R15 are the principal sources of heat release in H_2-O_2 flames [10]. The second oxidation pathway involves the endothermic, bimolecular chain-branching reactions R3 and R5, which have a high activation energy and are restricted to the high temperature zone of the flame. These chain branches are responsible for the exponential increase in rate and the resulting explosive nature of H_2-O_2 combustion.

TABLE 2

REACTIONS IN THE H_2-O_2 SYSTEM* [18]

No	Reaction	A (cm, mol, s)	b	E (kJ/mol)
R1	$OH+H_2 \rightarrow H_2O+H$	$1.2.10^9$	1.3	15.2
R2	$H+H_2O \rightarrow OH+H_2$	$4.5.10^9$	1.3	78.7
R3	$H+O_2 \rightarrow OH+O$	$2.2.10^{11}$	0	70.4
R4	$OH+O \rightarrow H+O_2$	$1.0.10^{13}$	0	0
R5	$O+H_2 \rightarrow OH+H$	$1.8.10^{10}$	1.0	37.3
R6	$OH+H \rightarrow O+H_2$	$8.3.10^9$	1.0	29.1
R7	$OH+OH \rightarrow H_2O+O$	$1.5.10^9$	1.14	0
R8	$O+H_2O \rightarrow OH+OH$	$1.6.10^{10}$	1.14	72.4
	Recombination reactions**			
R9	$H+H+M \rightarrow H_2+M$	$9.0.10^{16}$	-0.6	0
R10	$H+OH+M \rightarrow H_2O+M$	$2.2.10^{22}$	-2.6	0
R11	$H+O_2+M \rightarrow HO_2+M$	$2.3.10^{18}$	-0.8	0
	HO_2 Consumption			
R12	$H+HO_2 \rightarrow OH+OH$	$1.5.10^{14}$	0	4.2
R13	$H+HO_2 \rightarrow H_2+O_2$	$2.5.10^{13}$	0	2.9
R14	$OH+HO_2 \rightarrow H_2O+O_2$	$1.5.10^{13}$	0	0
R15	$O+HO_2 \rightarrow OH+O_2$	$2.0.10^{13}$	0	0
	H_2O_2 Formation and consumption			
R16	$OH+OH+M \rightarrow H_2O_2+M$	$9.1.10^{14}$	0	-21.4
R17	$H+H_2O_2 \rightarrow H_2O+OH$	$3.2.10^{14}$	0	37.5
R18	$H_2O_2+M \rightarrow OH+OH+M$	$3.0.10^{17}$	0	190.0

* $k = AT^b \exp(-E/RT)$

** $[M] = 6.0\ (H_2O) + (H_2) + 0.4\ (N_2) + 0.4\ (O_2)$

TABLE 3

HEATS OF FORMATION FOR SPECIES IN THE H_2–O_2 SYSTEM [14]

Species	Heat of Formation (kJ/mol)
H_2	0
H	217.8
OH	39.4
HO_2	20.9
H_2O	-241.6
H_2O_2	-136.0
O_2	0

An important group of reactions in this study are the recombination reactions R9, R10 and the aforementioned R11, since these are influenced differently by diluents having different third body efficiencies.

Generally, the third body efficiency of a molecule in termolecular reactions is related to collision frequency and the number of internal degrees of freedom over which a molecule can share collisional energy. This general trend is illustrated in Table 4, comparing third body efficiency coefficients (relative to H_2 = 1) for reaction R11 with calculated collision frequencies.

TABLE 4

COMPARISON OF COLLISION FREQUENCIES AND THIRD BODY EFFICIENCIES FOR SOME SIMPLE MOLECULES IN REACTION R11 $H + O_2 + M \rightarrow HO_2 + M$

Molecule	Third Body Efficiency Coefficient, m^* (relative to $H_2 = 1$) [15]	Collision Frequency (relative to H = 1)
He	0.3	0.6
Ar	0.3	0.38
N_2	0.4	0.46
O_2	0.4	0.42
H_2	1.0	1.0
CO_2	1.5	0.43
N_2O	1.4	0.43
H_2O	6.4	0.6

* $M = \sum_i m_i [i]$

The third body concentration [M], in the kinetic equations is an effective concentration made up from a sum of the concentrations of major species with coefficients m_i corresponding to their respective third body efficiencies relative to $H_2 = 1.0$.

$$[M] = [H_2] + m_{H_2O} [H_2O] + m_{O_2} [O_2] + \ldots$$

Referring to Table 4, experimental values of m_i for diatomic molecules are consistent with their respective collision frequencies. Values for He and Ar are somewhat lower, reflecting the absence of internal energy states. Triatomic molecules have considerably greater third body efficiencies than predicted by collision frequency, presumably due to their many internal states over which collisional energy can be shared.

Steam is unique in its outstanding third body efficiency in reaction R11. Walsh [19] attributed this to near-coincidence in the spacings of vibrational levels of H_2O and excited HO_2. Baldwin, et al. [20] found no support for this interpretation on the basis of studies with D_2O. While the exact mechanism of the high third body efficiency of H_2O in reaction R11 is still unclear, there is a considerable body of experimental data [15] indicating that the third body efficiency of steam is between 6.0 and 7.0 for reaction R11.

For reaction R10, the available experimental data for relative third body efficiencies of H_2, O_2, H_2O and N_2 are about the same as for reaction R11 [15]. The data for relative third body efficiencies in reaction R9 vary to such an extent that recommended values are not possible [15]. Thus the values from reaction R11 are used for R9 in this work. Other investigators [1,10] have apparently used this same rationale for reaction R9, and have used the same set of third body coefficients for all the termolecular reactions.

The reactions and rate parameters in Table 2 are those used in the one-dimensional flame code, with the exception of reactions R16 - R18, which

are included here for completeness, but are marginally acceptable by criterion (ii) [18].

The reactions in Table 2 are those important in flame propagation. Notably absent are reactions that lead to chain initiation, or ignition. Chain initiation is thought to arise from the heterogeneous reaction [13], and at higher temperatures, possibly from unimolecular dissociations

$$H_2 + O_2 \rightarrow OH + OH \qquad \log K = -0.5 \text{ at } 2000 \text{ K } [43]$$

$$H_2 + M \rightarrow H + H + M \qquad \log K = -10.8 \text{ at } 2000 \text{ K } [43]$$

$$H_2O + M \rightarrow H + OH + M \qquad \log K = -11.8 \text{ at } 2000 \text{ K } [43]$$

These reactions do not contribute significantly to the overall kinetics once the chain is initiated.

Diluent gases can affect the reaction kinetics and hence burning velocity in three ways:

(1) HEAT SINK: Diluent gases extract heat from the reaction in proportion to their heat capacities. The result is a lowering of the flame temperature, and since temperature appears as an exponent in the rate equations, the reaction rate is sensitive to relatively small changes in temperature. This is particularly true for reactions with high activation energies, R1 - R8.

(ii) CATALYST: Diluent gas molecules differ in their third body efficiency for the termolecular recombination reactions R9, R10 and R11. Molecules with high third body efficiencies produce

opposing effects on the overall reaction rate. A diluent molecule with a high third body efficiency will increase the rate of radical recombinations and thus produce a drain on chain carriers, and reduce the overall reaction rate. However, these radical recombinations are often highly exothermic and the heat released serves to speed up the reaction rate. The net effect on overall rate is the resulting balance between the loss of active species and the gain in available energy for endothermic chain-branching reactions.

(iii) RADICAL SINK: The diluent molecules may react directly with active species (H· O· or ·OH) in the flame. If the reaction constitutes a chain termination and is of a comparable rate to propagating and branching reactions in the flame, the overall rate of reaction will decrease.

3. REVIEW OF PREVIOUS WORK

3.1 INERT DILUENTS

The first systematic study of burning velocities in H_2-O_2-diluent systems was that by Jahn [21], for the diluents N_2 and CO_2. Jahn's data are widely regarded [8,9] as being low by about 20% due to a systematic error in the bunsen/ cone area method used. It was nonetheless an ambitious, self-consistent study, which has persisted in the literature, with the correction factor of 1.2.

Friedman [22] measured burning velocities of selected H_2-O_2-diluent mixtures with the diluents He, Ar, N_2 and CO_2. His interest was primarily in obtaining quenching distances. He admitted to poor absolute accuracy of his burning velocity data, and he relied mostly on the data of Jahn.

Mellish and Linnet [23] studied the effect of the diluents He and Ar on several flame phenomena, including burning velocity. Their values for burning velocity were consistently lower than currently accepted values. An attempt was made to correlate the observed diluent effects using both a thermal and a diffusion theory of flame propagation. The results were inconclusive, even for the simple case of He and Ar diluents. In the analysis, thermal conductivities for the mixtures were derived by a simple averaging formula of Friedman, which contains considerable errors for mixtures with H_2. Also they neglected to consider kinetic effects of changing the fuel equivalence ratio and treated excess O_2 and H_2 as simple diluents.

Morgan and Kane, at the National Bureau of Standards, for the Office of Naval Research and Bureau of Aeronautics [24], surveyed the effects of the inert diluents He, Ar and N_2 on flame speeds and temperatures. Because many fuels were studied, they restricted the measurements to stoichiometric compositions only. A reasonable correlation was made of burning velocity and flame thickness using a formulation similar to Equation (5).

France and Pritchard [25] studied burning velocities of multicomponent fuel-gas mixtures with diluents and observed that diluents

decrease the burning velocity in the order $CO_2 > N_2 > Ar > He$. Further, they found the reduction was linear with increasing diluent fraction. The general conclusion was that the effect of diluents on reducing the burning velocity is related to their heat capacity.

Takahashi, et al. [3] reported a series of measurements using the nozzle burner/cone angle method for H_2-air flames, where nitrogen in air was replaced by He and by Ar. They concluded that the maximum burning velocity decreased linearly with added diluent, and that the different diluents reduced the burning velocity in the order $N_2 > Ar > He$.

3.2 WATER VAPOUR

David and Mann [26] first observed moist flame temperatures to be 40-50°C higher than dry flame temperatures for open hydrogen-air flames, in contrast with the calculated temperature for moist mixtures which is 15°C lower than for dry mixtures.

Kuehl [27] observed an increase in burning velocity upon replacing N_2 with H_2O vapor in a low pressure (25 kPa) H_2-air flame at an unburnt gas temperature of 450°C. He concluded that the effect of water vapor was anomalous. Because of its greater heat capacity, water vapor should act as a heat sink and lower the flame temperature and hence the burning velocity. He postulated that water accelerated the burning velocity by participating in a mechanism of radiant heat transport from hot gases to water vapor in the unburnt gas. However, this conclusion was not supported by experiment or detailed calculations.

Levy [28], commenting on Kuehl's result, suggested a chemical kinetic interpretation for the accelerating effect of H_2O vapor on burning velocity. He suggested that H_2O vapor served to increase the OH radical concentration and thus increased the reaction rate through an increase in the number of chain carriers (i.e., OH radicals).

$$H_2O + HO_2 \rightarrow OH + H_2O_2$$
$$H_2O + H + O_2 \rightarrow OH + H_2O_2$$

His suggestion, however, did not account for the anomalous increase in flame temperature observed by David and Mann. Levy offered no calculations or experiments to support his suggestion, and concluded that a satisfactory explanation was still lacking.

Dixon-Lewis and Williams [29] gave further kinetic interpretation of Kuehl's result. On the basis of second explosion limit data, they implicated the low temperature oxidation reaction R11, and the high third body efficiency of H_2O vapor in that reaction, as a mechanism for steam increasing the reaction rate in low temperature flames. They argued that, at low flame temperatures ($\sim$ 900 K), the high activation energy chain-branching reaction R3 is slower than reaction R11, and an efficient third body such as H_2O will increase the reaction rate. However, it follows that at higher temperatures, as the ratio $\frac{k(3)}{k(11)}$ increases at a rate corresponding to the difference in Arhenius activation energy, reaction R11 becomes rapidly less important. Kuehl's data is for relatively high temperature flames (2400 K) where the ratio $\frac{k(3)}{k(11)}$ is high. Dixon-Lewis and Williams concluded with a statement that the HO_2 mechanism may "still retain some importance in

the hotter flames" and is a "not unreasonable" explanation for the effect of H_2O vapor on burning velocity. The role of reaction R11 in the preheating zone of the flame was overlooked. Dixon-Lewis has since done extensive modelling of the H_2-O_2-N_2 system, with particular emphasis on the HO_2 mechanism [10], but has not specifically addressed the effect of steam in this context.

More recently, Liu and MacFarlane [30] measured the burning velocities of H_2-air-steam mixtures as a function of temperature and composition. From their measurements, they derived an empirical correlation for burning velocities of H_2-air-steam between 25°C and 250°C. The data were, however, limited to steam fractions of less than 15%. Comparative data were not obtained for other diluents and chemical mechanisms were not considered.

The effect of steam in propane and ethylene flames was quantitatively studied recently by Müller-Dethlefs and Schlader [31]. Their results indicated that water vapor did not act as an inert diluent but instead gave rise to greater heat release that counteracted the cooling effect of the added steam. They offered no mechanism for the observed effect, but the data are noteworthy because they indicate that the anomalous behavior of water vapor observed in H_2 flames appears to exist in hydrocarbon flames as well.

The addition of water to combustors has been advocated since early in this century when it was found that steam could improve atomization of liquid fuels. The history of steam as an ancillary to combustion is the subject of a review by Dryer [32]. Water is an effective antiknock agent

and is receiving renewed attention in the light of environmental problems with fuel soluble additives such as tetraethyl lead [33]. Steam reduces sooting and carbon monoxide emission in hydrocarbon flames [34]. As well, steam is known to reduce NO_x emissions [32,35,36] in gas turbine combustion. The exact mechanisms for these effects are unresolved but are believed to arise from participation of H_2O in H-O-OH kinetics [32,36]. Fundamental studies of flame kinetics for the H_2-O_2-H_2O system are lacking.

3.3 EXCESS H_2 AND O_2

One of the unique features of H_2 combustion is the observation that the maximum burning velocity of H_2-air does not occur at the stoichiometric mixture ($\sim$ 29% H_2 in air) as occurs in hydrocarbon flames. For H_2-air flames, the maximum burning velocity is at $\sim$ 42% H_2 in air, corresponding to an H_2/O_2 ratio of about 3.6.

The burning velocity is a function of the rate of energy transfer to the unburnt gas. Whether energy transfer is via diffusion of free radicals or thermal conduction, both are dependent on flame temperature. However, in hydrogen flames there is an apparent contradiction. The maximum flame temperature occurs at 29% H_2-air (stoichiometric mixture); additional hydrogen reduces the flame temperature by acting as a heat sink but the burning velocity continues to increase [6,7,9,27]. Several explanations have been offered.

Kuehl [27] compared the burning velocity and temperature of H_2-air mixtures to which excess H_2 was added. He concluded that the increases in

the burning velocity by increased H atom diffusion has a greater effect on burning velocity than the decrease in flame temperature. At the time, Dixon-Lewis and Williams [29] disagreed, showing evidence that increasing the diffusion coefficient of H• in a specific flame decreased the burning velocity. They suggested a more likely explanation was that excess H_2 increased the thermal conductivity of the mixture. However, more recently Dixon-Lewis has supported an H• atom diffusion mechanism [10].

Behrens [37] progressively added excess H_2 and O_2 to stoichiometric mixtures of H_2-O_2-N_2 and observed, for both, an increase in burning velocity. This result was used as qualitative evidence that reactions in the H_2-O_2 flame are higher than zero order.

3.4 DEUTERIUM FLAMES

Deuterium flames are included in this study for both practical and theoretical reasons. From a practical standpoint a potential hazard exists from the buildup of D_2 and O_2 in the helium cover gas of CANDU reactors [38]. Dissolved D_2 and O_2 are produced by radiolysis in the D_2O moderator and, in the event of a moderator leak, out-gassing can occur and could result in a combustible mixture of D_2-O_2-He in the cover gas. Thus, it is important to understand the combustion behavior of these mixtures. In kinetic studies, isotope effects can provide important information on the role of H-H bond cleavage in complex multistep mechanisms.

Flame speeds of D_2 mixtures have been studied by Smith and Gray [39], but they did not measure burning velocities. Flame speed is the free

velocity of the flame in space, not referenced to the unburnt gas velocity. They obtained H_2/D_2 ratios of flame speeds of ~ 1.4 and attempted to relate this to differences in reactivity and transport properties.

To summarize the effect of diluents in hydrogen flame propagation, there is general agreement that diluents reduce the burning velocity to the extent that they act as a heat sink and reduce flame temperature. It is also recognized that diluents will alter the thermal diffusivity of the gas mixture. However, a quantitative, comprehensive, self-consistent study of diluent effects is lacking. In particular there has been no detailed study of the unique effects of steam as a diluent, insofar as a mechanism is not established for observed effects. The effect of excess H_2 has been widely observed in the context of H_2-air flames and is usually attributed to H atom diffusion and to the high thermal conductivity of H_2. The relative magnitudes of the two effects at different fuel fractions is uncertain, as is a mechanistic link between the generation of H atoms and their ultimate role in increasing the burning velocity.

4. EXPERIMENTAL

4.1 GENERAL

The initial challenge in physically measuring a laminar burning velocity is to devise an experimental approximation to the flat, one-dimensional flame imposed by the definition, in the absence of external heating,

cooling or perturbing aerodynamics. Flames of many configurations have been used to obtain a laminar burning velocity, each with their own merits and liabilities as to the ease of the physical measurement, and to their reliably creating the ideal surface of the definition. The subject of laminar burning velocity measurement has been critically reviewed recently by Andrews and Bradley [8], Rallis and Garforth [2], among others [6,7].

Of the recommended methods, the nozzle-burner/cone-angle method was chosen because it best accommodated the range of burning velocities in this study. In this method the flame surface is a stationary cone supported at the top of a vertical tube by a laminar flow of premixed combustible gas. Since the spatial velocity of the flame is zero, the burning velocity at any point on the flame cone is equal to the normal component of the unburnt gas velocity at that point. The burning velocity, S_u, can thus be expressed in terms of the unburnt gas velocity and the half angle of the flame cone [8] (see Figure 2).

$$\dot{m} = \rho_o U_o a_o = \rho_o S_u a_f$$

where $\dot{m}$ = mass-flow rate

ρ_o = unburnt-gas density

U_o = unburnt-gas velocity

a_o = cross-section area of the burner

a_f = area of the flame surface

S_u = burning velocity

(a)

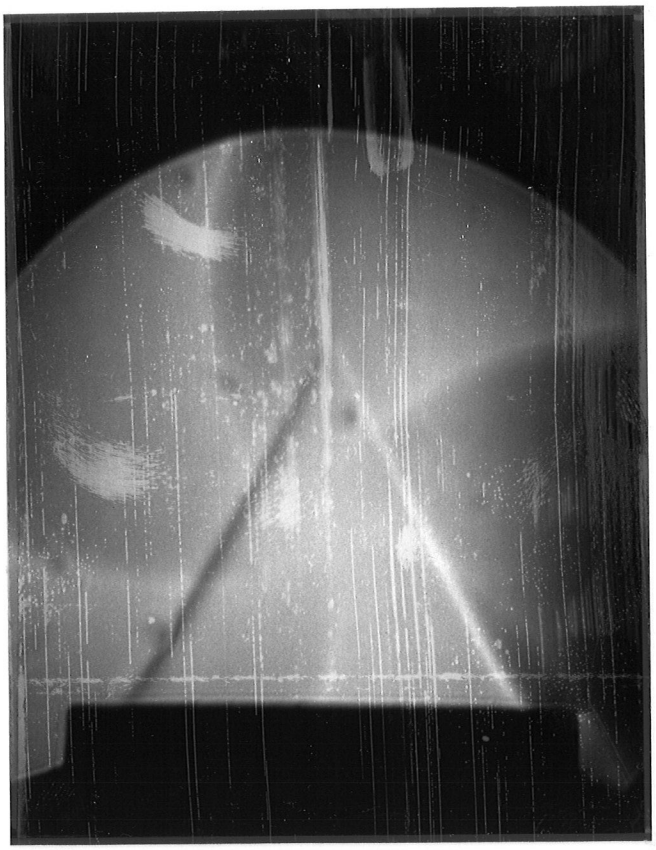

(b)

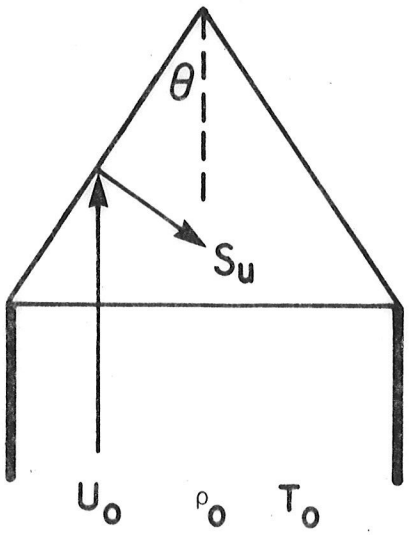

flame cone area = a_f

burner area = a_o

FIGURE 2: a) Actual schlieren photograph of a nozzle-burner flame cone

b) Schematic drawing of a flame cone illustrating the quantities used in deriving Equation (8)

Rearranging, $S_u = \frac{\dot{m}}{\rho_o a_f} = \frac{U_o a_o}{a_f}$,

and, $\frac{a_o}{a_f} = \sin \theta$.

$$S_u = U_o \sin \theta \qquad (8)$$

Equation (8) can be used to obtain the burning velocity if the following criteria are met. First, the quantities U_o and θ must be accurately determined. Second, the curved surface of the flame cone relative to the flame thickness must be an adequate approximation to an infinite plane. Finally, the velocity profiles of the unburnt gas must be laminar axisymmetric and uniform across the diameter of the burner exit.

4.2 LASER DOPPLER ANEMOMETER

The central requirement in the nozzle-burner/cone-angle method is that the unburnt gas velocity, U_o, can be reliably determined. The flame strongly influences the flow field so the unburnt gas velocity cannot be determined in the absence of the flame. Physical probes, such as Pitot tubes or hot-wire anemometers produce intolerable perturbations in flow and flame structure. Andrews and Bradley [8] recommend particle tracking, whereby the unburnt-gas velocity is deduced from tracks of stroboscopically illuminated particles seeded into the gas flow. While simple in principle, the method is time-consuming to use and sensitivity requirements dictate the use of rather large particles (5 μm or greater) for which fidelity of particle and gas velocities is uncertain [40].

Laser Doppler Anemometry (LDA) is a new alternative to particle tracking. Like particle tracking, it is non-intrusive but is easier to use and employs smaller light-scattering particles. LDA was pioneered as a non-intrusive flow diagnostic technique by Yeh and Cummin [41] in 1964. The theory and practice of LDA, in its many forms that have since evolved, are described in a book by Durst, Melling and Whitelaw [42]. The technique was used in combustion studies by France and Pritchard in 1976 [43]. A practical fringe model of the LDA phenomenon proposed by Rudd [44] and elaborated by Durst and Stevenson [45] illustrates the principle of the dual-beam, forward-scattering anemometer employed in this experiment.

Two focussed, intersecting light beams of equal intensity, having planar wavefronts will interfere to produce a set of parallel fringe planes in their volume of intersection. This is illustrated schematically in Figure 3. The accompanying photograph of an actual fringe pattern was obtained by inserting a 4 mm lens in the focal volume of the intersecting beams and projecting the image onto a screen. The distance between the fringe planes, d_f, is given by

$$d_f = \frac{\lambda}{2 \sin \phi} \tag{9}$$

where, λ = wavelength of the laser light

ϕ = the crossing angle of the two beams

when a small particle with a velocity component, $u_\perp$, perpendicular to the fringe planes passes through this volume of intersection, it generates a rising and falling intensity of scattered light. The frequency, f_D, of the

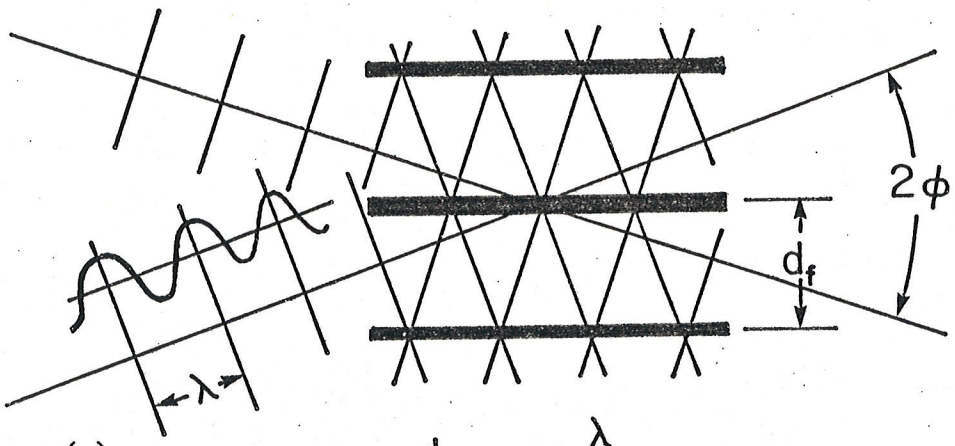

(a)

$$d_f = \frac{\lambda}{2 \sin \phi}$$

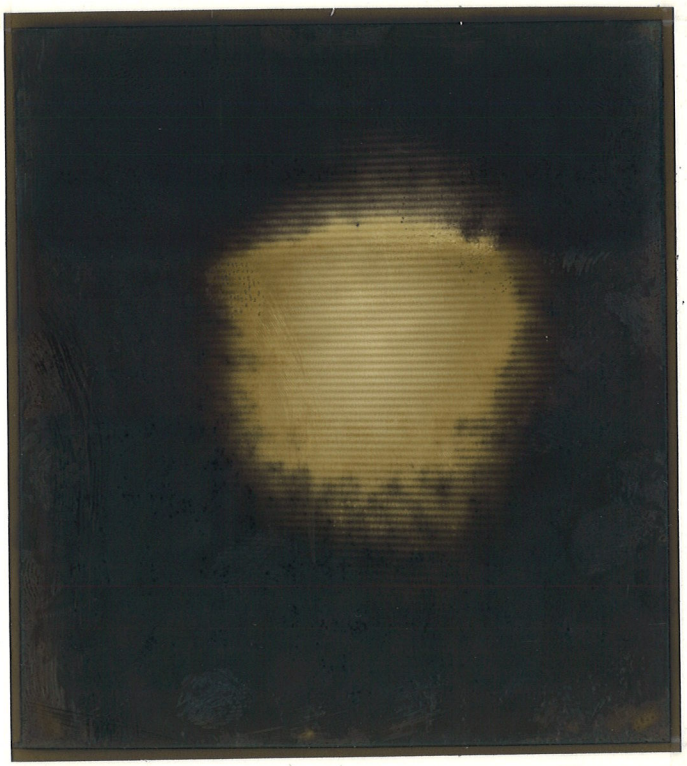

(b)

FIGURE 3: a) Schematic representation of the interference fringe planes in the LDA sample volume [45]

b) Photograph of a projected image of the LDA sample volume, showing the fringe planes

scattered light intensity variation is proportional to the velocity of the particle and the spacing of the fringe planes, d_f.

$$f_D = \frac{u_\perp}{d_f} = 2\, u_\perp \left(\frac{\sin \phi}{\lambda}\right) \tag{10}$$

The scattered light signal from particles (0.3 μ alumina) traversing the probe volume is detected by a photomultiplier tube (RCA 8645, S-20 response). The signal is fed to a signal conditioner and frequency counter (TSI model, 1990), which outputs a voltage proportional to f_D. The velocity of the particle $u_\perp$ is obtained from Equation (10). Rearranging,

$$u_\perp = f_D \frac{\lambda}{2 \sin \phi} \tag{11}$$

The fringe spacing determines the size of particles to be used. For optimum signal-to-noise ratio the particle diameter d_p should be less than the fringe spacing. A minimum ratio d_f/d_p of 4 is recommended [42]. In this experiment, $\phi = 7.1°$ and $\lambda = 632.8$ nm. From Equation (9), the fringe spacing is 2.6 μm. Thus, particle diameters are in the sub-micron range, a considerable improvement over the 5 μm particles required for photographic particle tracking. In this experiment particle diameter was 0.3 μm. The dimensions of the probe volume are of the order of the diameters of the focussed beam waists, which exceed the requirements of this experiment for spatial resolution. The counter electronics reject signals that do not contain a predetermined number of cycles, or signals that arise from more than one particle in the sample volume. For combustion studies the minimum possible number of particles in the gas flow is desired because

of possible catalytic effects in the flame. Particle seeding rates were kept very low, with the voltage output of valid signals recorded on a chart recorder and an average taken of about one hundred separate particles. Particles were entrained into the gas flow by a single-stage cyclone particle generator.

4.3 FLAME VISUALIZATION

The cone angle, 2θ, is most easily obtained from an enlarged photograph of the flame. Hydrogen flames, unlike flames containing carbon, do not luminesce and cannot be photographed directly by visible light. Moreover, the luminous zone of a flame is not suitable for burning velocity measurements because it does not represent the plane of first interaction between the unburnt gas and the combustion wave [2]. Other methods of flame visualization that better represent the surface of interest are shadowgraph and schlieren photography. Both use the refraction of transmitted light at the steep temperature (density) gradient of the flame front to generate an image of the flame.

In the shadowgraph method the flame is illuminated by a point source and the shadow of the flame is recorded on a photographic plate. The displacement of light is proportional to the second derivative of the density and represents a zone very near the first temperature rise. However, the position of the shadowgraph edge will vary depending on the distance to the recording surface. There is also the complication of a second, outer edge at a higher temperature which is not well-defined. Most authors consider shadowgraph unreliable for burning velocity measurements [2,6,7,8].

In schlieren photography, the flame is illuminated by parallel light and brought to focus at a knife edge. The image is formed by light refracted past the knife edge to the photographic plate. The schlieren image represents the first derivative of the density, which is at its maximum at ~ 200°C [2], very near to the point of first temperature rise. The location of the schlieren edge is independent of distance at which the image is recorded. While technically more complex than shadowgraphy, schlieren photography is the recommended method of photographing flames for burning velocity measurements [2,6,7,8].

The schlieren system in this experiment employed a 150 W xenon lamp with achromatic lenses for focussing and recollimating. A schematic diagram of the optical layout is given in Figure 4, showing the schlieren and LDA optical axis at right angles for simultaneous measurement of the cone half-angle and the unburnt gas velocity. The schlieren image was photographed on 4x5 polaroid film. The cone half-angle θ was determined directly from the photographs by measuring the base b and height h of the cone.

$$\theta = \tan^{-1} \left(\frac{b}{2h}\right) \qquad (12)$$

4.4 BURNER AND GAS HANDLING

The burner and gas handling system are shown schematically in Figure 5. Gases were metered by thermoelectric mass-flow controllers, (Brooks Instruments Model 8850C) individually calibrated for each gas used.

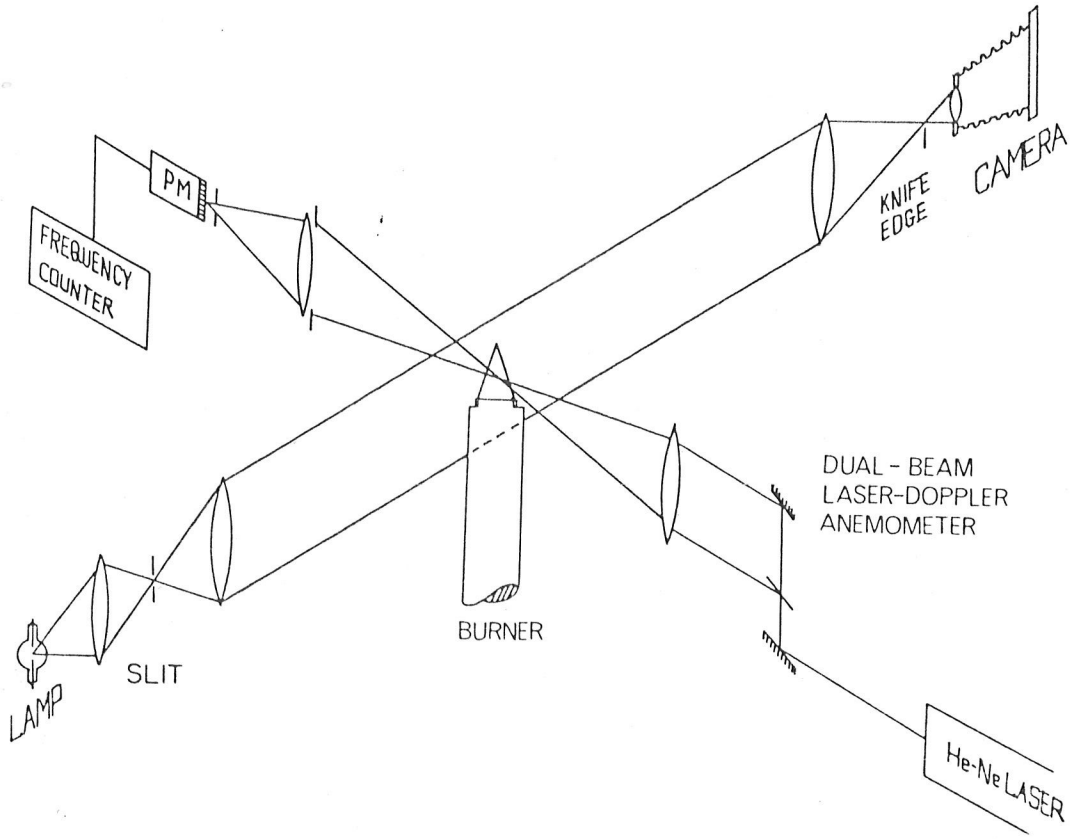

FIGURE 4: Schematic drawing of the layout of the LDA and Schlieren optics [29]

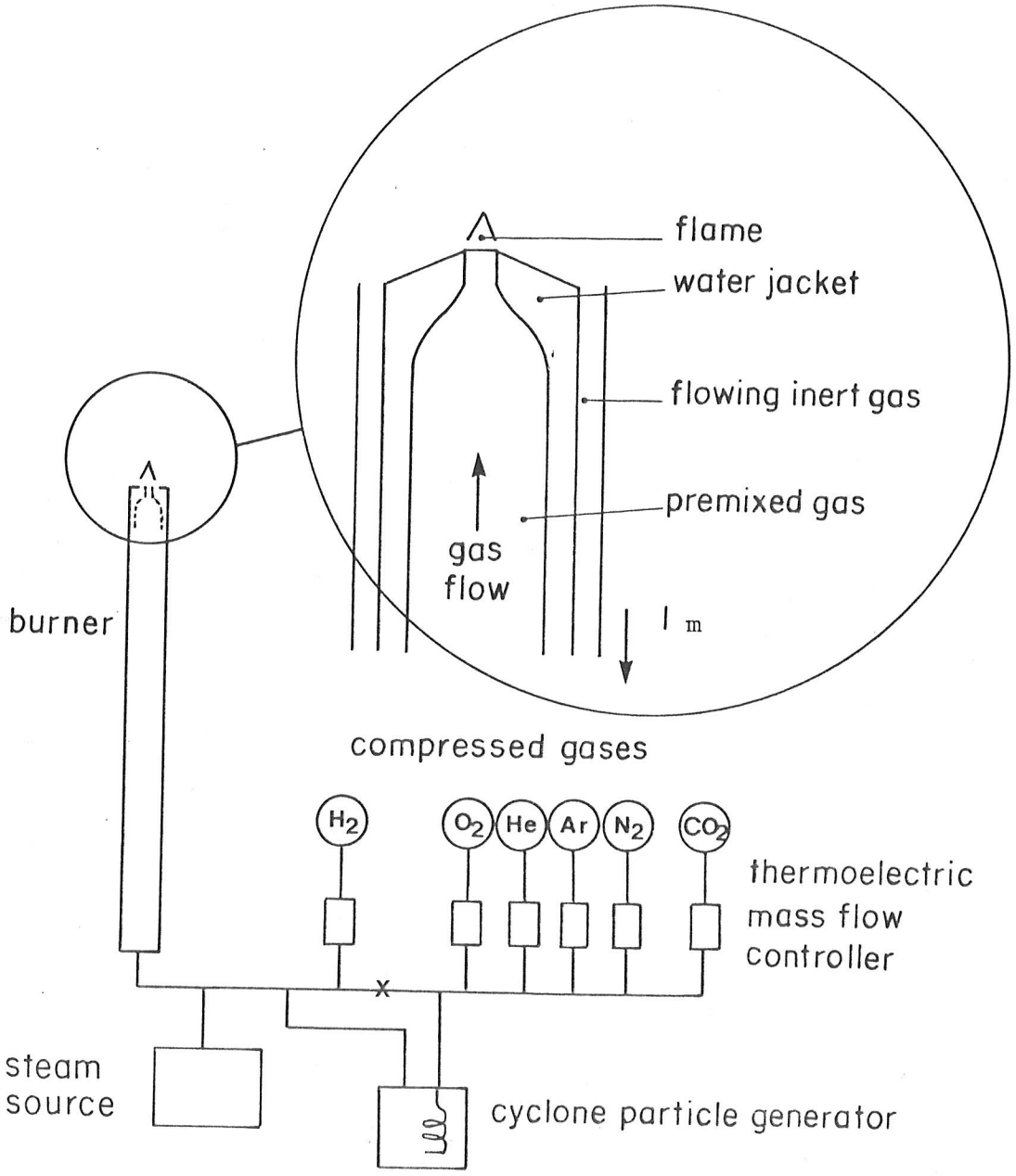

FIGURE 5: Schematic drawing of the burner and gas handling system

A uniform volume flow of steam was provided by the smooth evaporation of a precisely metered flow of distilled, degassed liquid water. The metered gases were blended and mixed over about a meter length. The mole fractions of the gas mixture were assumed to be proportional to the volume flow rates.

The burner consisted of a 0.8 m straight pipe tapered at the open end to a Mach-Hebra nozzle. The use of a tapered nozzle at the burner exit produces a uniform velocity profile for a distance of several diameters beyond the nozzle exit. The uniform velocity profiles were verified by point measurements across the diameter of the nozzle exit up to 1 cm above the nozzle. Figure 6 shows typical gas velocity profiles on the 5 mm nozzle.

The burner was fitted with an annular chamber over its entire length to within 0.5 mm of the nozzle exit. Water was circulated through the chamber from a constant temperature bath, providing accurate control of unburnt gas temperatures and cooling of the nozzle. A second chamber was installed for flowing an inert gas curtain around the flame to prevent entrainment of atmosphere air.

One criticism of the nozzle burner method is that flame curvature can lead to significant departure from the ideal one-dimensional flame, and can result in erroneous burning velocities. This effect was quantified by making measurements on burners of different diameters (hence flames of different radii of curvature). The measured burning velocity was observed

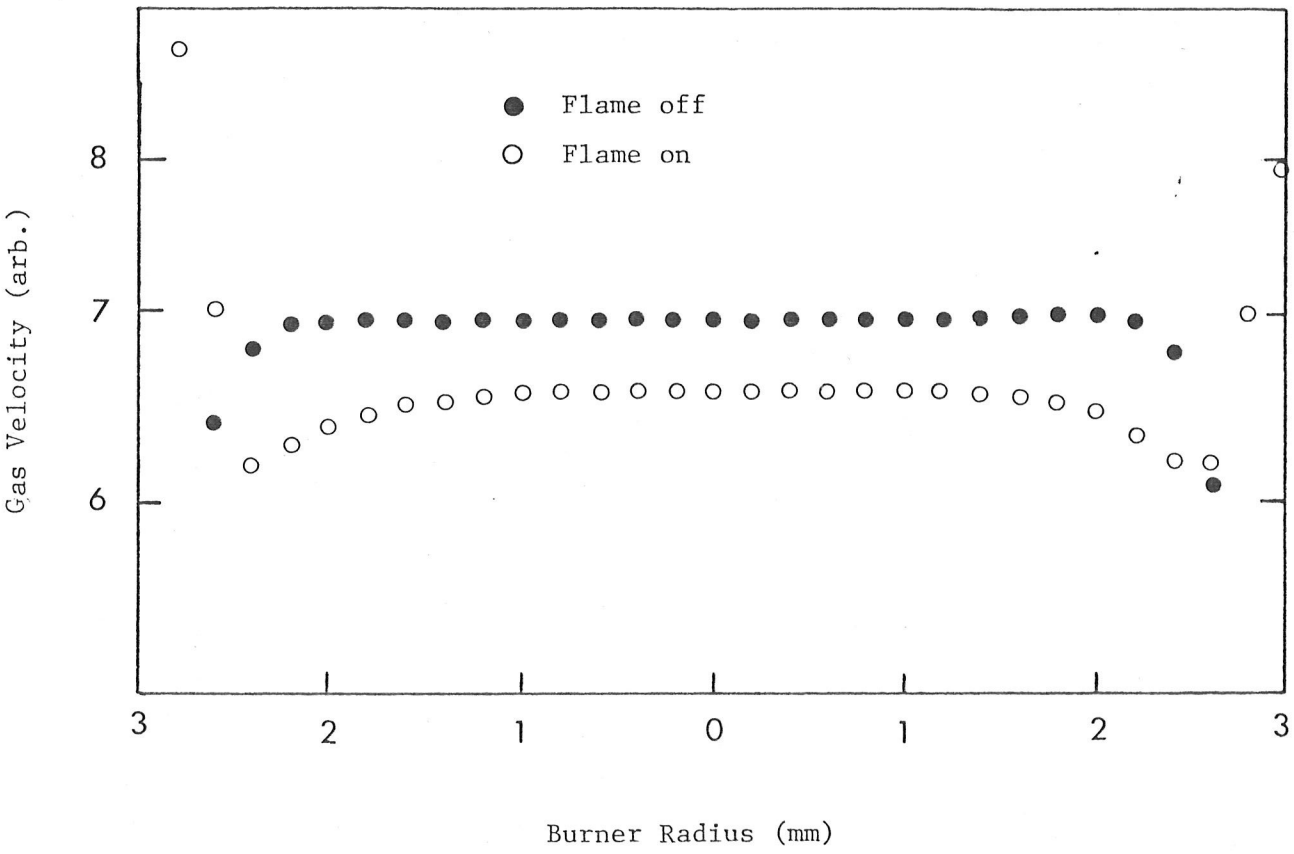

FIGURE 6: Representative velocity profile of gases exiting the 5-mm nozzle. Measurements were taken with and without a flame at a height of 1 mm

to decrease with increasing burner diameter (Figure 7). At a 5 mm nozzle diameter, the measured burning velocity approaches a constant value, indicating that errors due to flame curvature become negligible beyond this diameter. France and Pritchard [43] reported no effect of nozzle diameter on measured burning velocity for 8 mm to 12 mm burner diameters. Thus, it appears that a conical flame of 5 mm diameter or greater is a reasonable approximation to a one-dimensional surface. For burning velocities greater than 6 $m \cdot s^{-1}$, which exceeded the critical Reynolds number for laminar flow on the 5 mm burner, a 3 mm burner was used and the burning velocities were corrected by subracting 0.28 $m \cdot s^{-1}$.

A burning velocity measurement was made as follows: The desired volume flow rates of oxygen and diluent were dialed on the flow controllers. Hydrogen was then introduced into the mixture while holding a spark ignition source over the burner. The flow of H_2 was increased until the flame ignited as observed by the schlieren image. Once the desired volume of flow of H_2 was established, the flame height was adjusted by diverting a variable fraction of the total flow to a bleed line vented to atmosphere. The velocity of the unburnt gas was continuously monitored by a chart record of the LDA output, while a 4x5 polaroid photograph was taken of the flame. The cone half-angle θ was measured directly from the photograph and combined in Equation (8) with the unburnt gas velocity to obtain the burning velocity.

4.5 EXPERIMENTAL UNCERTAINTY

The experimentally determined quantity is the laminar burning velocity. The burning velocity data are reported in the figures as a function of mixture composition.

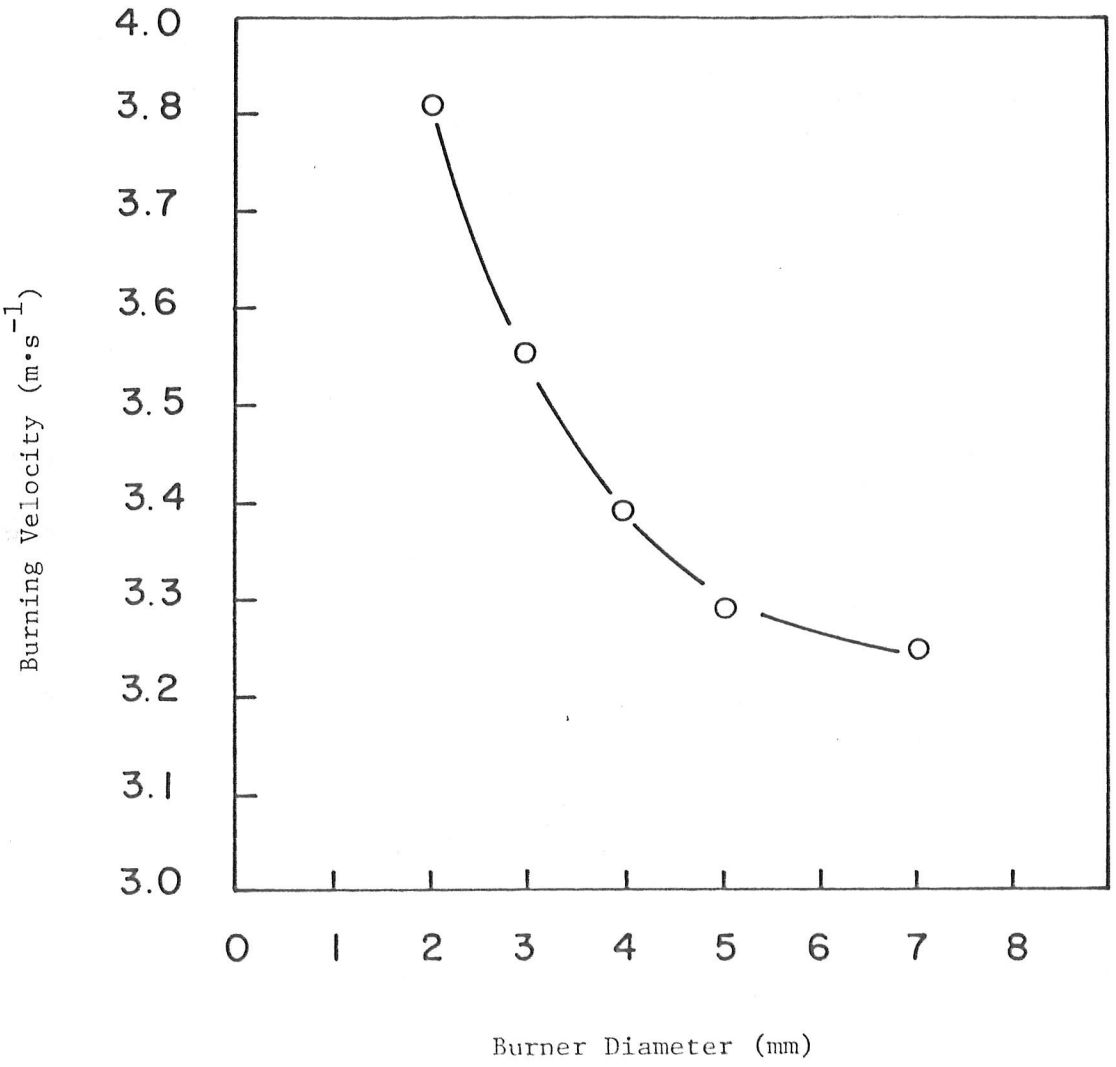

FIGURE 7: The effect of nozzle diameter on measured burning velocity for 42% of H_2 in air

The thermoelectric mass flow controllers were individually calibrated at the factory, for each gas, to within ± 0.1% of the total flow capacity (5L/min). Therefore the uncertainty in mixture composition was better than ± 1% and was periodically verified by mass spectrometry.

Two experimental quantities, the cone angle 2θ and the unburnt gas velocity U_o, are combined in Equation (8) to obtain the burning velocity. The cone angle measurement has the greatest possibility of error, since it depends on the quality of the particular flame cone image. In near-stoichiometric flames the flame cones were straight-sided and the steep temperature gradients produced a sharp schlieren image. The unceratinty in measuring θ was ± 0.2°, contributing to an error in sin θ of ± 1%.

In very lean mixtures ($H_2/O_2 \leq 0.5$), and particularly in lean mixtures containing Ar and CO_2, polyhedral flames were observed. The phenomenon of polyhedral flames has been previously studied in detail [48]. It is attributed to differential rates of mass diffusion of fuel and oxidant, resulting in spatial periodicities in gas composition within the flame. The high mobility of H_2, relative to O_2, makes H_2 flames particularly prone to this problem. The result is an increased uncertainty in θ of ± 1° for H_2-O_2 ratio less than 0.5. The uncertainty in sin θ is ± 3.8%.

A deterioration in flame quality was also observed for very rich ($H_2O_2 \leq 5$) and flames containing large fractions of diluent ($X_{dil} \geq 0.6$). The schlieren image was diffuse due to the thicker reaction zone, lower flame temperature and the corresponding decrease in refractive index gradient. In the worst cases, the uncertainty in sin θ approached ± 5%.

The uncertainty in the LDA-measured U_o was ± 2% for an individual particle which, after averaging the signals from a hundred or more particles, was better than ± 1%.

Thus the least uncertainty in burning velocity, for flames of near-stoichiometric composition, and diluent fractions less than 0.5, was better than ± 3%. Most of the analysis concerned mixtures in this category. The uncertainty in burning velocity for the extreme lean and rich mixtures was ± 7%.

5. EXPERIMENTAL RESULTS

5.1 APPROACH AND RATIONALE

The strong coupling of kinetic and transport processes in flames presents a problem to the experimentalist studying mechanisms of flame propagation. That is, there is the difficulty of altering one property of a combustible mixture while leaving all others unaffected. The simplest change that can be made to a mixture is the substitution of one chemically-inert diluent gas in the mixture for another. This is the strategic basis for the present investigation of the H_2-O_2 flames. Diluent gases are systematically replaced in H_2-O_2 flames in order of increasing complexity, and the effect on burning velocity measured.

The simplest case is the replacement of He for Ar. Both gases are assuredly inert and have identical heat capacities and, thus, the same adiabatic flame temperatures. The only properties relevant to flame propagation that are different are density and thermal conductivity, and these are accounted for by the thermal diffusivity (Equation 7). The study of He and Ar diluents serves to quantify the effect of thermal diffusivity in H_2-O_2 flame propagation.

The next level of complexity is introduced with N_2, a diatomic molecule with a greater heat capacity, which serves to lower the flame temperature. Since N_2 has the same thermal diffusivity as Ar, the effect on S_u of replacing Ar by N_2 can be linked directly to their relative roles as "heat sinks" in reducing flame temperature. Thus, the effect of flame cooling on burning velocity can also be quantified.

The next level of complexity is diluents that may have concurrent physical and chemical effects (i.e. non-inerts), H_2O and CO_2. In addition to having higher heat capacities than N_2, H_2O and CO_2 are both known to be highly effective catalysts in three-body radical recombinations, and participate to a degree in direct reactions with radicals in the flame. Once the contributions of flame cooling and thermal diffusivity to an observed effect are determined from experiments with He, Ar and N_2, the magnitude of the catalytic and kinetic effects of H_2O and CO_2 can be measured. These results are then analysed with a one-dimensional flame code.

Interpretation of diluent effects is greatly complicated by concurrent kinetic rate effects of changing H_2/O_2 equivalence ratios (ratio

of H_2/O_2 to the stoichiometric ratio). Recognizing this, care is taken in this study to determine relative effects of diluents only in the context of constant fuel equivalence ratio. The unique effects of equivalence ratio are studied separately. Excess H_2 and excess O_2 are treated strictly as diluents in a stoichiometric mixture. Then, effects on flame cooling and transport properties of the mixture are calculated and corrected using the same method proven valid for inert diluents. The remaining effect, due to changes in reaction rates, is then studied in isolation using the one-dimensional flame code.

To summarize, this work employs the systematic replacement of diluents in H_2-O_2 flames as a vehicle for eludicating fundamental mechanisms of flame propagation. This requires an accurate self-consistent data base of burning velocities for the many combinations of H_2-O_2 mixtures with the seven diluents.

5.2 PRELIMINARY

A considerable range of burning velocity measurements are undertaken in this study, from 14 $m \cdot s^{-1}$ for undiluted H_2-O_2 at 100°C, to less than 1 $m \cdot s^{-1}$ for highly diluted mixtures at room temperature. It is necessary to ensure that the method of measurement is reliable over the complete range. In the low to intermediate range of this study, extensive literature is available for the H_2-air system. Figure 8 shows that the present work with the 5 mm nozzle is in good agreement with the results of Edmonson and

Heap [46], using a 10.4 mm nozzle with particle tracking; Andrews and Bradley [47], using double kernel ignition in a closed vessel; France and Pritchard, using a 7 mm nozzle burner with LDA particle tracking [25]; and with the calculations of Warnatz [18]. Included also are the calculated burning velocities from the one-dimensional flame code used in this study. The code results are slightly high, which is reasonable, since the calculation is made adiabatically and a small heat loss is expected in a real flame, from radiation.

For the upper extreme of our range there are some published burning velocities of undiluted H_2-O_2 with which to compare. Figure 9 shows our values for undiluted H_2-O_2 compared with the results of Jahn (x 1.2) [21], the calculations of Warnatz [18], and the predictions of our one-dimensional flame code. Thus, our measurements are shown to be in agreement with published work over the complete range of the study.

5.3 MIXTURES WITH He, Ar, N_2 AND CO_2

Burning velocities were measured for H_2-O_2 mixtures containing the diluents He, Ar, N_2 and CO_2 at ambient temperature and pressure. Measurements were made for selected ratios of H_2-O_2 of 0.5:1 to 9:1 with each diluent over the range of diluent fractions that provided a stable flame. The results are summarized in Figures 10, 11 and 12 for lean, stoichiometric and rich mixtures, respectively.

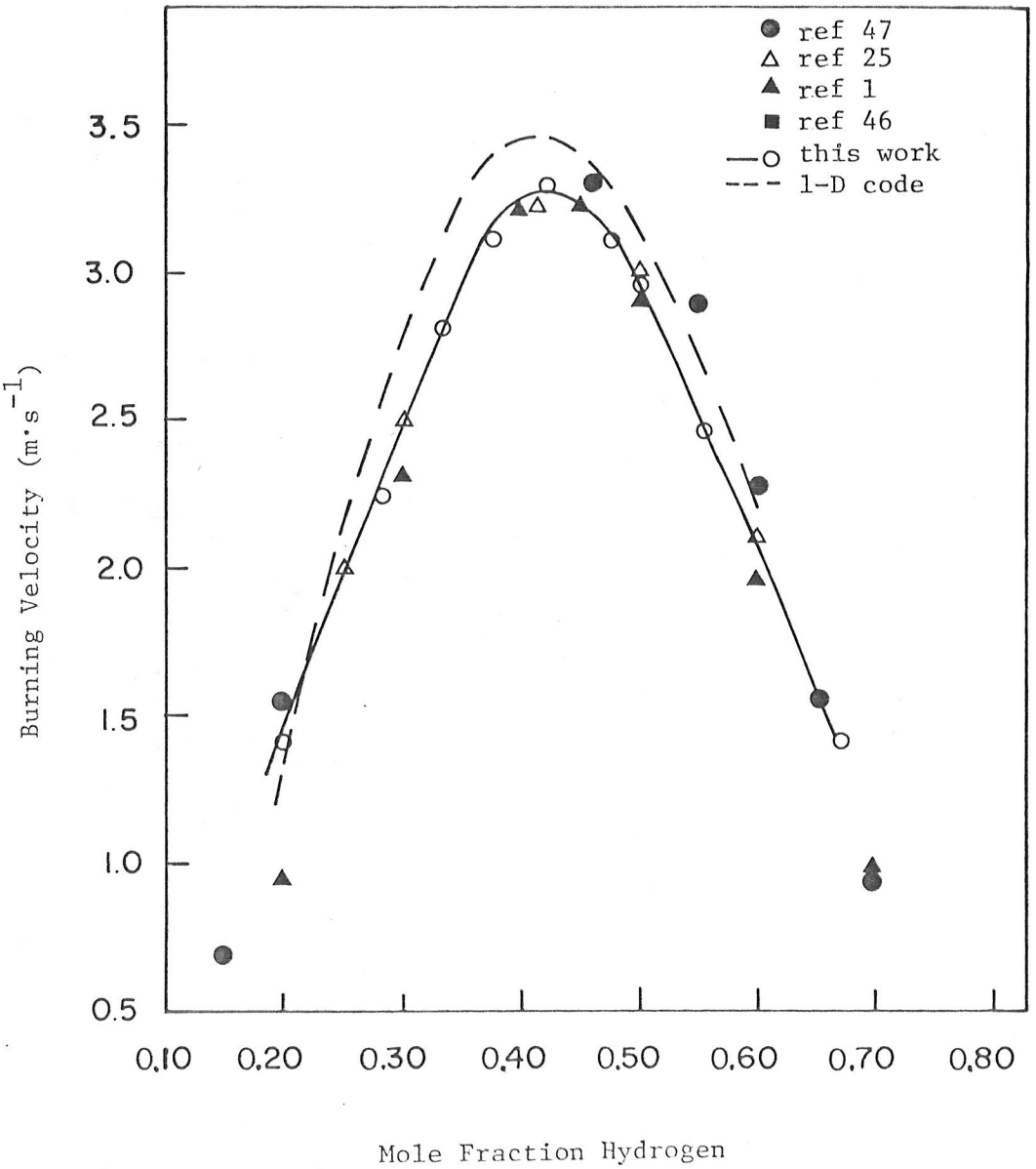

FIGURE 8: Burning velocities for H_2-air at 298 K

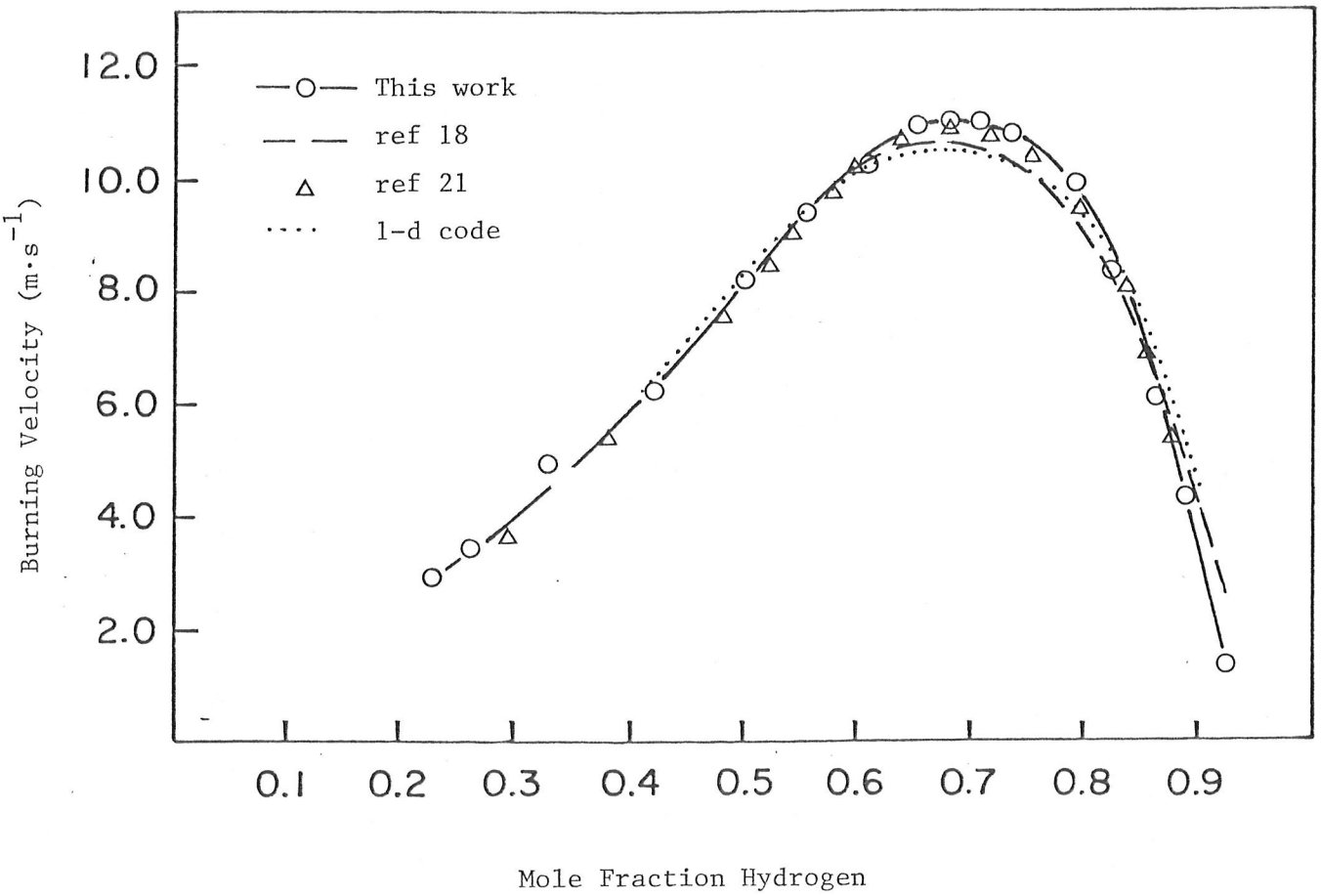

FIGURE 9: Burning velocities for H_2-O_2 at 298 K

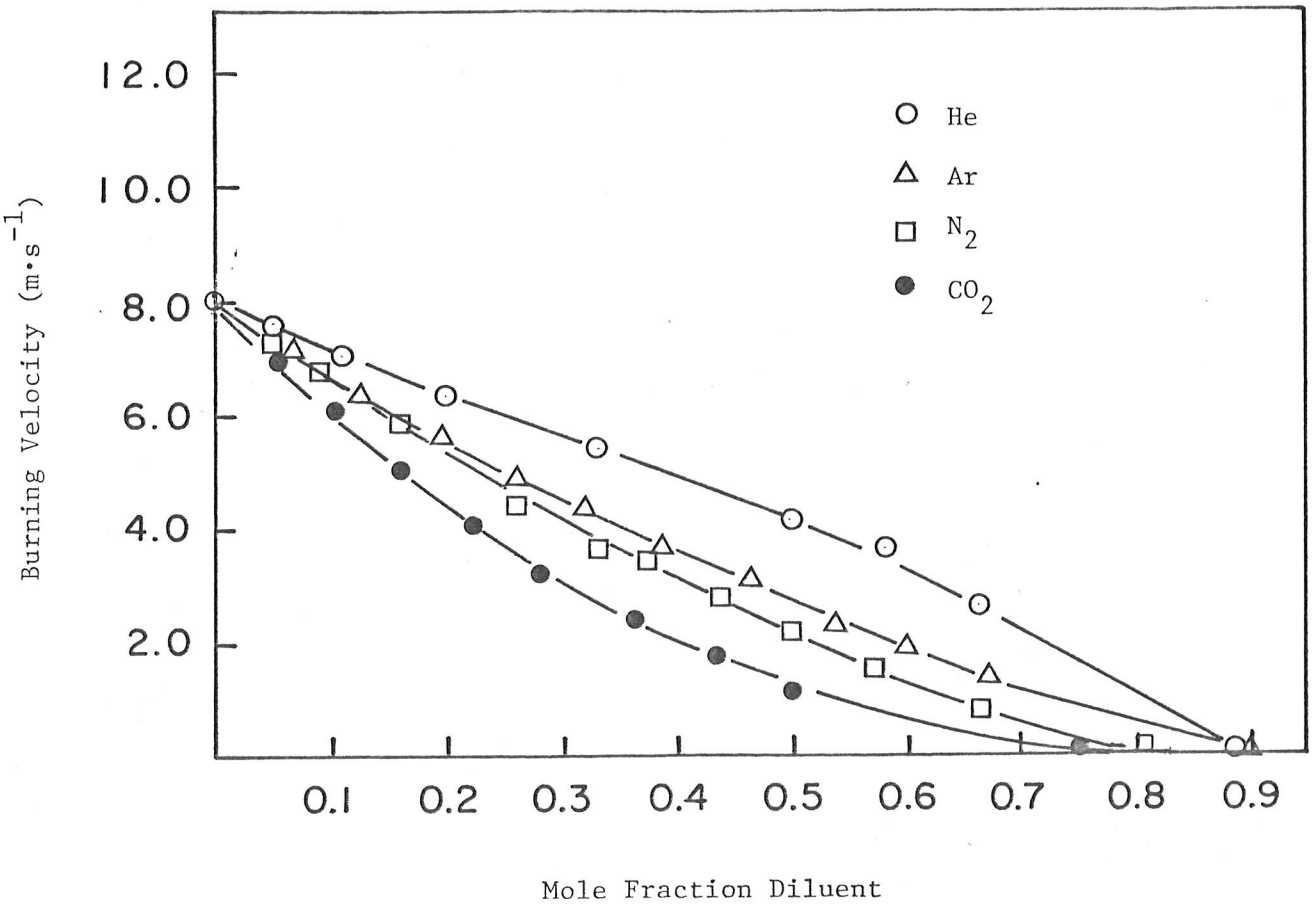

FIGURE 10: Burning velocities of 1:1 H_2-O_2 at 298 K with the diluents, He, Ar, N_2 and CO_2

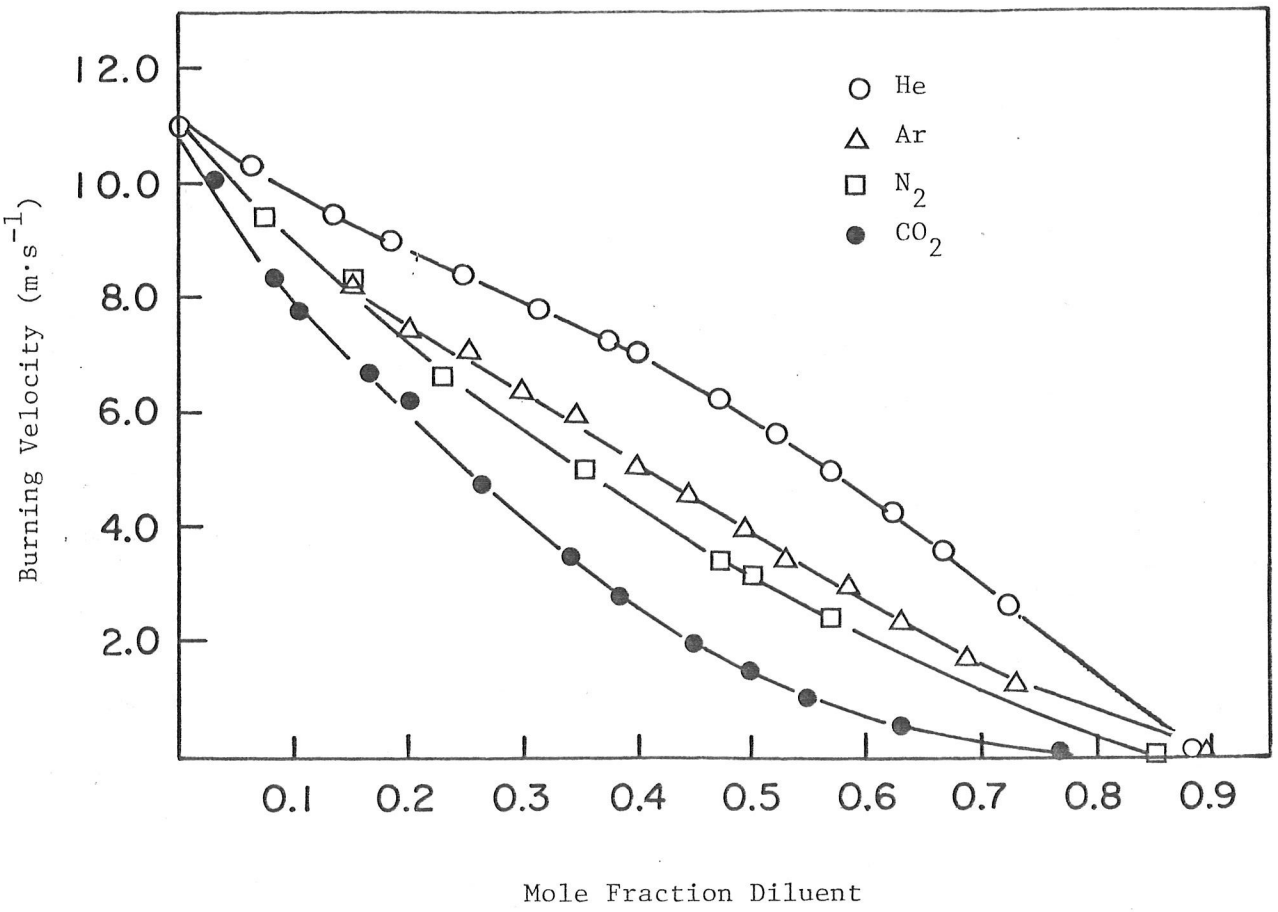

FIGURE 11: Burning velocities of 2:1 H_2-O_2 at 298 K with the diluents, He, Ar, N_2 and CO_2

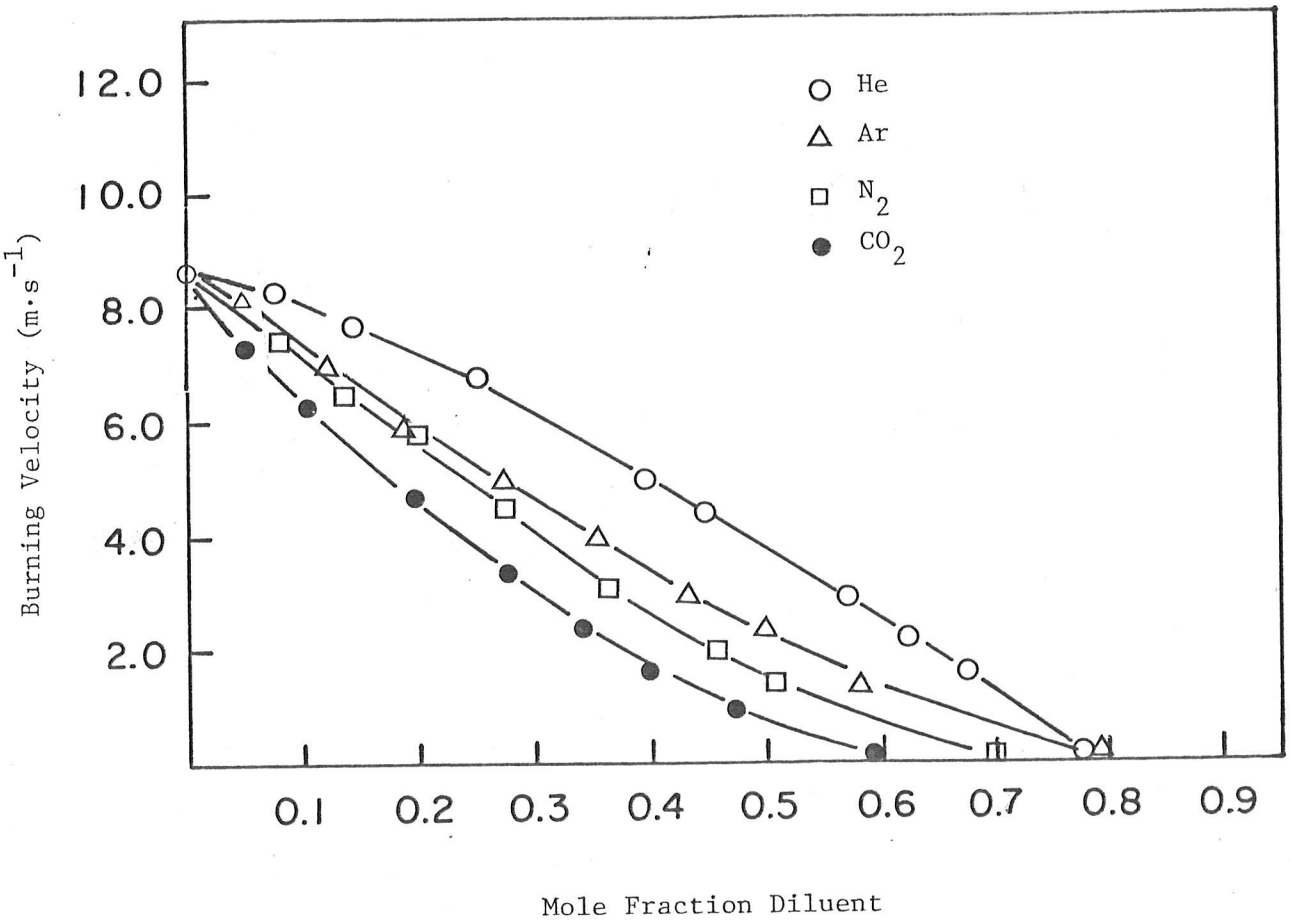

FIGURE 12: Burning velocities of 5:1 H_2-O_2 at 298 K with the diluents, He, Ar, N_2 and CO_2

A general result for all cases is, for a constant H_2-O_2 ratio, the burning velocity decreases with increasing fractions of diluent gas. The decrease extrapolates smoothly to intercept the x-axis at the diluent fraction independently measured [49] as the flammability limit for the mixture. This is generally predictable. As the diluent fraction increases, the burning velocity decreases as a natural consequence of there being less fuel per unit volume (i.e., less heat produced) and a greater fraction of the heat of combustion being required to bring the diluent to the flame temperature. Ultimately, the fuel becomes sufficiently dilute and the thermal load sufficiently great that the flame cannot sustain itself. This inerting diluent fraction is given the symbol X_L and is the point in the figures at zero burning velocity, taken from Kumar and Hollinger [49].

More important are the considerable differences in burning velocity for the same fraction of different diluents. The diluents reduce the burning velocity in the order $CO_2 > N_2 > Ar > He$, which is qualitatively consistent with previous work. The mechanisms causing these differences are examined in detail in Section 6.

5.4 EXCESS H_2 AND O_2

Excess oxygen was added as a diluent to a stoichiometric mixture of H_2-O_2. The results are shown in Figure 13 along with the results obtained by replacing the excess oxygen with nitrogen. This comparison is made because O_2 and N_2 have nearly identical thermal diffusivities and heat capacities so the higher burning velocities in mixtures with excess O_2 are

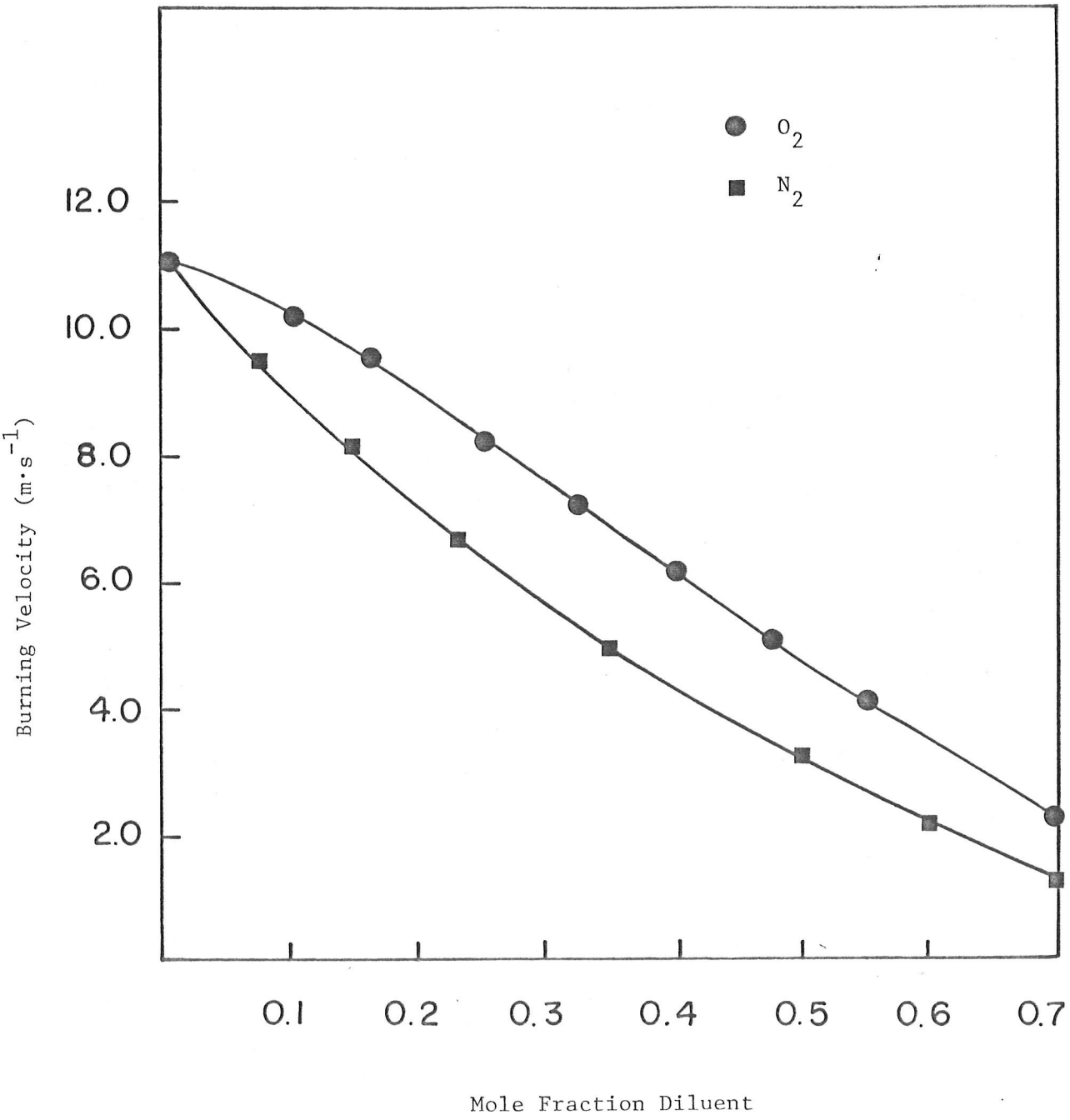

FIGURE 13: Burning velocities of 2:1 H_2-O_2 with N_2 diluent and with N_2 replaced by O_2

attributable to reaction kinetics effects. Similarly, excess hydrogen was added to a stoichiometric H_2-O_2 mixture and the burning velocities are compared in Figure 14 with corresponding mixtures containing He. These observations will be analysed in detail in Sections 6.5 and 6.8, with the aim of better understanding the nature of flame propagation in lean and rich flames.

5.5 MIXTURES WITH STEAM

Burning velocity measurements with steam diluent were made at 100°C for stoichiometric H_2-O_2 mixtures containing 0% to 70% steam. For comparison, burning velocities were also measured at 100°C for corresponding mixtures containing N_2 and CO_2. The results are shown in Figure 15. Steam appears unique among the inert diluents in that its effect on burning velocity is not consistent with its high heat capacity. This and other factors regarding the behaviour of steam diluent will be analysed later.

Because of the lack of data in the literature for burning velocities of H_2-air-steam mixtures, and given the relevance of this system to practical situations, measurements were made for mixtures of 20% to 65% hydrogen in air, containing up to 50% steam. This extends previously published data [30] which were limited to 15% steam. The burning velocities of the H_2-air-steam mixtures are plotted in Figure 16.

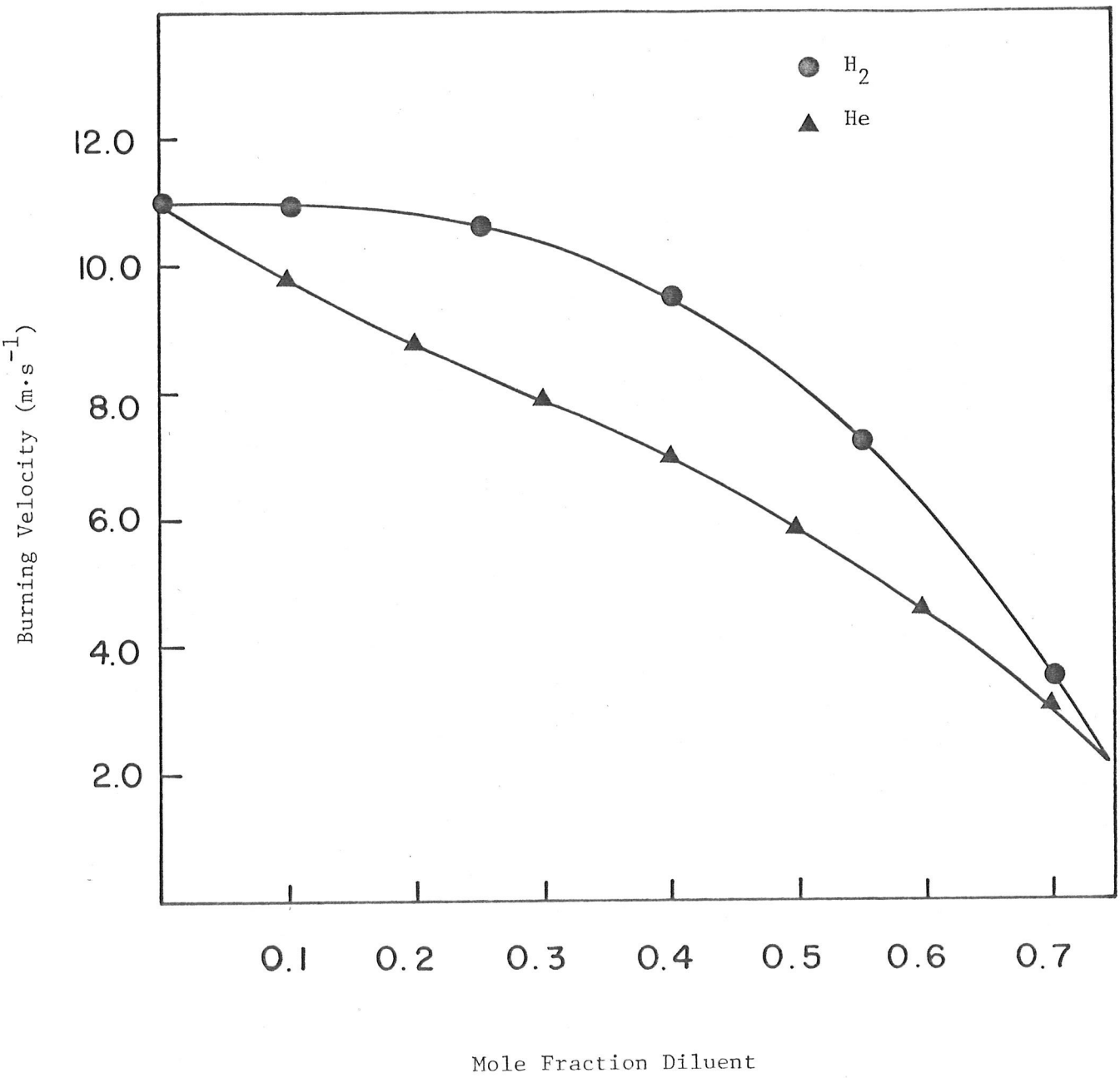

FIGURE 14: Burning velocities of 2:1 H_2-O_2 with He diluent and with He replaced by H_2

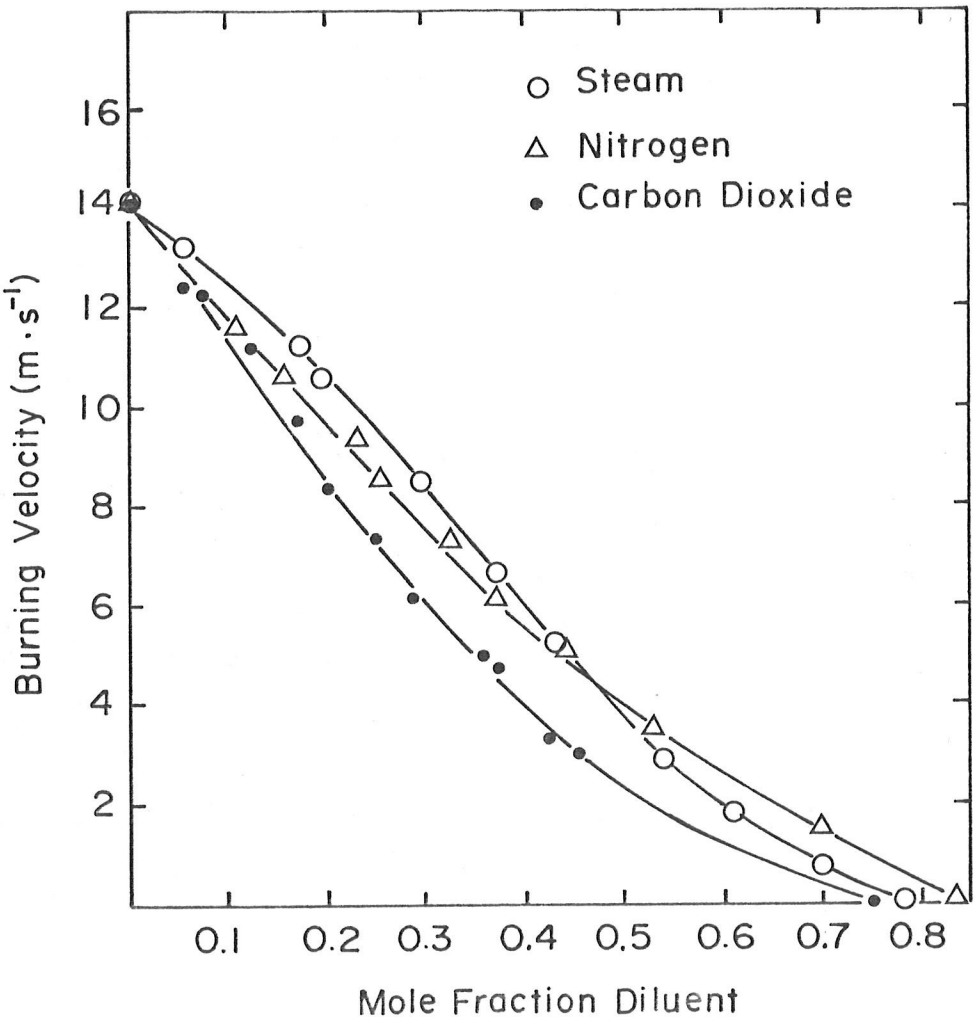

FIGURE 15: Burning velocities of 2:1 H_2-O_2 at 273 K with the diluents N_2, CO_2 and steam

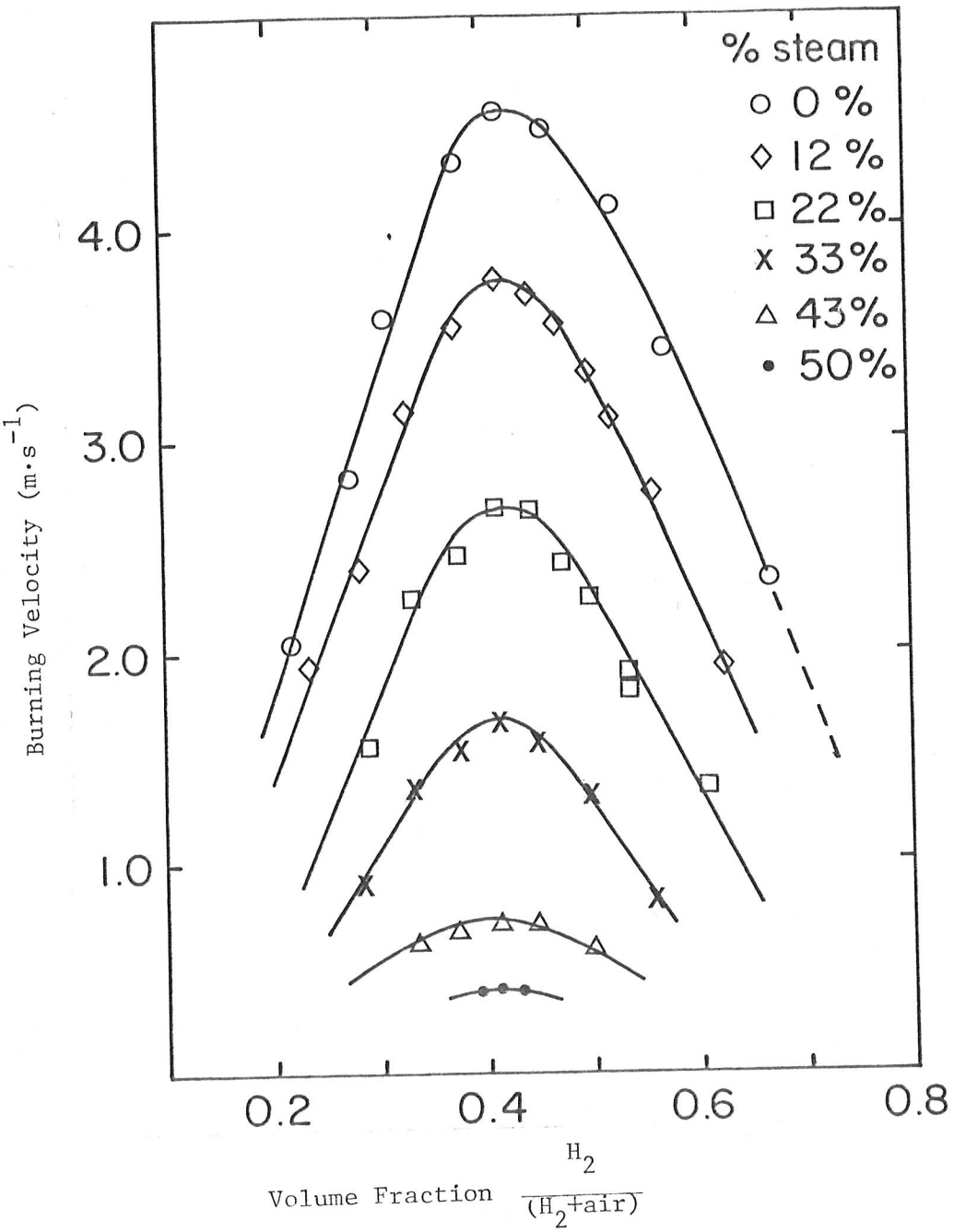

FIGURE 16: Burning velocities of H_2-air-steam at 373 K

5.6 DEUTERIUM FLAMES

The isotope effect on burning velocity was determined by measuring burning velocities for selected mixtures containing Deuterium (D_2). Burning velocities were measured for mixtures of D_2/air, D_2/O_2 and D_2/O_2/He. The results are shown in Figures 17, 18 and 19, respectively, with the corresponding results from H_2 flames for comparison. In all cases, replacement of H_2 with D_2 resulted in a lowering of the burning velocity. The ratio, $\frac{S_u(H_2)}{S_u(D_2)}$, is 1.36 for undiluted stoichiometric mixtures and decreases to about 1.26 with added diluent.

6. ANALYSIS AND DISCUSSION

6.1 GENERAL METHOD

In the following sections, the effect of each diluent on the burning velocity is analysed in detail in order of increasing complexity of effect. Analysis consists of first assessing the effect of the diluent in terms of the general flame equation.

$$S_u = \underbrace{\left(\frac{\lambda}{\rho C_p}\right)^{\frac{1}{2}}}_{\text{transport term}} \cdot \underbrace{(\text{reaction rate})^{\frac{1}{2}}}_{\text{rate term}} \qquad (6)$$

Replacement of one kinetically inert diluent for another will alter the transport term if the diluents differ in density, heat capacity or thermal

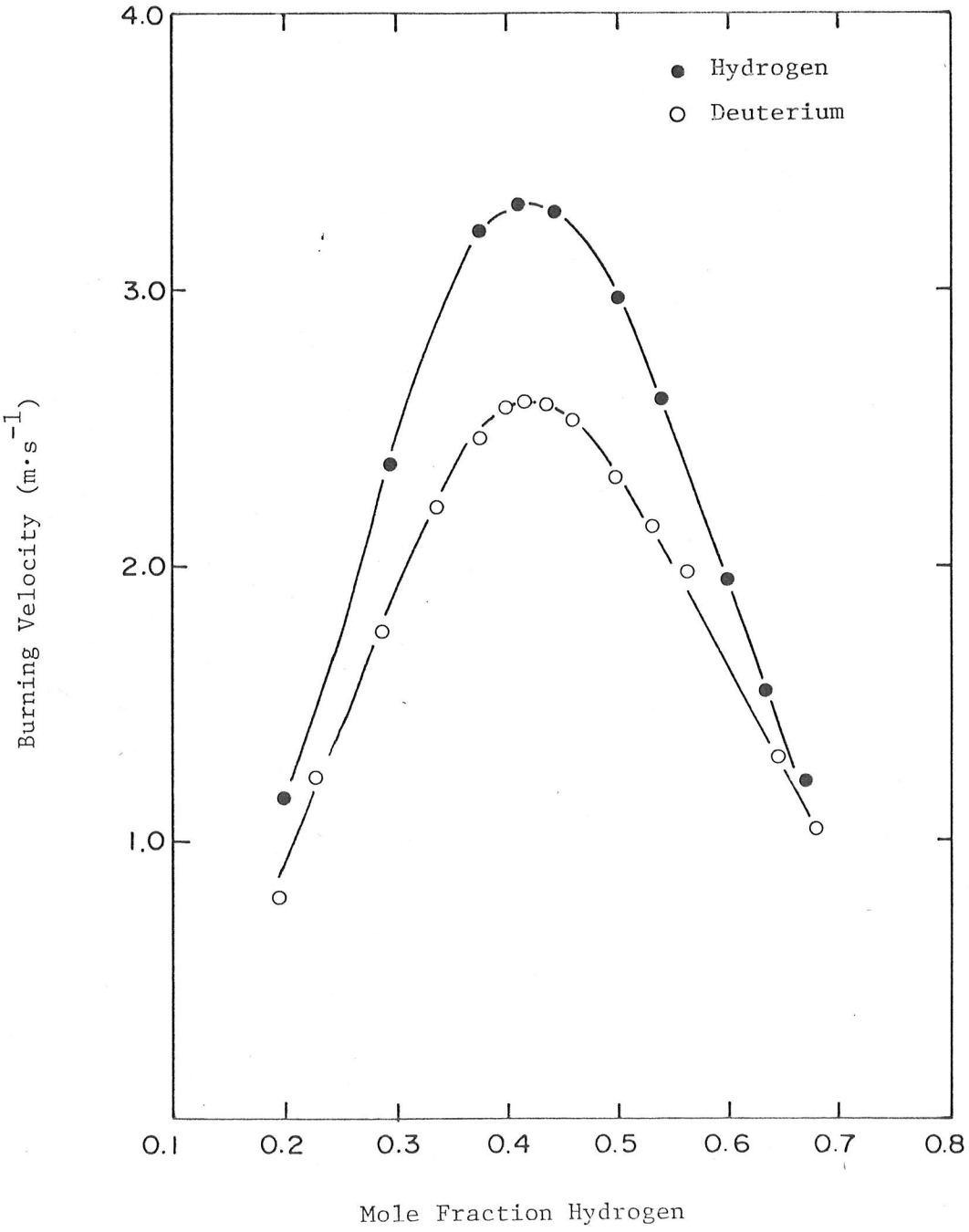

FIGURE 17: Burning velocities of D_2-air and H_2-air at 298 K

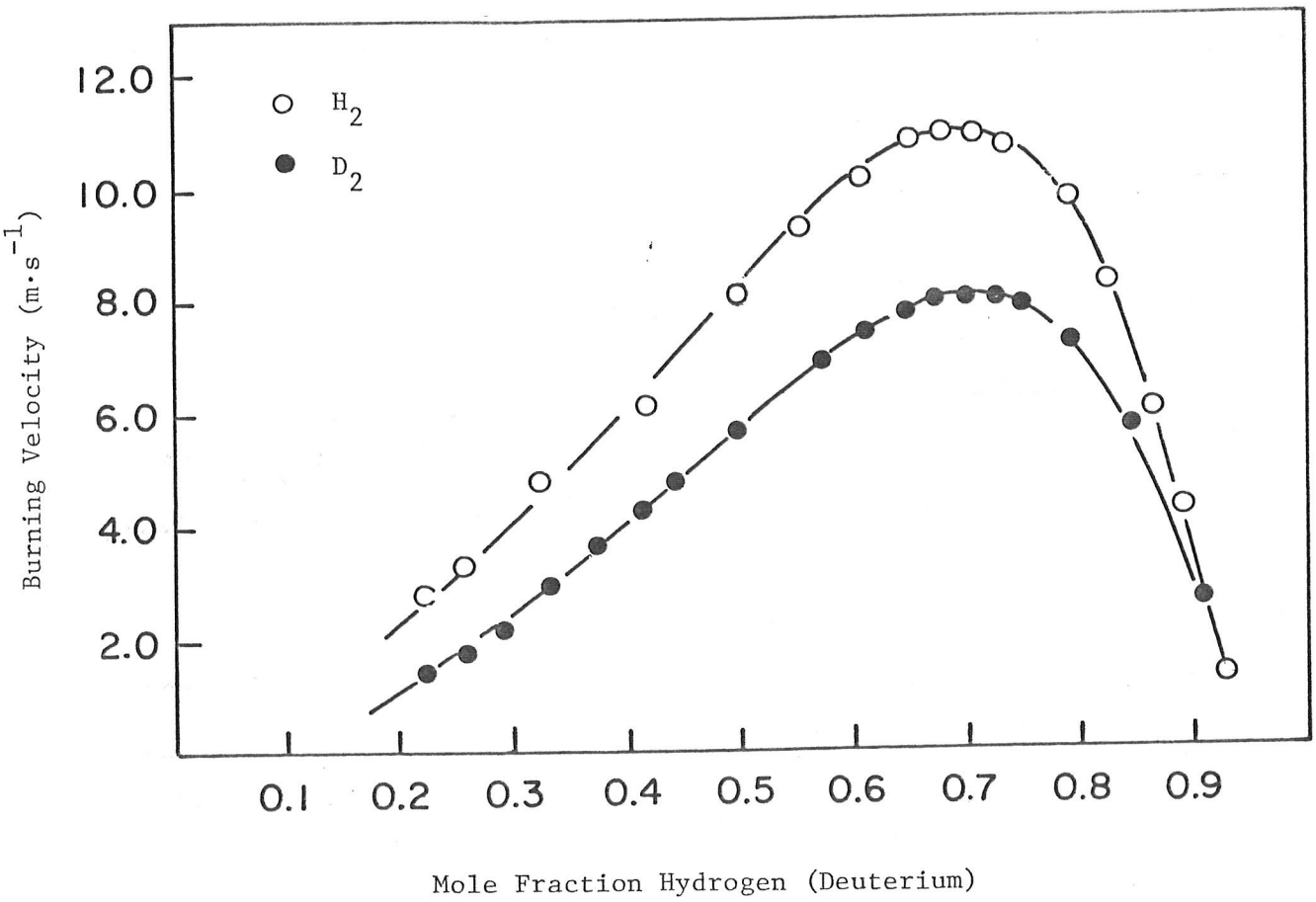

FIGURE 18: Burning velocities of D_2-O_2 and H_2-O_2 at 298 K

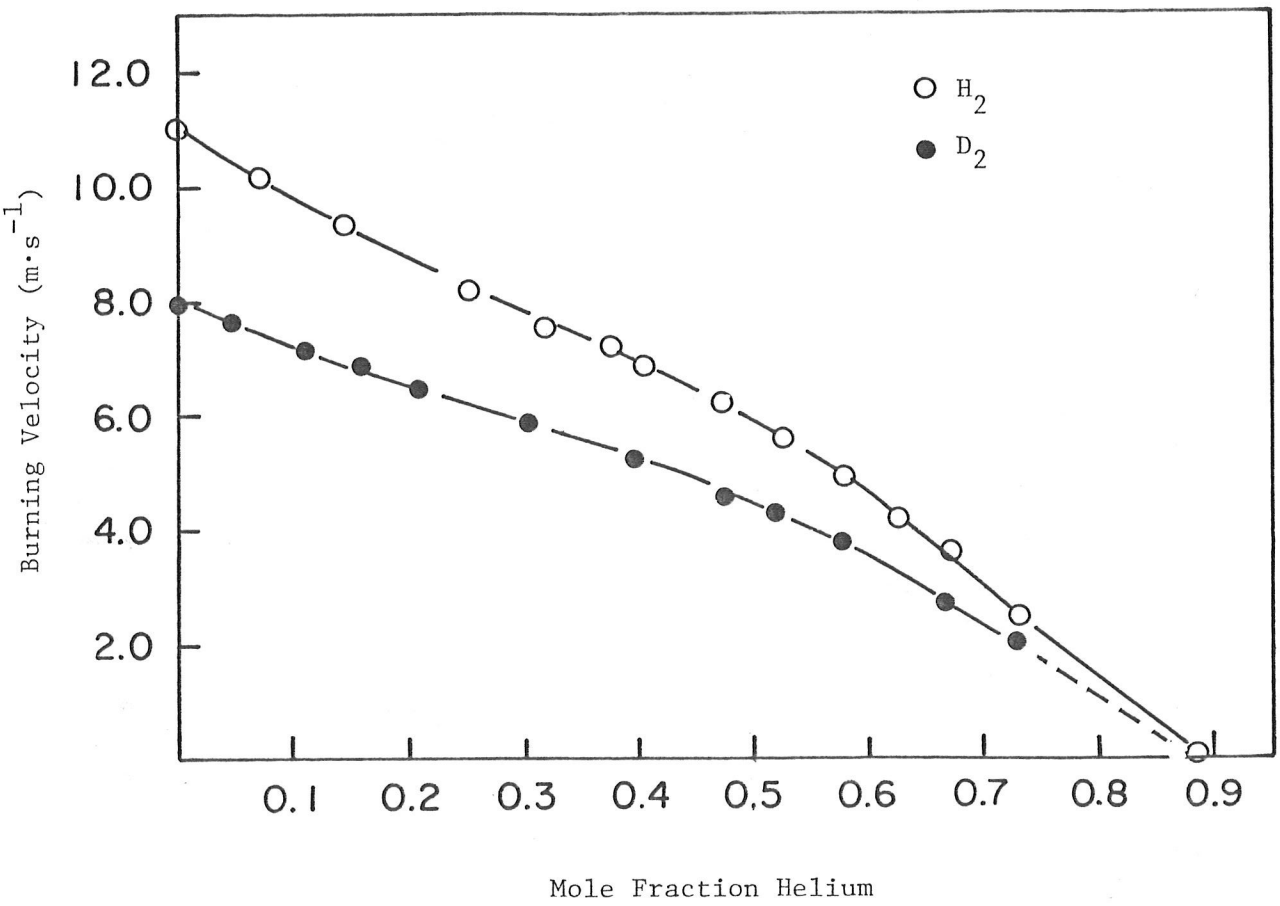

FIGURE 19: Burning velocities of 2:1 D_2-O_2 and 2:1 H_2-O_2 with He diluent

conductivity. Diluents differing in heat capacity will also change the rate term to the extent that they act as a heat sink, reducing flame temperature. Non-inert diluents produce the usual changes to the transport term and affect the rate term through flame temperature and, in addition, through direct or catalytic participation in reaction kinetics.

The transport term, represented by the thermal diffusivity, α, is calculated in detail for each mixture containing diluent and normalized for zero diluent to account for the contribution of the added diluent to the transport term.

In calculating α for the mixture, C_p and ρ are derived by averaging the values for individual gases.

$$C_p \text{ (mix)} = \Sigma C_{pi} Y_i \tag{13}$$

Y_i = mass fraction = $\dfrac{X_i M_i}{\Sigma X_i M_i}$

X_i = mole fraction

M = molecular weight

$\rho_{mix} = \Sigma \rho_i X_i$

Estimation of thermal conductivity, λ, is made by the method of Mason and Saxena [50].

$$\lambda(\text{mix}) = \sum_{j=i}^{n} \frac{X_i \lambda_i}{\sum_{j=1}^{n} X_i \phi_{ij}} \tag{14}$$

where

$$\phi_{ij} = \frac{1}{\sqrt{8}} \left(1 + \frac{M_i}{M_j}\right)^{-\frac{1}{2}} \left[1 + \left(\frac{\mu_i}{\mu_j}\right)^{\frac{1}{2}} \left(\frac{M_j}{M_i}\right)^{\frac{1}{4}}\right]^2 \qquad (15)$$

μ = viscosity

Table 1 lists the values of the constants used in the calculation. Calculated thermal diffusivities are tabulated in Appendix B.

The calculated values of thermal diffusivity for each mixture containing diluent, α, and for the pure fuel/oxidant, α_o, are combined to give the dimensionless quantity,

$$\left(\frac{\alpha_o}{\alpha}\right) = \text{relative thermal diffusivity} \qquad (16)$$

Relative thermal diffusivity is a measure of the contribution of any added diluent to the transport term of Equation (6), relative to the undiluted mixture. If the measured burning velocities are multiplied by the square root of the relative thermal diffusivities of the mixture, then the effect of the diluent on thermal diffusivity is removed from the burning velocities. Thus differences between corrected burning velocities for the various diluents can be attributed to the rate term.

Thus identified, rate effects are analysed by use of the one-dimensional flame code by testing the sensitivity of calculated burning velocities to changes in relevant rate parameters.

6.2 EFFECT OF HELIUM AND ARGON

The burning velocities of H_2-O_2 mixtures containing He are as much as 60% greater than for corresponding mixtures containing Ar (see Figures 10, 11 and 12). The two diluents are kinetically inert, have identical molar heat capacities, and, as a result, have the same adiabatic flame temperature [6]. They do, however, differ considerably in density and thermal conductivity and, thus, in thermal diffusivities. Therefore, the He and Ar experiments serve to test the premise that inert diluents affect burning velocity only through their effect on heat transport properties of the gas mixture, as represented by the thermal diffusivity.

The measured burning velocities were corrected for changes by the diluent to the thermal diffusivity by the factor $(\frac{\alpha_o}{\alpha})^{\frac{1}{2}}$, and were replotted. The result is shown in Figures 20, 21 and 22 along with the prediction of a correlation equation from Section 6.4, to follow. In each case (for lean, rich and stoichiometric flames), applying the transport correction produced an identical result (within the error of the original measurements) for He and Ar. Furthermore, the result showed a linear dependance of $S_u(\frac{\alpha_o}{\alpha})^{\frac{1}{2}}$ with added diluent fraction. The x-intercept of the straight line was unchanged at the diluent fraction corresponding to the flammability limit for downward propagation, as measured by Kumar and Hollinger [49].

Thus, the differences in burning velocity between He and Ar diluents is attributable entirely to differences in the thermal diffusivities of the mixture. The factor $(\frac{\alpha_o}{\alpha})^{\frac{1}{2}}$ is shown to accommodate an order of

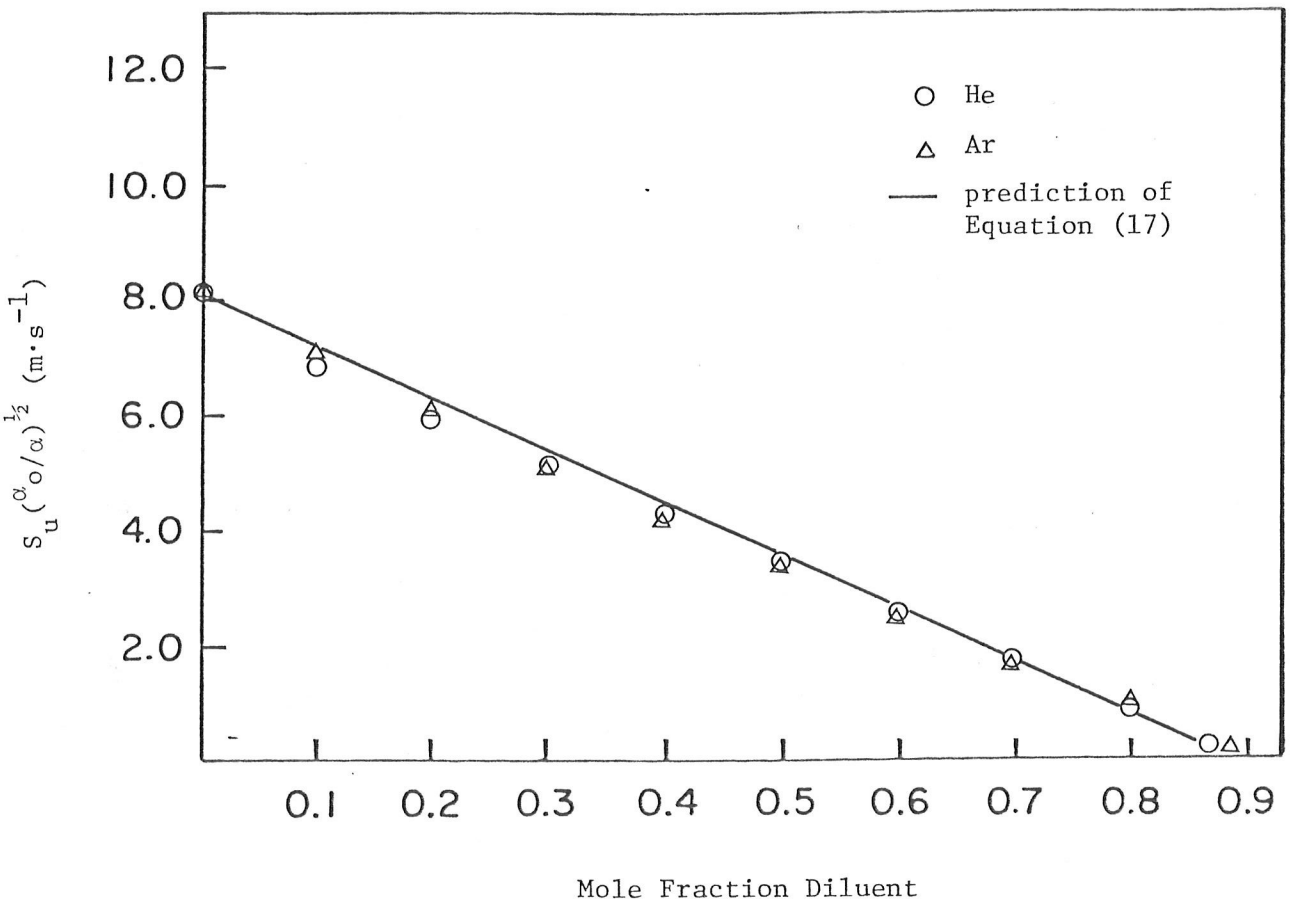

FIGURE 20: Burning velocities of 1:1 H_2-O_2 with He and Ar diluents, corrected for relative thermal diffusivity

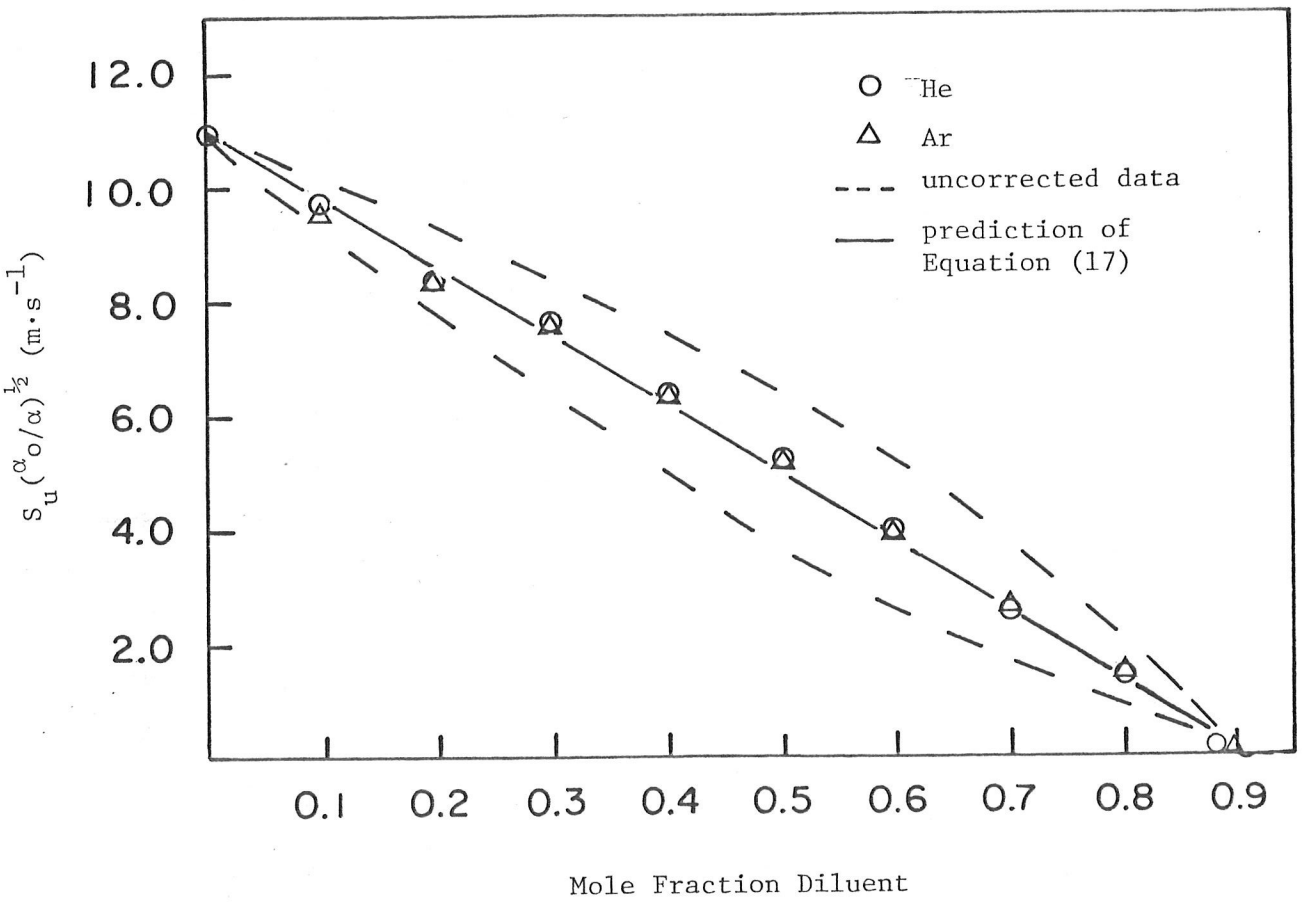

FIGURE 21: Burning velocities of 2:1 H_2-O_2 with He and Ar diluents, corrected for relative thermal diffusivity

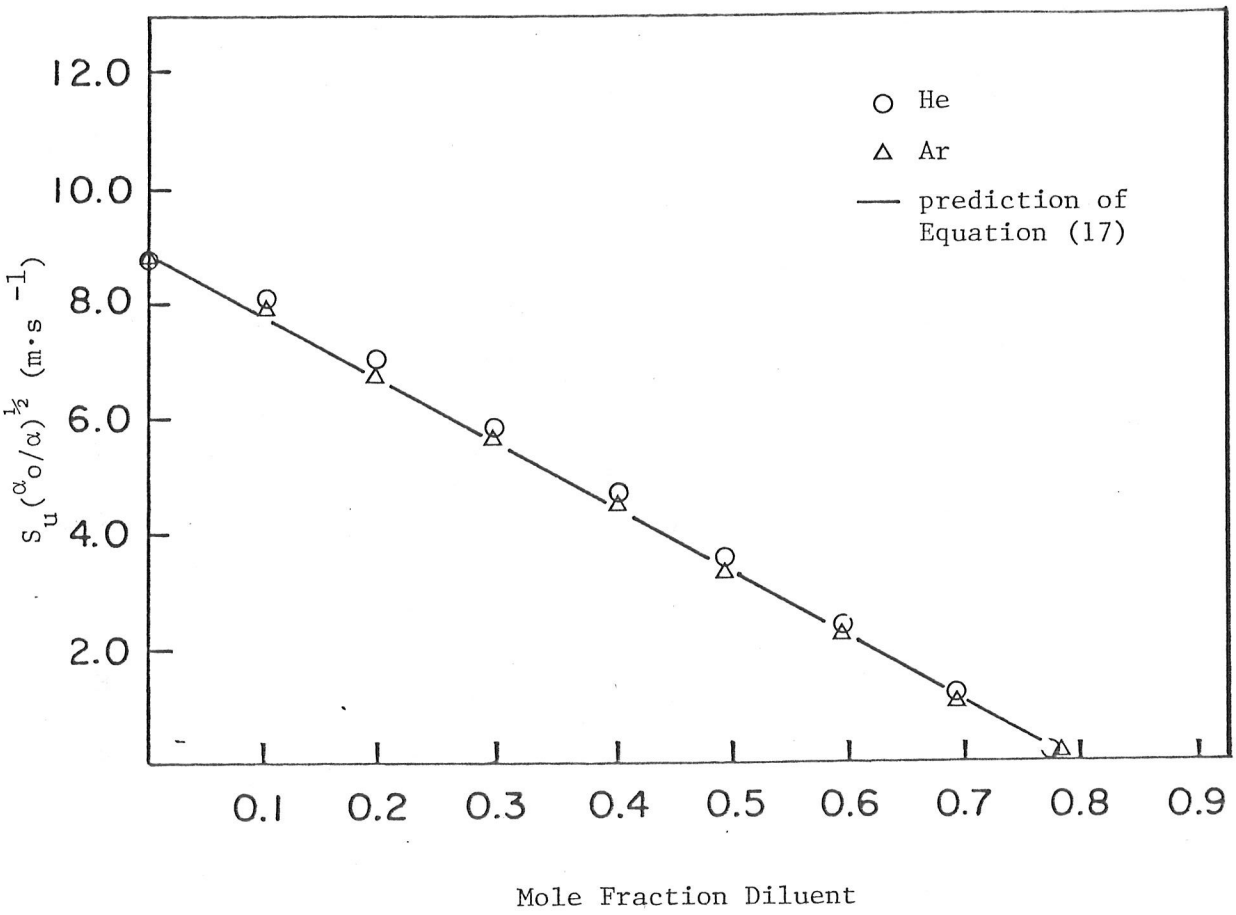

FIGURE 22: Burning velocities of 5:1 H_2-O_2 with He and Ar diluents, corrected for relative thermal diffusivity

magnitude difference in density and thermal conductivity between He and Ar, which is as great a range as occurs between any of the gases in this study. Therefore it is assumed that the relative thermal diffusivity, as calculated above, reliably represents the contribution of added diluent to the transport properties of the gas mixture, to the extent that it affects the burning velocity.

6.3 THE EFFECT OF NITROGEN

N_2 and Ar have nearly identical thermal diffusivities. This enables differences in their effects on burning velocities to be interpreted in terms of different flame temperatures arising from their different heat capacities.

The measured burning velocities for N_2 diluent were corrected for relative thermal diffusivity in the same way as the burning velocities for the He and Ar diluents. The resulting plots of $S_u(\frac{\alpha_o}{\alpha})^{\frac{1}{2}}$ versus mole fraction diluent are shown in Figures 23, 24 and 25. As was the case for He and Ar, the correction resulted in a straight line plot that intercepted the x-axis at the mole fraction of N_2 corresponding to the flammability limit for downward propagation, X_L. The difference between N_2 and the noble gases is that X_L occurs at lower fractions of diluent than for the noble gases. This is reasonable since flammability limits are strongly dependent on the heat capacity of the gas mixture [49] and mixtures with N_2 have a higher heat capacity than the equivalent mixtures containing noble gases. What is important is that a change in the heat capacity of the diluent only changes the slope of the transport-corrected plot of burning velocity versus diluent fraction.

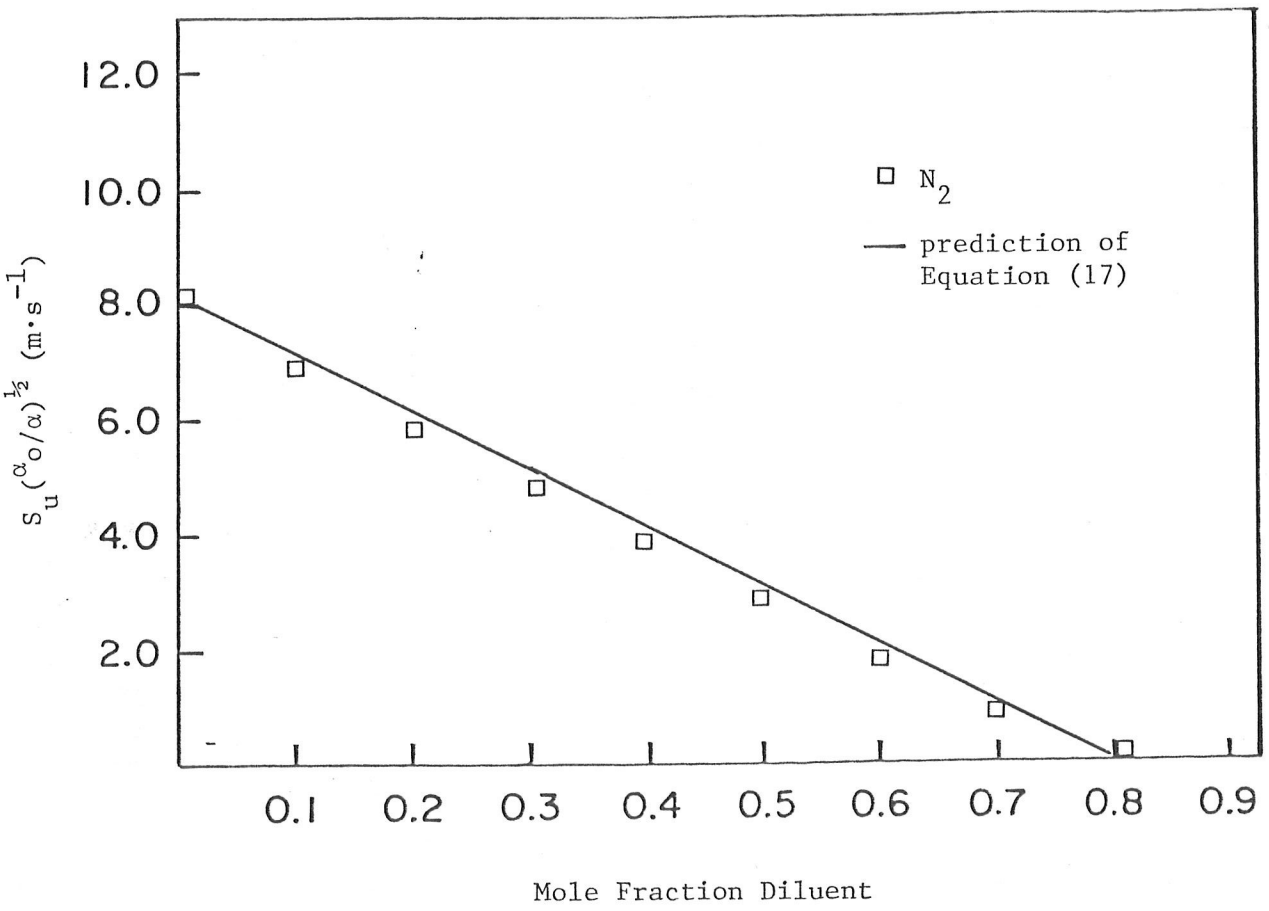

FIGURE 23: Burning velocities of 1:1 H_2-O_2 with N_2 diluent, corrected for relative thermal diffusivity

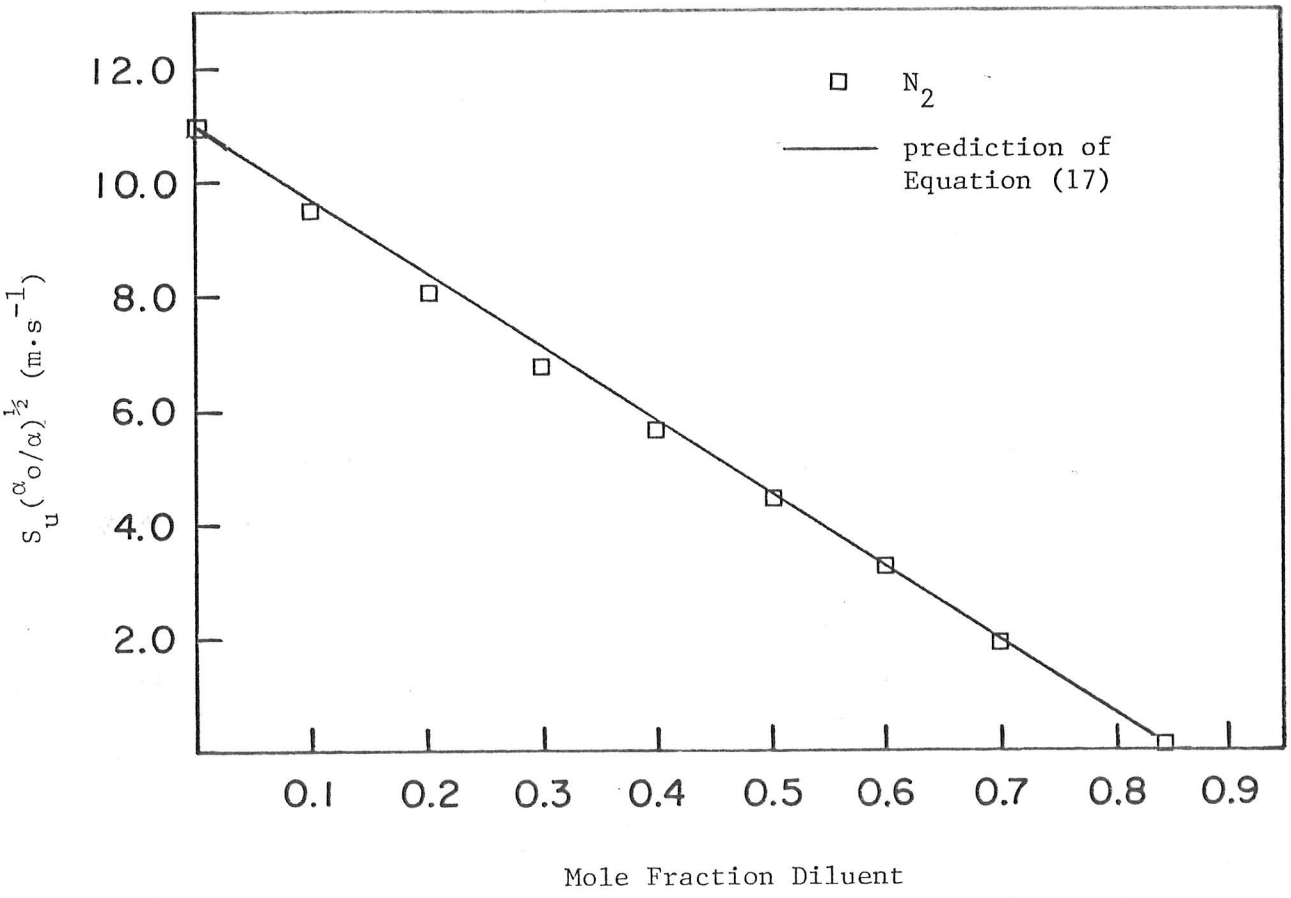

FIGURE 24: Burning velocities of 2:1 H_2-O_2 with N_2 diluent, corrected for relative thermal diffusivity

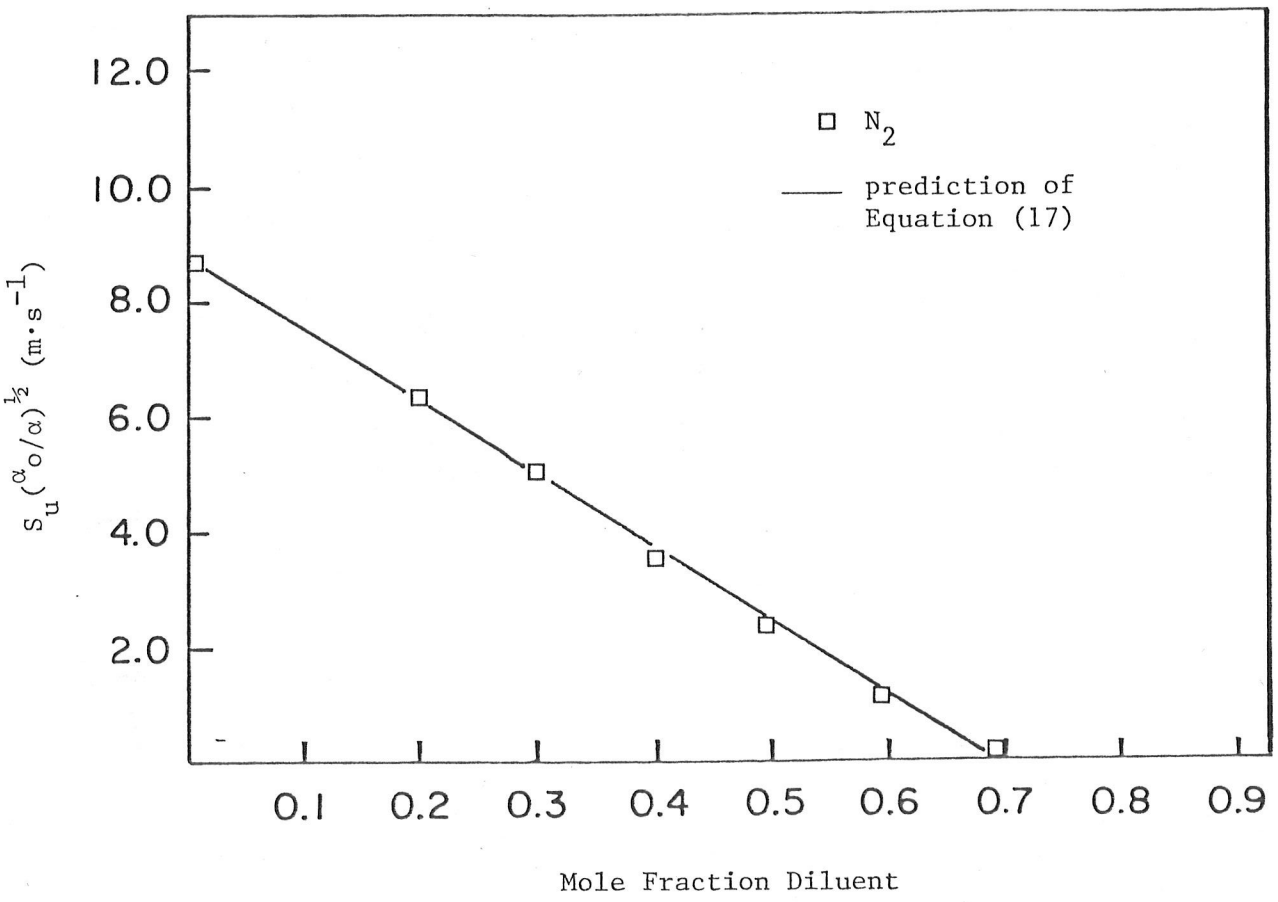

FIGURE 25: Burning velocities of 5:1 H_2-O_2 with N_2 diluent, corrected for relative thermal diffusivity

6.4 CORRELATION EQUATION FOR INERT DILUENTS

The good agreement between the intercepts of the $S_u(\frac{\alpha_o}{\alpha})^{\frac{1}{2}}$ plots and the independently measured inerting diluent concentrations, X_L, along with the linear behavior of $S_u(\frac{\alpha_o}{\alpha})^{\frac{1}{2}}$ with diluent concentration, together form the basis of a useful correlation for predicting burning velocities. Given the burning velocity for the pure fuel/oxidant, S_{u_o}, and the inerting diluent concentration X_L, the burning velocity for any fraction of diluent (X_{dil}) can be estimated by,

$$S_u(\frac{\alpha_o}{\alpha})^{\frac{1}{2}} = S_{u_o} - X_{dil}(\frac{S_{u_o}}{X_L}) \qquad (17)$$

S_{u_o} is obtained directly from Figure 9. Data for the inerting diluent fraction X_L are provided in Appendix C. Values for α and α_o were calculated for the temperature of the unburnt gas mixture, (298 K) and are given in Appendix B.

The significance of the S_{u_o} term in Equation (17) deserves mention. From the data presented in Figures 14 and 15 it was observed that excess H_2 and excess O_2 did not behave as simple diluents. Excess H_2 and O_2 accelerate the burning velocity through complex mechanisms in the rate term. This is a point that has often been overlooked in previous attempts to correlate burning velocities with thermal properties [22,23,24,27]. S_{u_o}, which is the burning velocity of the undiluted H_2-O_2 mixture, already contains the kinetic effect of the equivalence ratio on burning velocity. The specific effects of excess H_2 and excess O_2 are studied separately in the following sections.

Equation (17) provides a simple means of predicting the burning velocity of H_2-O_2 with chemically inert diluents. Notably, Equation (17) correctly predicts the full range of H_2-air burning velocities. However the present purpose is to correct for the physical effects of a diluent on burning velocity in order that chemical kinetic effects can be identified for the non-inert diluents to follow.

At this point it is possible to anticipate that the simple correlation of Equation (17) will overpredict burning velocities for mixtures with diluents that have a strong temperature dependence of the heat capacity. Figure 26 shows the heat capacities of molecules used in this study, as a function of temperature [51]. The flammability limits that are correlated with burning velocity in Equation (17) are determined largely by the heat capacity of the diluent at the temperature of the flame near the flammability limit, which is a relatively low temperature (typically ~ 700 K - 1000 K). The heat capacities of the diluents that follow the correlation (He, Ar and N_2) do not have a significant temperature dependence. However, the heat capacities for CO_2 and steam increase with temperature, making these molecules more effective heat sinks in a high temperature, propagating flame than at the relatively low temperature flammability limit used in the correlation. This will be discussed further in the following Sections 6.6 and 6.7.

6.5 EFFECT OF EXCESS O_2

N_2, as a diluent, affects the burning velocity in an "ideal" way; that is, its behavior can be predicted by Equation (17). N_2 and O_2 have

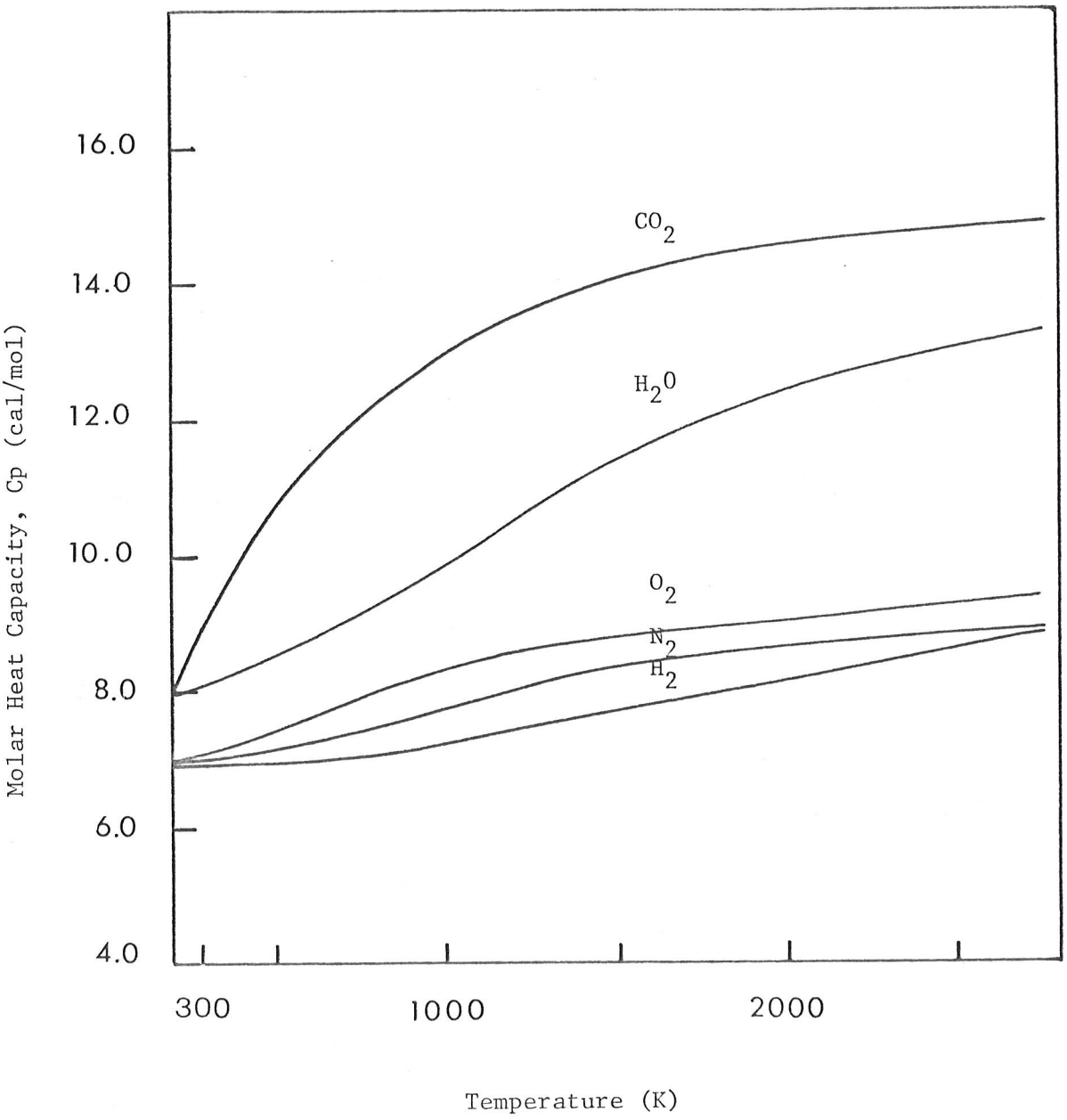

FIGURE 26: Molar heat capacities of combustion gases as a function of temperature [51]

nearly identical C_p, λ and ρ, so replacement of N_2 diluent with O_2 in a stoichiometric mixture will not change the thermal diffusivity or the adiabatic flame temperature significantly. However, as shown in Figure 13, replacement of N_2 by excess O_2 resulted in a considerable increase in the burning velocity. In the stoichiometric mixture the burning velocity increased from 6.5 $m \cdot s^{-1}$ to 8.3 $m \cdot s^{-1}$, when 25% N_2 was replaced with 25% excess O_2. This is a suitable situation to test the assumption that departures from the predicted behavior of Equation (17) arise through participation of the diluent in chemical reactions. Furthermore, the case of N_2 and O_2 diluents is independent of any assumptions contained in the derivation of Equation (17) because N_2 and O_2 are nearly identical for the quantities used in the calculation.

Molecular oxygen participates directly in two reactions in the reaction scheme in Table 2, reactions R3 and R11.

$$H + O_2 \rightarrow OH + O \qquad (R3)$$

$$H + O_2 \rightarrow HO_2 + M \qquad (R11)$$

Reaction R3 is a chain-branching reaction with a high activation energy, producing O and OH atoms required for reactions R1 and R5, and forms the initiating step for the high-temperature oxidation process. Thus, reaction R3 is primarily a radical source. Reaction R11 initiates the low temperature, heat-releasing oxidation process. Reaction R11 is exothermic by about 200 kJ/mol and the subsequent reactions of HO_2 in reactions R12 to R15 are also exothermic by a similar amount [15]. Thus, reaction R11 is primarily a heat source. Both reactions R3 and R11 are likely to be important.

The rate equation for reaction R3 is

$$\text{rate} = k_3 [O_2] [H\bullet]$$

Replacing N_2 with O_2 in a mixture containing 50% H_2 + 25% O_2 + 25% N_2 will double $[O_2]$ in the mixture, and effectively double the rate of reaction R3. If, instead, k_3 is doubled, the rate will also be doubled.

The rate equation for reaction R11 is,

$$\text{rate} = k_{11} [O_2] [H] [M]$$
$$\text{where} \quad [M] = [H_2] + 6 [H_2O] + 0.4 [O_2] + 0.4 [N_2]$$

Exchanging O_2 and N_2 leaves [M] unchanged since O_2 and N_2 have the same third body efficiency coefficients (Table 4). The effect of doubling $[O_2]$ (i.e., replacing N_2) will result in a doubling of the rate, as for reaction R3. Similarly, doubling k_{11} will have the same effect as doubling $[O_2]$.

Four experiments were done with the one-dimensional flame code. First, combustion of the mixture containing 50% H_2 + 25% O_2 + 25% N_2 was analysed using the rate parameters in Table 2. Next, the experiment was repeated with the N_2 replaced by O_2. The result, runs 1 and 2 of Table 5, was an increase in burning velocity from 6.8 $m \cdot s^{-1}$ to 8.3 $m \cdot s^{-1}$, in good relative agreement with the values 6.5 $m \cdot s^{-1}$ and 8.1 $m \cdot s^{-1}$ observed experimentally.

TABLE 5

SUMMARY OF THE ONE DIMENSIONAL FLAME CODE EXPERIMENTS

Code Run	Mixture Composition	Variable /control	S_u ($m \cdot s^{-1}$) Code	Exp.	T(K)* at 0.012 cm	Ta(K)**	$\dot{Q}^{***}_{max}$	Location of $\dot{Q}$ max (cm)	Maximum species mass fractions HO_2	H	O	OH	Initial Temperature T_i
1	$0.5\ H_2 + 0.25\ O_2 + 0.25\ N_2$	control	6.8	6.5	1150	2890	0.081	0.016	0.0020	0.007	0.034	0.043	298
2	$0.5\ H_2 + 0.5\ O_2$	control	8.3	8.1	1500	2915	0.150	0.012	0.0040	0.005	0.076	0.090	298
3	$0.5\ H_2 + 0.25\ O_2 + 0.25\ N_2$	$k_3 \times 2$	7.4	-	1220	2890	0.092	0.014	0.0020	0.007	0.046	0.049	298
4	$0.5\ H_2 + 0.25\ O_2 + 0.25\ N_2$	$k_3 \times 2$ $k_{11} \times 2$	8.2	-	1440	2890	0.125	0.010	0.0034	0.0067	0.045	0.052	298
5	$0.5\ H_2 + 0.25\ O_2 + 0.25\ N_2$	control	8.9	8.4	1100	2904	0.070	0.016	0.0017	0.007	0.032	0.063	373
6	$0.5\ H_2 + 0.25\ O_2 + 0.25\ H_2O$	control	9.8	9.3	1320	2801	0.080	0.0012	0.0052	0.0065	0.019	0.070	373
7	$0.5\ H_2 + 0.25\ O_2 + 0.25\ H_2O$	m_{H_2O}=0.4	7.8	-	950	2801	0.060	0.014	0.0020	0.010	0.037	0.036	373
8	$0.5\ H_2 + 0.25\ O_2 + 0.25\ H_2O$	m_{H_2O}=0.4 $k_{11} \times 4$	9.9	-	1320	2801	0.074	0.010	0.0043	0.0082	0.035	0.059	373
9	$0.8\ H_2 + 0.2\ O_2$	control	8.7	9.5	1030	2831	0.098	0.018	0.0043	0.023	0.024	0.035	298
10	$0.8\ H_2 + 0.2\ O_2$	$k_1 \times 2$ $k_5 \times 2$	9.7	-	1080	2831	0.114	0.016	0.0044	0.026	0.014	0.022	298

* T at 0.012 cm is the temperature at an arbitrary 0.012 cm from the unburnt gas, for comparative use. A greater temperature, here, is an indication of a steeper temperature gradient.

** Ta is the final adiabatic flame temperature calculated using a code from NASA [52].

*** $\dot{Q}$ is the net volumetric heat release rate normalized with enthalpy and time.

The next experiment, run 3 in Table 5, analysed combustion of the mixture containing 25% N_2, with k_3 doubled in the reaction scheme to simulate the effect on reaction R3 of replacing the N_2 with O_2. The result was an increase in the burning velocity from 6.8 $m \cdot s^{-1}$ to 7.4 $m \cdot s^{-1}$, making up nearly half the total observed effect of doubling $[O_2]$.

Finally k_3 and k_{11} were both doubled, to simulate the combined effect on burning velocity of reactions R3 and R11 when $[O_2]$ is doubled. The result (run 4, Table 5) was a burning velocity of 8.2 $m \cdot s^{-1}$ which is nearly the same as 8.3 $m \cdot s^{-1}$ obtained in run 2. Thus, the increase in burning velocity when N_2 is replaced by O_2 is attributable entirely to the increase in rates of reactions R3 and R11. Furthermore, the relative importance of the two reactions have been determined. Of the observed 23% increase in burning velocity when N_2 is replaced by excess O_2, 10% and 13% are contributed by the increased rates of reactions R3 and R11, respectively. It is somewhat surprising that reaction R11 is of equal or greater importance than reaction R3 in a high-temperature flame. It is widely held that at high temperatures, the chain-branching reactions dominate H_2-O_2 kinetics. However, in terms of the burning velocity, it is important to consider the heat-releasing effect of the low temperature reaction R11 in the preheat zone and its subsequent effect on the temperature profile. Note in Table 5, the increase in heat release rate $\dot{Q}$ and the shift of the $\dot{Q}$ maximum towards the unburnt gas upon doubling k_{11} (Runs 3 and 4). This change in flame structure results in a large enhancement of the thermal conduction, or the $\lambda \frac{dT}{dx}$ term of Equation (2). Even though the final flame temperature T_a is nearly the same in all four cases, an increase in reaction R11 increases the temperature gradient, $\frac{dT}{dx}$, in the region of the flame nearest the unburnt gas.

Finally, the above experiments demonstrate that deviations from the prediction of Equation (17) can be quantitatively linked to the participation of the diluent in the reaction kinetics of the combustion process.

6.6 THE EFFECT OF STEAM

Figure 15 showed that replacement of N_2 diluent with steam in a stoichiometric H_2-O_2 mixture increased the burning velocity. This is contrary to what was expected on the basis of the higher heat capacity and lower thermal diffusivity of steam relative to N_2. A more exact representation of the effect of steam is shown in Figure 27, where the data for steam were corrected for relative thermal diffusivity and plotted along with the prediction of Equation (17) for ideal diluent behavior. Equation (17) underpredicted the burning velocity by 20% (for the mixture containing 25% steam). Given the previous success of the prediction, the evidence is strong that, like oxygen, steam influences the burning velocity through mechanisms other than flame cooling and heat transport.

Kuehl [27] suggested a mechanism of radiative heat transport from the flame to unburnt gas, independent of thermal diffusion whereby hot species in the flame (OH, H_2O) emit infra-red radiation, which is absorbed by H_2O in the unburnt gas, raising its temperature. Since temperature appears as an exponent in kinetic equations, small changes in temperature could produce significant changes in burning velocity. While the mechanism is a legitimate one, estimates of the amount of heat thus transferred vary widely and are complicated by viewing integrals, abnormal vibrational/rotational temperatures of OH [53] and an inexact knowledge of the emissivities

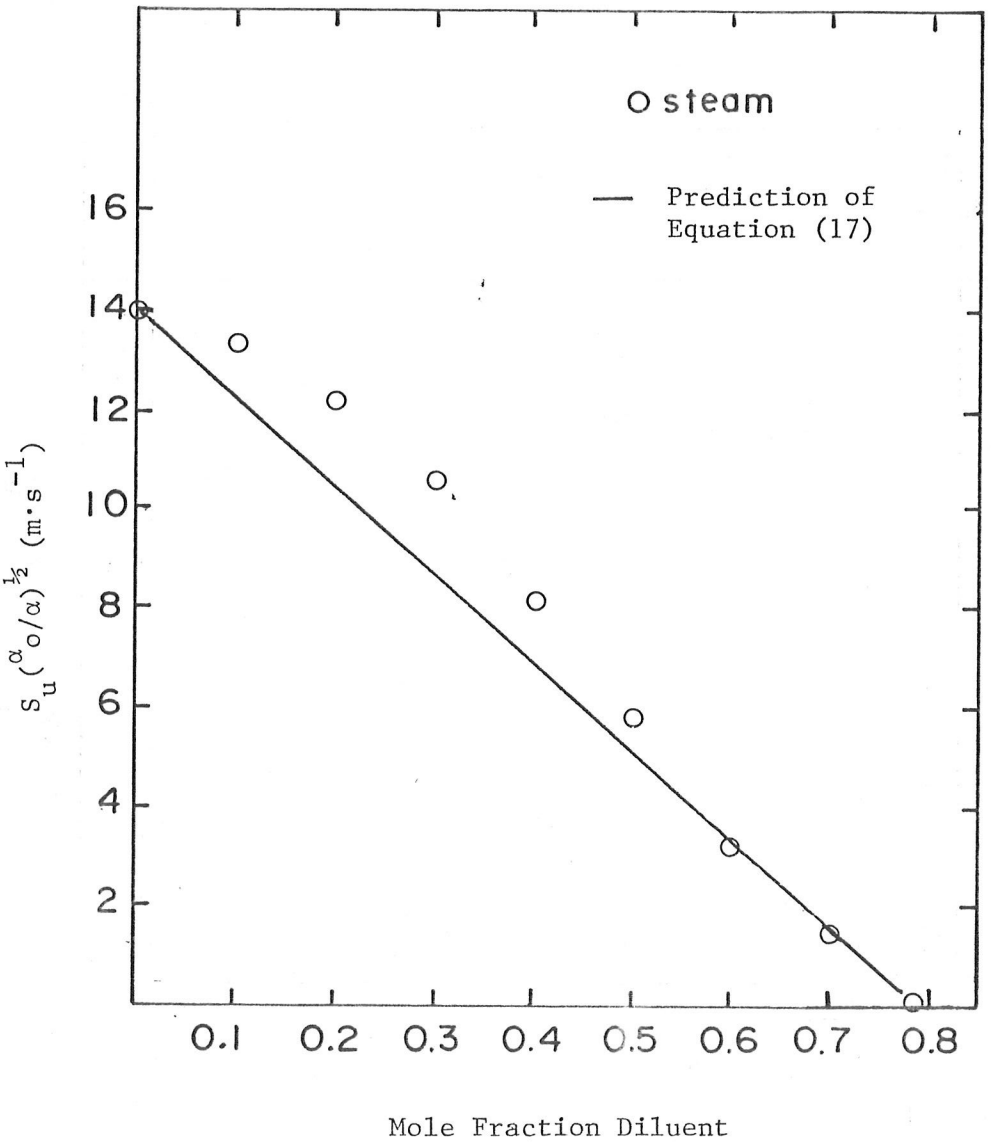

FIGURE 27: Burning velocities of 2:1 H_2-O_2 at 373 K with steam diluent, corrected for relative thermal diffusivity

of the flame gases [54]. Because of these difficulties, the effect of radiation is not directly considered here. We have focussed on kinetic and catalytic mechanisms, which are quantified to an extent that allows an upper limit to be determined for the magnitude of the radiative heat transfer mechanism.

As for oxygen, kinetic mechanisms were evaluated by use of the one-dimensional flame code described in Appendix A. The reaction scheme used in the code is given in Table 2. In the reaction scheme, steam is a participant in the bimolecular reactions R2 and R8, and is a catalyst in the recombination reactions R9, R10 and R11.

Since reaction R2 is endothermic by ~ 60 kJ $\cdot$mol^{-1}, increasing the rate of reaction R2 by addition of steam should lower the burning velocity, if there is any affect at all.

Reaction R8 is significant in that it is a chain branch, yielding 2 OH from one O atom. The activation energy is high, but is comparable to other sources of OH in the flame, such as reaction R3. The influence of chain-branching reactions should not be underestimated in flame propagation, but it will be shown later that reaction R8 is unimportant in the steam effect.

The role of steam as a third body catalyst in reactions R9, R10 and R11 is of greater interest.

$$H + H + M \rightarrow H_2 + M \qquad \Delta H = -435 \text{ kJ/mol} \qquad (9)$$

$$H + OH + M \rightarrow H_2O + M \qquad \Delta H = -500 \text{ kJ/mol} \qquad (10)$$

$$H + O_2 + M \rightarrow HO_2 + M \qquad \Delta H = -196 \text{ kJ/mol} \qquad (11)$$

where $[M] = 6[H_2O] + [H_2] + 0.4[O_2] + 0.4[N_2]$.

All three reactions are highly exothermic. However, reactions R9 and R10 are chain-terminating reactions and increasing their rates could be an effective drain on active species, and may decrease the burning velocity. Reaction, R11 on the other hand, is essentially a chain propagating reaction, producing HO_2 that participates further in the exothermic reactions 12-15.

$$HO_2 + H \rightarrow H_2 + O_2 \qquad \Delta H = -240 \text{ kJ/mol} \qquad (12)$$

$$HO_2 + H \rightarrow OH + OH \qquad \Delta H = -160 \text{ kJ/mol} \qquad (13)$$

$$HO_2 + OH \rightarrow H_2O + O_2 \qquad \Delta H = -300 \text{ kJ/mol} \qquad (14)$$

$$HO_2 + O \rightarrow OH + O_2 \qquad \Delta H = -230 \text{ kJ/mol} \qquad (15).$$

Furthermore, by virtue of its requirement for molecular oxygen and its high rate at low temperatures, reaction R11 predominates in the zone of the flame nearest the unburnt gas. Thus, an increase in the rate of reaction R11 leads to a significant release of heat in a heat-deficient region of the flame. In addition, one of the subsequent reactions, R13, is a significant source of OH radicals in what is also a radical-deficient region of the flame.

The effect on burning velocity of a more efficient third body (such as steam) would be the net result of the individual effects of reac-

tions R9, R10 and R11, of which reaction R11 is expected to dominate. In what follows, we first examine in detail the sensitivity of the calculated burning velocity and flame structure to changes in the third body efficiency coefficient. Then the net effect of the third body coefficient on burning velocity is separated into the effect of reactions R9 and R10 as radical sinks and the effect of reaction R11 as a heat source.

First, the flame structure and burning velocity was calculated for a stoichiometric H_2-O_2 mixture at 100°C containing 25% N_2 and for the corresponding mixture where N_2 was replaced by steam, using the rate parameters in Table 2 (i.e., $[M] = 6\ [H_2O] + [H_2] + 0.4\ [O_2] + 0.4\ [N_2]$). The results are shown graphically in Figures 28 and 29 as well as in tabular form in Table 5, runs 5 and 6. The calculated burning velocities were 8.9 $m \cdot s^{-1}$ and 9.8 $m \cdot s^{-1}$ for N_2 and steam diluents, respectively, and are in good relative agreement with the experimentally measured values of 8.4 $m \cdot s^{-1}$ and 9.3 $m \cdot s^{-1}$. It is reasonable that the calculated values were systematically higher by a small amount than the experimental values because the calculation assumed an adiabatic system.

With regard to flame structure, the key features are the mass fractions of HO_2, the heat release rate, $\dot{Q}$, and the temperature profile. For the mixture with steam diluent, the HO_2 concentration is greater by a factor of 3. The heat-release profile is higher and shifted towards the unburnt gas. The temperature profile is also shifted towards the unburnt gas, reflecting the change in the heat release profile. These quantities are plotted separately in Figure 30 to illustrate the connection between $[HO_2^{\bullet}]$ and heat-release rate, $\dot{Q}$. The differences in flame structure between

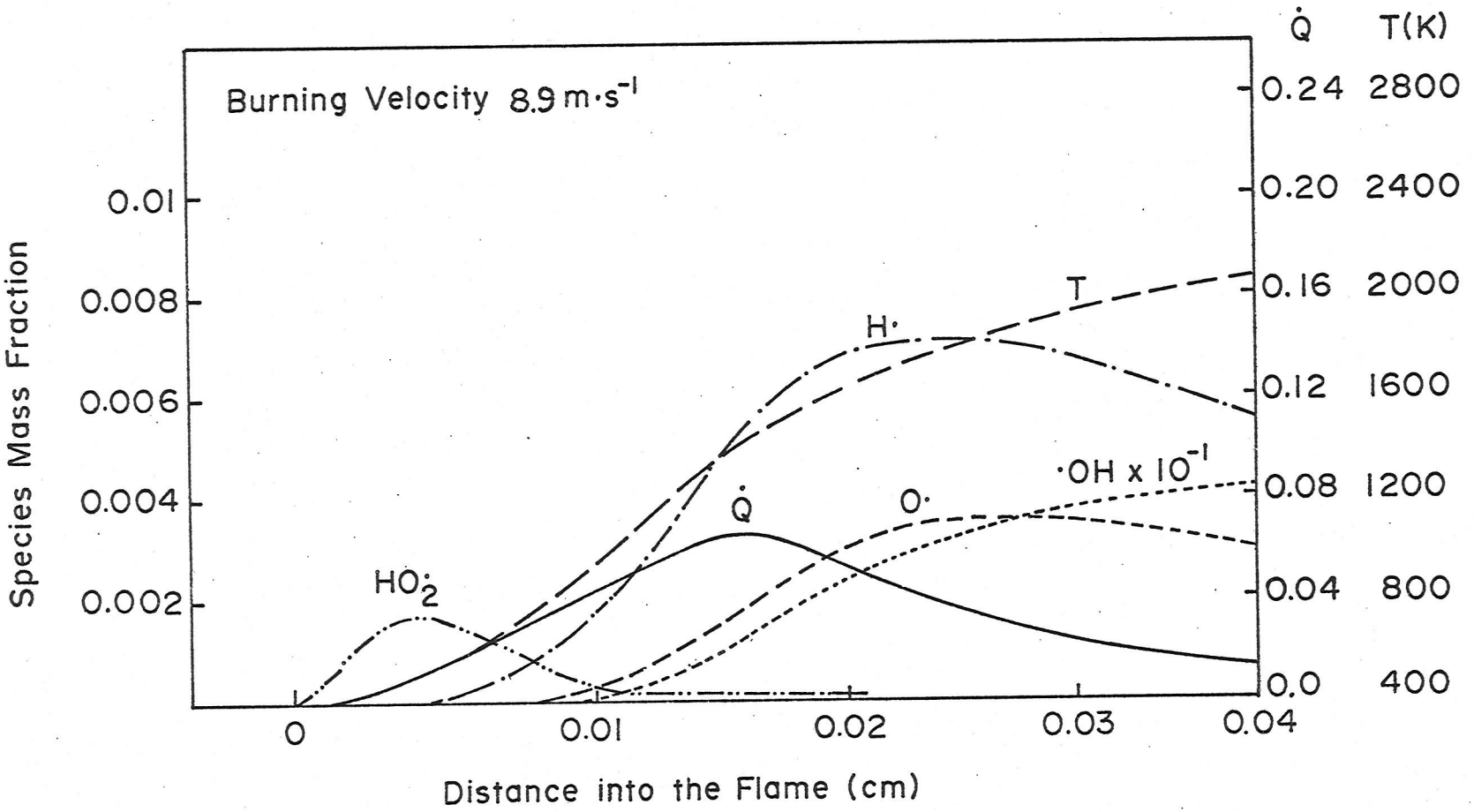

FIGURE 28: Calculated flame structure of 2:1 H_2-O_2 at 373 K, containing 25% N_2 diluent by volume

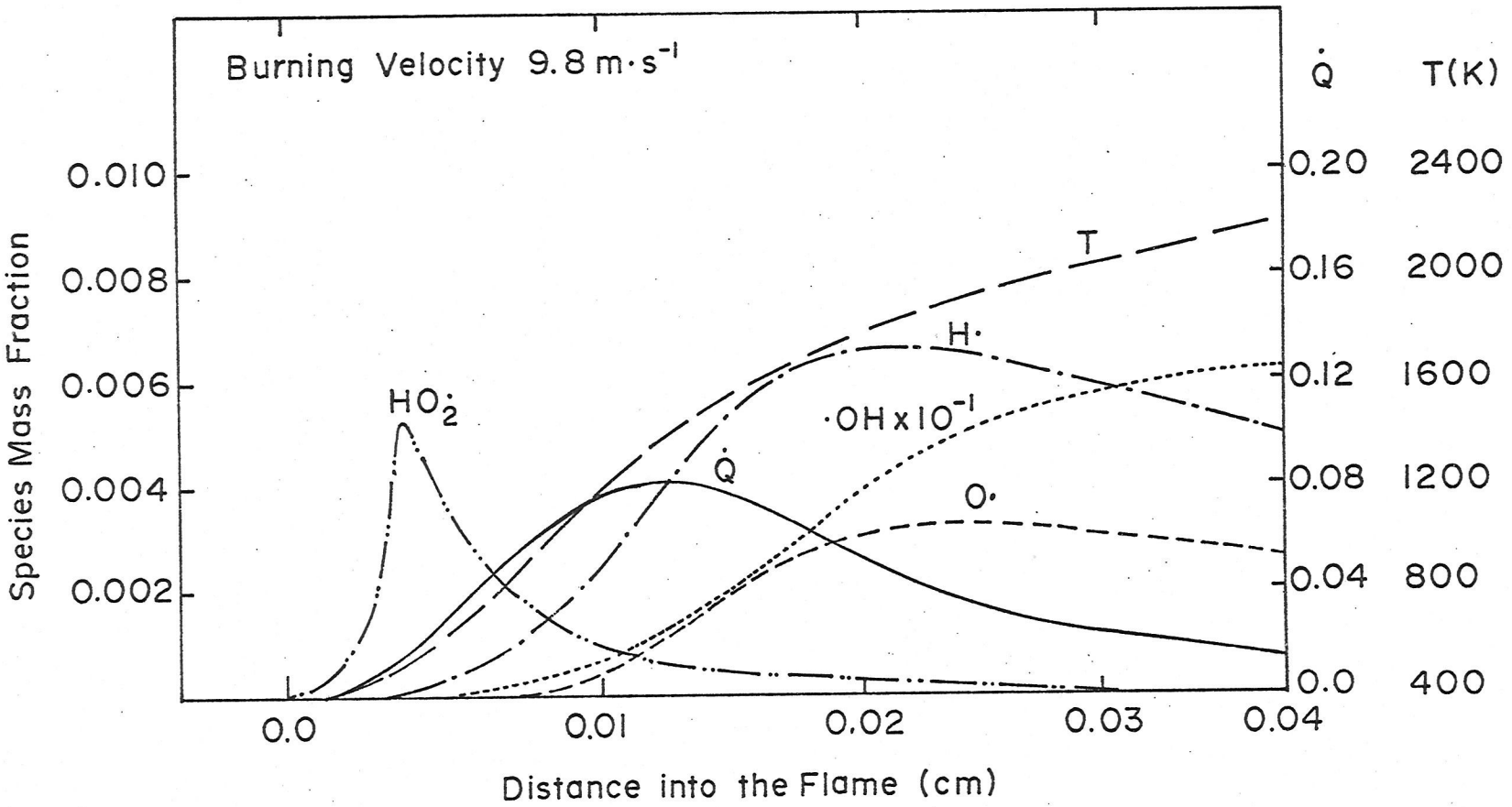

FIGURE 29: Calculated flame structure of 2:1 H_2-O_2 at 373 K, containing 25% steam by volume

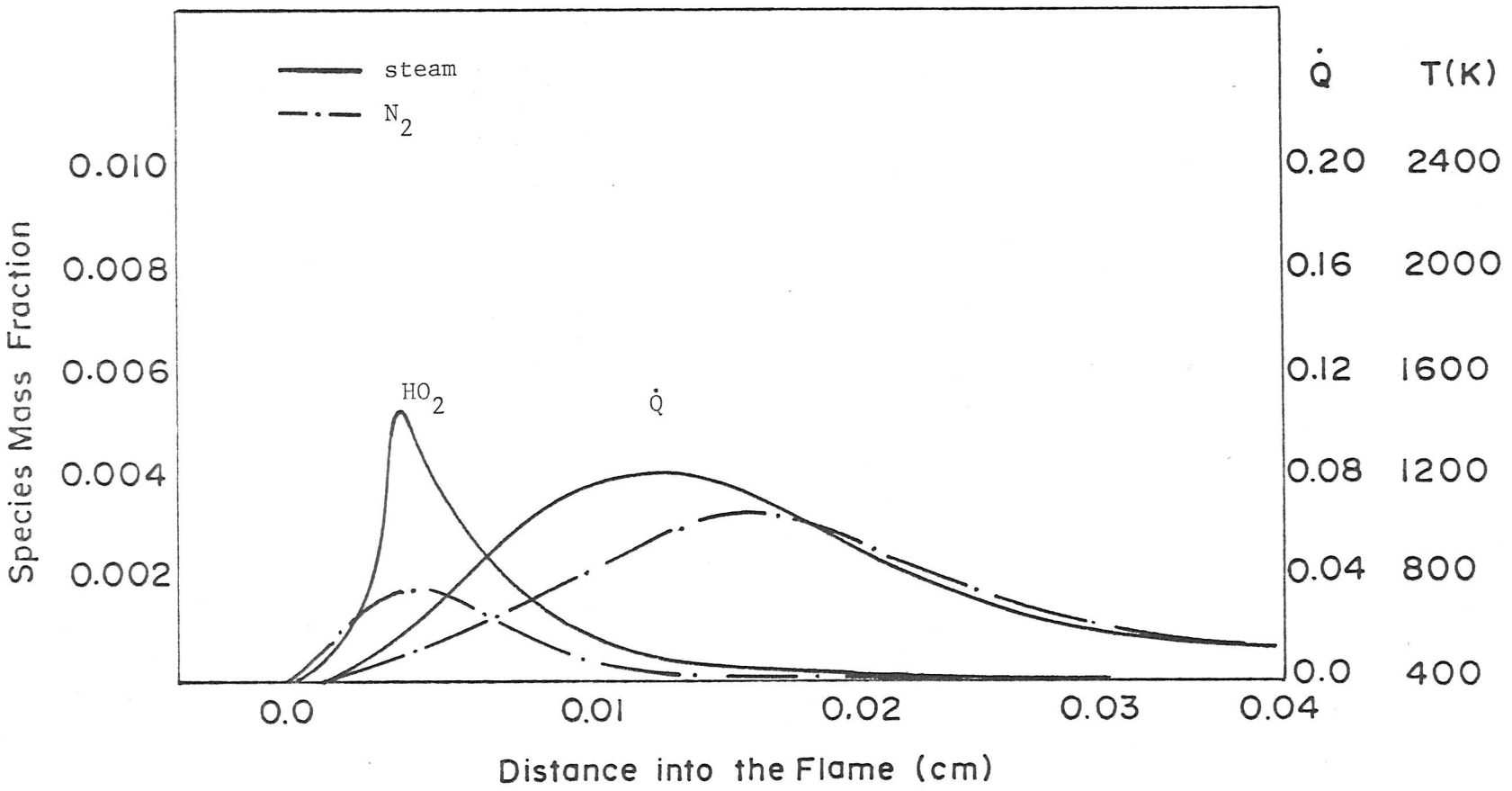

FIGURE 30: Comparison of calculated heat release rates, $\dot{Q}$, and $HO_2^{\bullet}$ concentrations in 2:1 H_2-O_2 flames containing 25% N_2 and steam diluents

steam and N_2 diluent are all consistent with an increase in the rate of reaction R11 resulting from the higher third body efficiency of steam and with the experimentally observed increase in burning velocity.

In the next code experiment, the third body coefficient for steam was artificially changed to that of N_2, i.e., from 6.0 to 0.4. The results are shown in Figure 31 as well as run 7 in Table 5. The burning velocity decreased from 9.8 to 7.8 $m \cdot s^{-1}$, a difference of 28%. $[HO_2]$ and $\dot{Q}$ were lower, and were nearly indistinguishable from the case of N_2 diluent in run 5. The most notable change was the large decrease in the flame temperature profile. The calculated temperature profiles for runs 5, 6 and 7 are plotted for comparison in Figure 32. In the absence of its high third body efficiency steam exhibited the effect expected on the basis of its high heat capacity, i.e., the burning velocity was lowered due to a reduction of the flame temperature in the reaction zone.

It is interesting to compare the burning velocity obtained by the code for $m_{H_2O} = 0.4$ in run 7 with the prediction of Equation (17) for "ideal" diluent behavior. The code calculated Su = 7.8 $m \cdot s^{-1}$. As the code results were 0.5 $m \cdot s^{-1}$ higher than experimental results, the code value should be adjusted to about 7.3 $m \cdot s^{-1}$, to strictly compare the results with the experimental data used in Equation (17).

$$\left(\frac{\alpha_o}{\alpha}\right)^{\frac{1}{2}} Su = Su_o - X_{dil} \left(\frac{Su_o}{X_L}\right) \qquad (17)$$

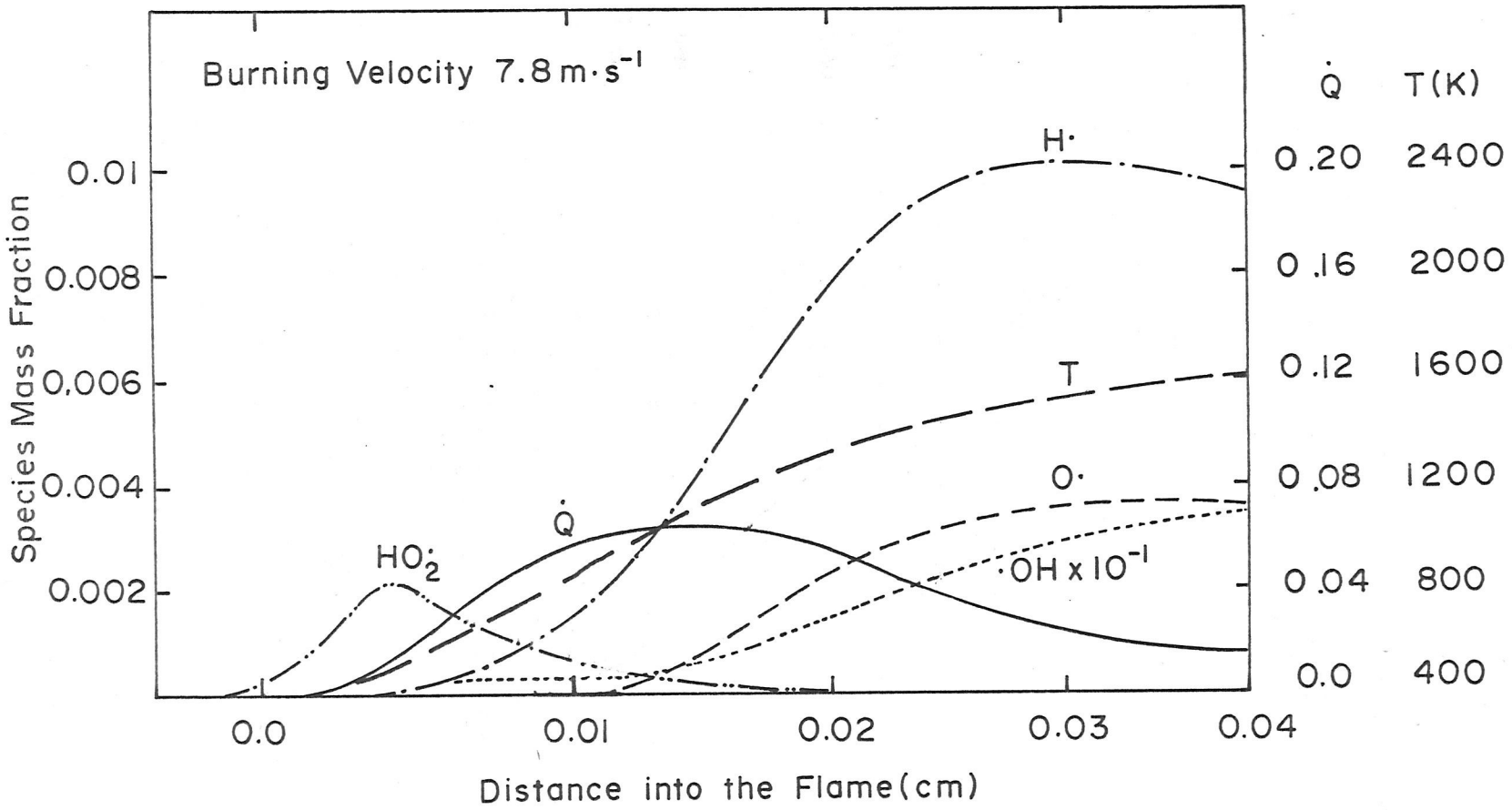

FIGURE 31: Calculated flame structure of 2:1 H_2-O_2 at 373 K, containing 25% steam diluent with $m_{H_2O} = 0.4$

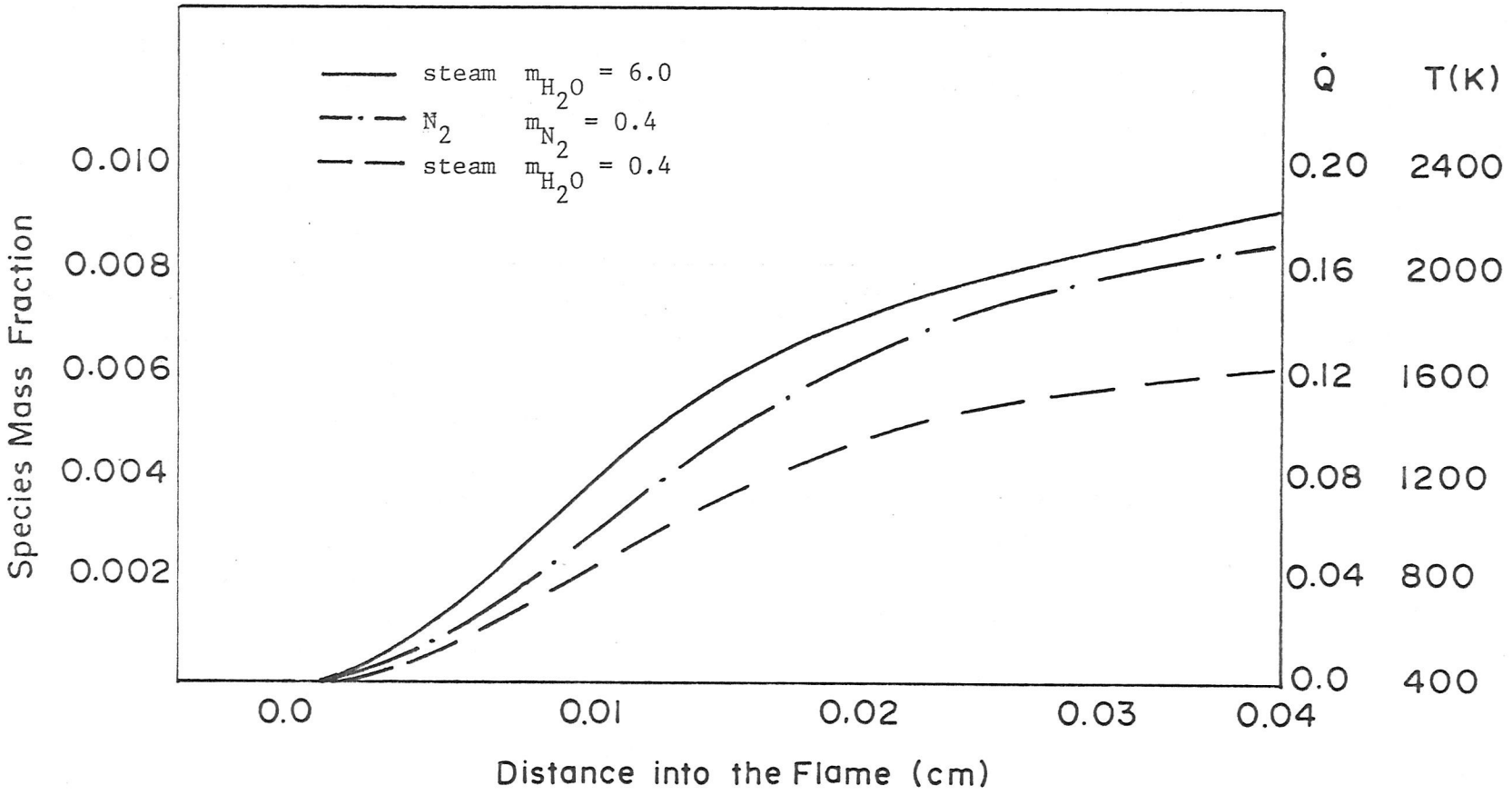

FIGURE 32: Comparison of calculated temperature profile for 2:1 H_2-O_2 flames containing 25% N_2 diluent, 25% steam diluent (m_{H_2O} = 6.0) and 25% steam diluent with m_{H_2O} = 0.4

For 25% steam in a stoichiometric H_2-O_2 mixture: $\alpha_o^{\frac{1}{2}} = 0.937$ and $\alpha^{\frac{1}{2}} = 0.779$, from Appendix B; $S_{u_o} = 14.0$, from Figure 15; $X_{dil} = 0.25$ and $X_L = 0.78$ from Appendix C. Substituting into Equation (17) yields $S_u = 7.9\ m \cdot s^{-1}$, which slightly overpredicts the adjusted code result of $7.3\ m \cdot s^{-1}$ for $m_{H_2O} = 0.4$.

In Section 6.4, it was anticipated that Equation (17) would overpredict the burning velocity of steam diluent due to the increase in the heat capacity of steam with temperature. The magnitude of this effect is small relative to the catalytic effect but it can be estimated reasonably well by determining an "effective X_L" consistent with the higher C_p of H_2O at the flame temperature. This is obtained from Figure 33, where X_L for several diluents is plotted as a function of their heat capacities. Admittedly, factors other than C_p influence the flammability limit X_L but C_p is the dominant factor.

The heat capacity of steam at the flame temperature is ~ 12 cal/mol•K (from Figure 26). From extrapolation of the graph in Figure 33, this corresponds to an "effective X_L" of ~ 0.65. Using this value for X_L in Equation (17) yields Su = $7.2\ m \cdot s^{-1}$, in good agreement with the corrected code result of $7.3\ m \cdot s^{-1}$.

By artificially reducing the third body efficiency of steam in the code to that of N_2, the calculated burning velocity agrees with the prediction of Equation (17) for "ideal" diluent behavior. It appears, then, that the high third body efficiency of steam is the principal cause of the high burning velocities observed with steam diluent. It remains, now, to

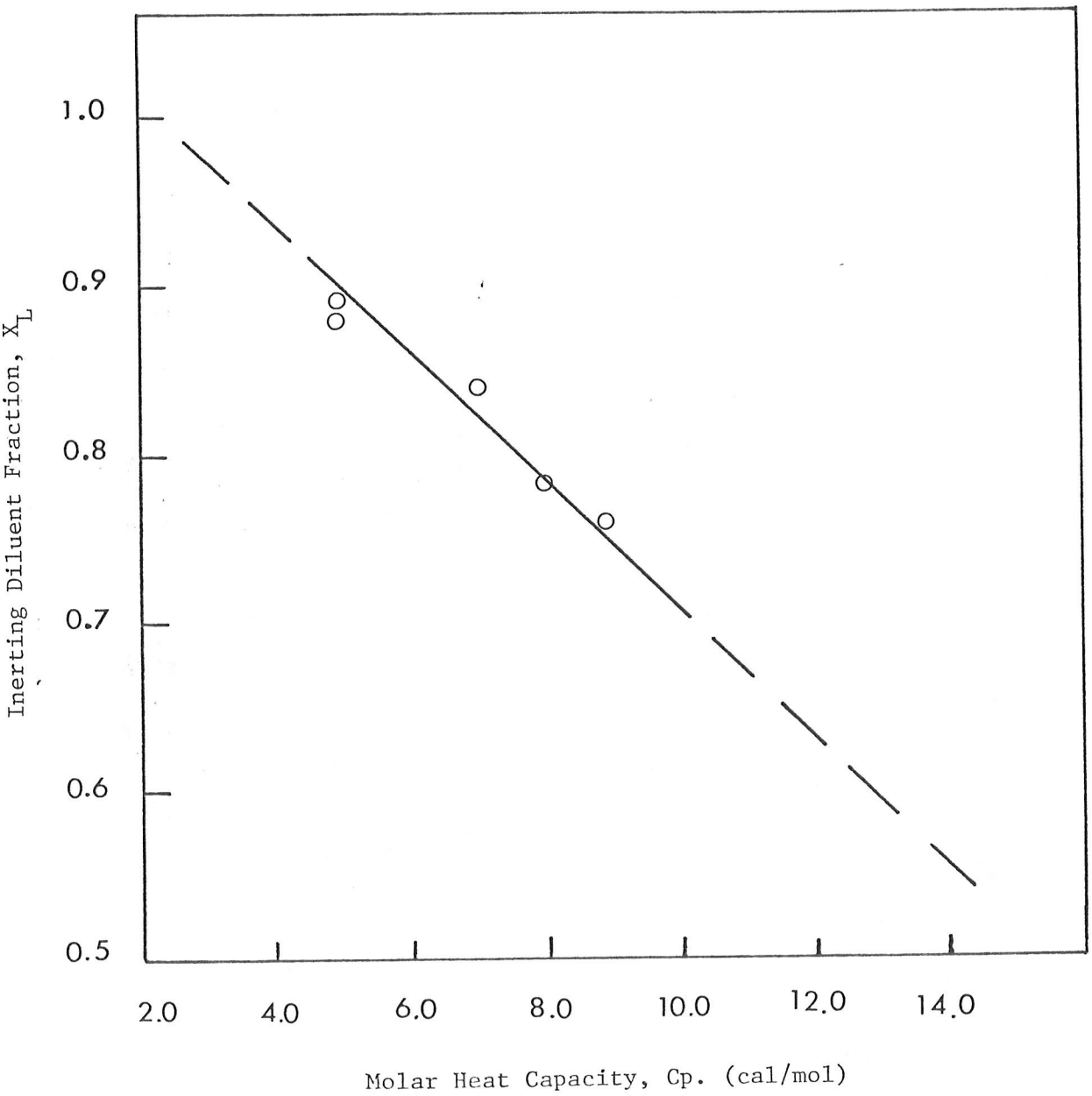

FIGURE 33: Inerting diluent concentration, X_L, for 2:1 H_2-O_2 as a function of molar heat capacity of the diluent

separate the net effect of the third body efficiency into the relative effects of reactions R9 and R10 as radical sinks and reaction R11 as a heat source.

Consider again the previous run where m_{H_2O} was reduced in the code from 6.0 to 0.4 for stoichiometric H_2-O_2 containing 25% steam. This changed [M], and hence the overall rates of each of the reactions R9, R10 and R11 by a factor of $\frac{1}{4}$. The effect on the calculated burning velocity was a decrease from 9.8 $m \cdot s^{-1}$ to 7.8 $m \cdot s^{-1}$. In the next code experiment, m_{H_2O} remained at 0.4, but the reduction in [M] was compensated in reaction R11 by increasing k_{11} by a factor of 4. The results are shown in run 8 of Table 5. The burning velocity increased to 9.9 $m \cdot s^{-1}$. From this it can be deduced that the effect of reactions R9 and R10 combined was a 0.1 $m \cdot s^{-1}$ suppression of the burning velocity, which was insignificant. In fact, the calculated structure in run 8 was nearly indistinguishable from run 6, where all three recombination reactions were increased. The only difference was the mass fractions of H atoms increased in run 8 because of the reduced rates of recombinations in reactions R9 and R10. Thus, run 8 conclusively shows that the steam effect is due to the increase in the rate of reaction R11 and the rates of reactions R9 and R10 are almost insignificant. It is interesting to note that the substantial increase in concentration of H atoms in run 7 has no apparent effect in increasing the burning velocity. This will be discussed further in the context of the effect of excess hydrogen.

The net effect of steam diluent on the burning velocity is the sum of the effects of flame cooling, thermal diffusivity and third body efficiency. Equation (17), with modifications, predicts the effect of steam

arising from changes to the heat capacity and thermal diffusivity of the mixture. The 20% by which experimental measurements of burning velocity exceed the unadjusted prediction of Equation (17) is accounted for by the high third body efficiency of steam in reaction R11, initiating the low temperature heat releasing cycle of reactions R12 - R15. The concurrent drain on chain carriers in reactions R9 and R10 is of minor importance in its effect on burning velocity. Furthermore, there remains a vanishingly small role for the radiant heat transport mechanism proposed by Kuehl and for reaction R8 in the observed effect of steam on burning velocity.

6.7 THE EFFECT OF CO_2

CO_2 was observed to produce the greatest suppression of burning velocity of the diluents studied. This is consistent with CO_2 having the highest heat capacity and the lowest thermal diffusivity. However, upon closer examination the suppression of burning velocity by CO_2 appears extraordinary. In Figures 34, 35 and 36, the burning velocity data for CO_2 diluent were corrected for relative thermal diffusivity and plotted along with the prediction of Equation (17) for ideal diluent behavior. Equation (17) overpredicts the burning velocities with CO_2 as diluent in lean and stoichiometric flames (Figures 34 and 35, respectively) by as much as 70%, but more closely predicts the effect of CO_2 in rich mixtures (Figure 36). The large suppression of burning velocity by CO_2 in lean flames is evidently absent, or masked, in rich flames.

A possible kinetic mechanism for CO_2 to suppress the burning velocity is by direct reaction with one or more of the chain carriers: H•, O•,

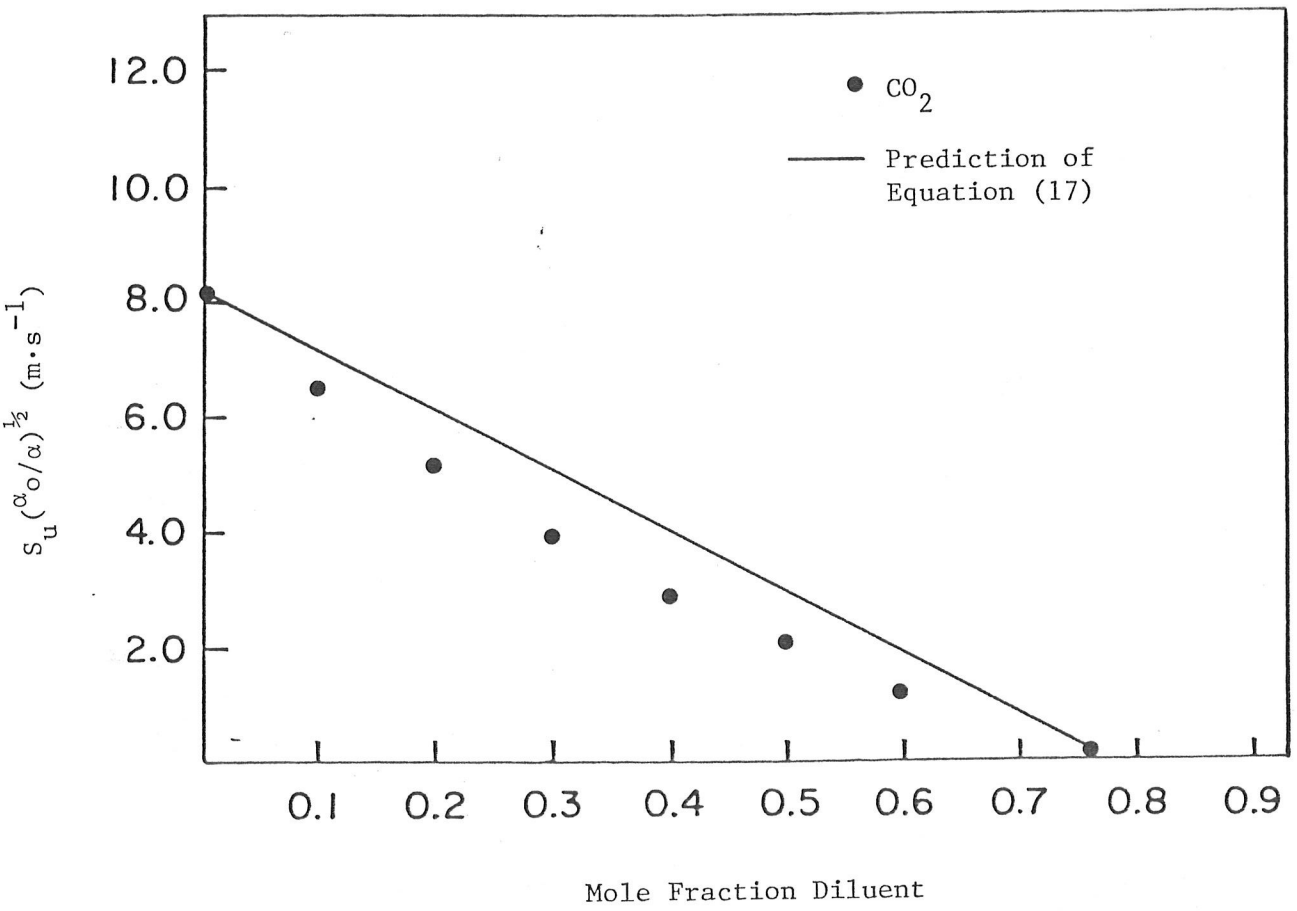

FIGURE 34: Burning velocities of 1:1 H_2-O_2 with CO_2 diluent, corrected for relative thermal diffusivity

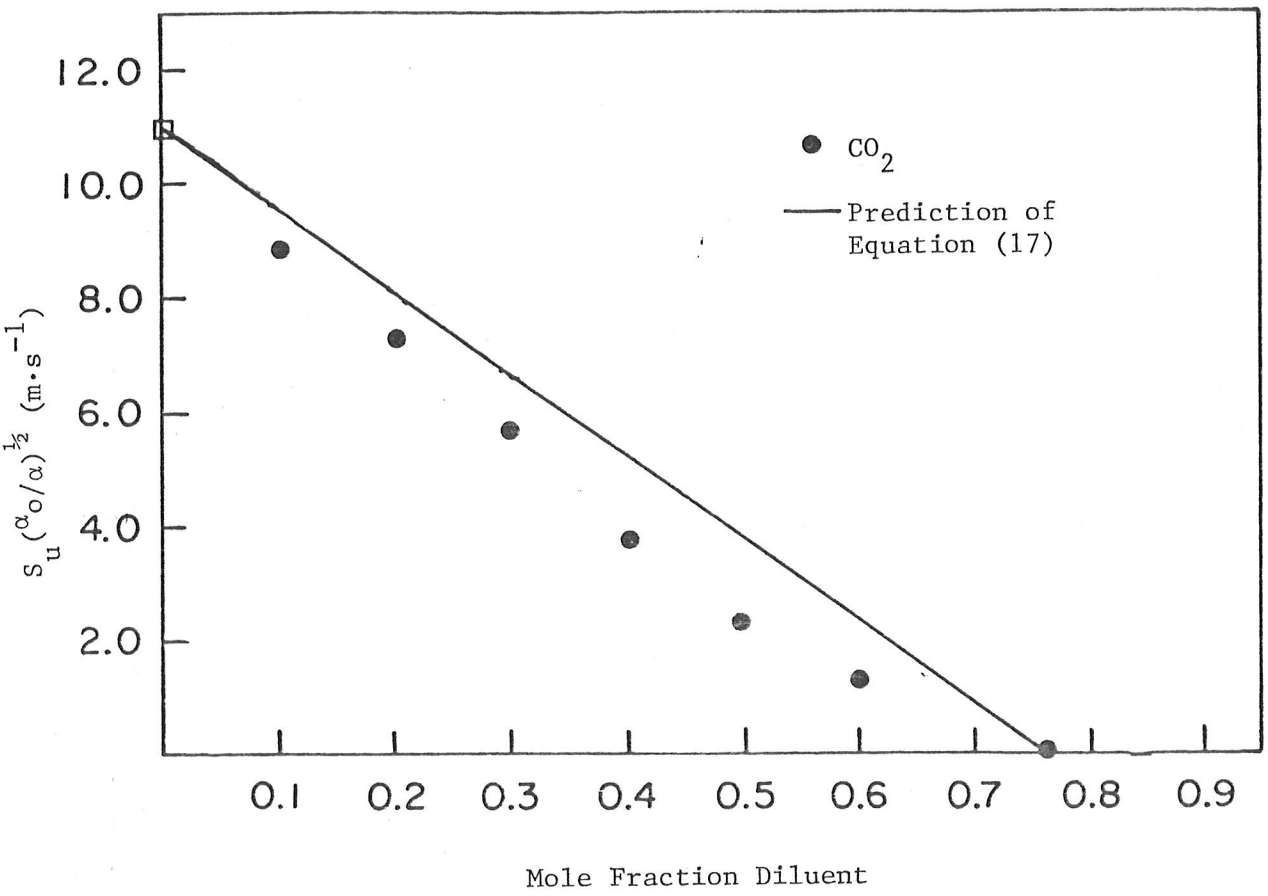

FIGURE 35: Burning velocities of 2:1 H_2–O_2 with CO_2 diluent, corrected for relative thermal diffusivity

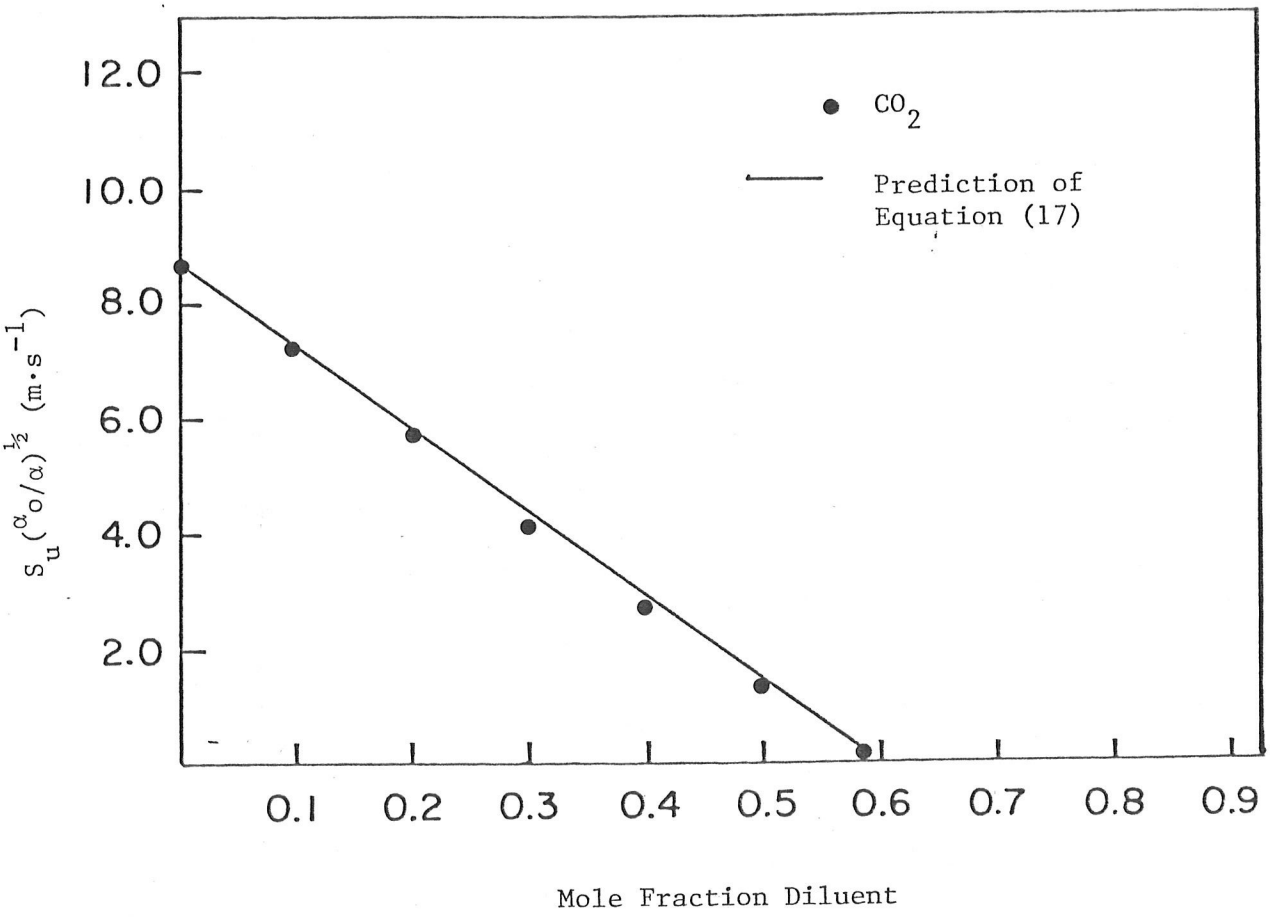

FIGURE 36: Burning velocity of 5:1 H_2-O_2 with CO_2 diluent, corrected for relative thermal diffusivity

or •OH. The known reactions of CO_2 with H•, O• and •OH [17] were examined, and compared with the reactions of H_2 and O_2 with H•, •OH and O• in the reaction scheme of Table 2, in order to identify reactions with CO_2 that could significantly compete for radicals in the flame. From this exercise, two reactions were identified as candidates for explaining the observed effect of CO_2, reactions R19 and R20.

$$H + CO_2 \overset{k}{\underset{\leftarrow}{\rightarrow}} CO + OH \qquad \log K = -0.35 \text{ at } 2000 \text{ K} \qquad \text{(R19)}$$

$$k = 1.0 \times 10^{11} \text{ mol} \cdot \text{cm}^{-3} \cdot \text{s}^{-1} \text{ at } 2000 \text{ K}$$

$$O + CO_2 \overset{\rightarrow}{\leftarrow} O_2 + CO \qquad \log K = 0.293 \text{ at } 2000 \text{ K} \qquad \text{(R20)}$$

$$k = 3.0 \times 10^{7} \text{ mol} \cdot \text{cm}^{-3} \cdot \text{s}^{-1} \text{ at } 2000 \text{ K}$$

$$H + O_2 \overset{\rightarrow}{\leftarrow} OH + O \qquad \log K = -6.4 \text{ at } 2000 \text{ K} \qquad \text{(R3, R4)}$$

$$k = 3.2 \times 10^{12} \text{ mol} \cdot \text{cm}^{-3} \cdot \text{s}^{-1} \text{ at } 2000 \text{ K}$$

$$O + H_2 \overset{\rightarrow}{\leftarrow} OH + H \qquad \log K = 0.135 \text{ at } 2000 \text{ K} \qquad \text{(R5, R6)}$$

$$k = 1.0 \times 10^{9} \text{ mol} \cdot \text{cm}^{-3} \cdot \text{s}^{-1} \text{ at } 2000 \text{ K.}$$

Reaction R19 will compete with O_2 for H atoms in the flame, but the reaction is not a chain terminating one; it results in the production of another active species. The net effect is not likely to be a significant drain on the radical pool and thus, not likely to suppress the burning velocity.

Reaction R20 is a chain-terminating reaction, in competition for O atoms with reaction R5. The rate constant of the forward reaction for reac-

tion R20 is $\sim 10^{-2}$ that of reaction R5 so its effect is also likely to be small.

The overprediction by Equation (17) for CO_2 diluent is most likely due to the failure of the correlation for diluents with a strong temperature dependence of C_p, already discussed in Section 5.5 and in Section 5.7 with steam diluent. CO_2 is a more extreme case. The estimate of an effective X_L for CO_2 requires considerable extrapolation of Figure 33 to $C_p \sim 14$ cal/(mol•K) for CO_2 at 2000 K. Owing to the extreme slope of C_p versus T for CO_2, separate estimates of an effective X_L are required for each diluent fraction of interest. The result is an improvement of the correlation but only to within about 10% - 20% of the measured values. Since a more satisfactory means to quantitatively account for this effect is not immediately available, this remains a limitation of Equation (17).

The observation that Equation (17) successfully predicts the behavior of CO_2 in rich flames is evidence to suggest that rich flame propagation is not sensitive to changes in flame temperature to the same extent as lean flames. This is discussed further in the next Section on rich flame propagation.

6.8 THE EFFECT OF EXCESS HYDROGEN

The effect on burning velocity of hydrogen added as a "diluent" to a stoichiometric mixture is expected to be complex. The most predictable effect is its behavior as a simple diluent, increasing the burning velocity by its high thermal diffusivity relative to the gases it is replacing.

Since the hydrogen diluent is not inert, it is expected to also participate in the reaction kinetics. The effect on burning velocity is further complicated by the role of the highly mobile H atoms in rich flame propagation. The following is an attempt to interpret the effect of excess hydrogen in terms of the relative roles of each of these mechanisms.

First, it is necessary to quantify the role of excess hydrogen as a simple diluent in a stoichiometric mixture. Figure 37 compares the burning velocities with excess H_2, corrected for relative thermal diffusivity, with the prediction of Equation (17) for ideal diluent behavior. The difference between the curves, is the effect from the participation of the H_2 "diluent" in reaction kinetics. It is significant that a kinetic rate effect is clearly identified since the effect of excess H_2 has previously been attributed to increased thermal diffusivity, [29] H atom diffusion [18,27] or both. The present treatment is unique in that the effects of H_2 as a simple diluent are eliminated and the kinetic rate effect is identified and treated separately. H atom diffusion will be shown to arise as a natural consequence of changes in reaction kinetics due to excess H_2.

Molecular H_2 participates directly in only two elementary reactions, reactions R1 and R5 in Table 2.

$$OH + H_2 \rightarrow H_2O + H \qquad \text{R1}$$

$$O + H_2 \rightarrow OH + H \qquad \text{R5}$$

Addition of excess hydrogen will increase the overall rates of these reactions in proportion to the amount of H_2 added. The effect this has on

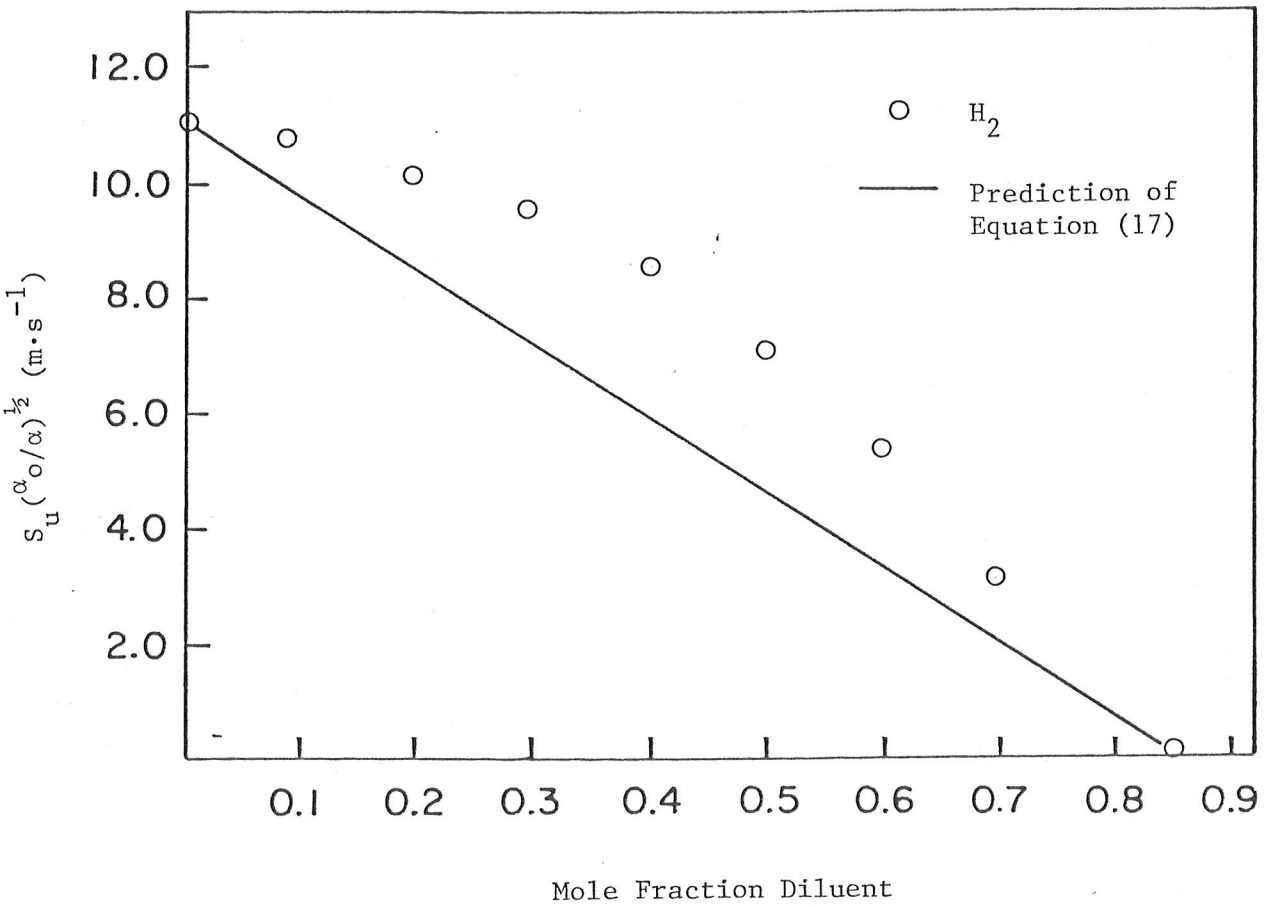

FIGURE 37: Burning velocities of 2:1 H_2-O_2 at 298 K with excess H_2, corrected for relative thermal diffusivity

burning velocity, however, is not straightforward. Neither reaction is exothermic and therefore would not directly contribute to thermal propagation. Both reactions do, however, generate H atoms, and it has been shown experimentally [55] and confirmed by calculations [18], that burning velocity correlates linearly with [H•].

It can be demonstrated analytically that H atom concentration is sensitive to molecular hydrogen concentration. Equilibrium exists between H•, •OH and O• at temperatures above 1500 K [10,18]. This enables analytical expressions to be derived for the concentrations of these species in terms of stable species [18]. From reactions R1 to R6,

$$X_{H\bullet} = \left(\frac{k_1^{\,3}\, k_3\, k_5\, X_{O_2}\, X^3_{H_2}}{k_2^{\,2}\, k_4\, k_6\, X^2_{H_2O}} \right)^{\frac{1}{2}}$$

$$X_{O\bullet} = \frac{k_1\, k_3\, X_{O_2}\, X_{H_2}}{k_2\, k_4\, X_{H_2O}}$$

$$X_{OH} = \left(\frac{k_3\, k_5\, X_{O_2}\, X_{H_2}}{k_4\, k_6} \right)^{\frac{1}{2}}$$

From these expressions we observe that $X_{H\bullet}$ is strongly influenced by X_{H_2}. There exists, then, a qualitative link between increases in hydrogen concentration, increased H atom yield and increased burning velocity. The following code experiments are aimed at establishing a more concrete assessment of these rather general correlations.

Combustion of a mixture containing 80% H_2 and 20% O_2 was analysed with the rate parameters unchanged from Table 2 and then, with the rate constants for reactions generating H atoms (reactions R1 and R5) doubled, to simulate the effect of an increase in $[H_2]$ on the reaction rates. The results appear in Table 5, runs 9 and 10. The calculated burning velocity increased by more than 10%, from 8.7 $m \cdot s^{-1}$ to 9.7 $m \cdot s^{-1}$. The calculated H atom concentration also increased by about 10% from a maximum mass fraction of 0.0023 to 0.0026. This again supports the correlation of burning velocities and H atom concentrations and also demonstrates that an increase in $[H\bullet]$ is inextricably linked to an increase in reaction rates. However, it is still not clear by what mechanism this increased $[H\bullet]$ actually produces the increase in the burning velocity.

Important evidence as to the fate of the H atoms was provided by the significant shift of the $\dot{Q}$ maximum towards the unburnt gas when the rate constants for reactions R1 and R5 were doubled in run 8. The H atoms presumably attack molecular oxygen in reactions R3 and R11.

$$H + O_2 \rightarrow OH + O \qquad \text{R3}$$

$$H + O_2 + M \rightarrow HO_2 + m \qquad \text{R11}$$

Since reaction R3 is endothermic, the increased heat release is the result of H atoms diffusing upstream from the reaction zone and participating specifically in the exothermic reaction R11 in the preheat zone. This is consistent with a previous observation with steam diluent, where the shift of $\dot{Q}_{max}$ towards the unburnt gas was also a result of an increase in the rate of reaction R11. Furthermore, for steam diluent and for excess O_2, reaction

R11 as a heat source was shown to be a potent factor in the burning velocity. This is not to underestimate the importance of the chain-branch reaction R3, but it is likely that due to the low equilibrium constant ($k_3/k_4 \sim 10^{-1}$ at 1500 K) [15] for reactions R3 and R4, the majority of H atoms are regenerated by reaction R4, and by reaction R5, and proceed ultimately to reaction R11.

In the present context, some additional points on the effect of steam are noted. In runs 6 and 7 in Table 5 (also Figures 29 and 30), reducing the third body efficiency coefficient of steam from 6.0 to 0.4 was shown to produce a large (27%) decrease in the burning velocity. At the same time the concentration of H atoms increased by ~ 60%, due to the decreased rate of their recombinations when the third body efficiency was lowered. This large increase in [H•], concurrent with a decrease in burning velocity, appears to contradict much previous work indicating that burning velocity increases with [H•]. Upon closer examination we find that the effect of H atom diffusion is only masked and this is actually strong support for the exclusive role of reaction R11 in the H atom diffusion mechanism. Even though the availability of H atoms was increased by 60% by reducing m_{H_2O}, the rate of reaction R11 was reduced by 400%. Since reaction R3 is not affected by third body coefficients, a 60% increase in [H•] should have increased the burning velocity via reaction R3. This was not observed, suggesting reaction R3 is relatively unimportant in the H atom diffusion mechanism.

This section will conclude with two figures that provide a basis for some general remarks about hydrogen flame propagation and diluent

effects. In Figures 38 and 39 the maxima of the species profiles, burning velocities and temperatures, as output from the computer model, are plotted as a function of H_2 concentration in air and in O_2, respectively.

Figure 38 shows the contradiction of the continued increase in the burning velocity beyond the stoichiometric amount of hydrogen ($\sim$ 29% H_2) where O• and •OH concentrations and temperature are all declining. In the lean to stoichiometric flames, the burning rate appears to be dominated by thermal mechanisms. Beyond the stoichiometric mixture (29% H_2) the temperature is decreasing due to the heat requirement of warming excess H_2 to the flame temperature, but the decrease in temperature with excess H_2 is accompanied by a sharply increasing concentration of H atoms as predicted by the analytical expression. The burning velocity increase from 30% to 42% H_2 is due to the increasing influence of H atom diffusion. At this point the mixture is already quite rich, (H_2:O_2 $\approx$ 4:1). Between 42% and 50% H_2, the H atom concentration is still increasing but is unable to sustain the maximum burning velocity, with losses in thermal diffusion caused by decreasing flame temperatures. As well, the growing scarcity of O_2 is lowering the effectiveness of H atom diffusion. At still greater concentrations of H_2, the temperature drop is influencing the rates of high activation reactions generating H atoms, [H•] decreases, and the burning velocity drops sharply.

The yield of HO_2• increases through the lean regions and then remains constant through to the extreme rich mixtures. Since the formation of HO_2• does not depend on high temperatures, [HO_2•] does not follow the temperature profile as do [•OH] and [O•], but [HO_2•] should be sensitive to

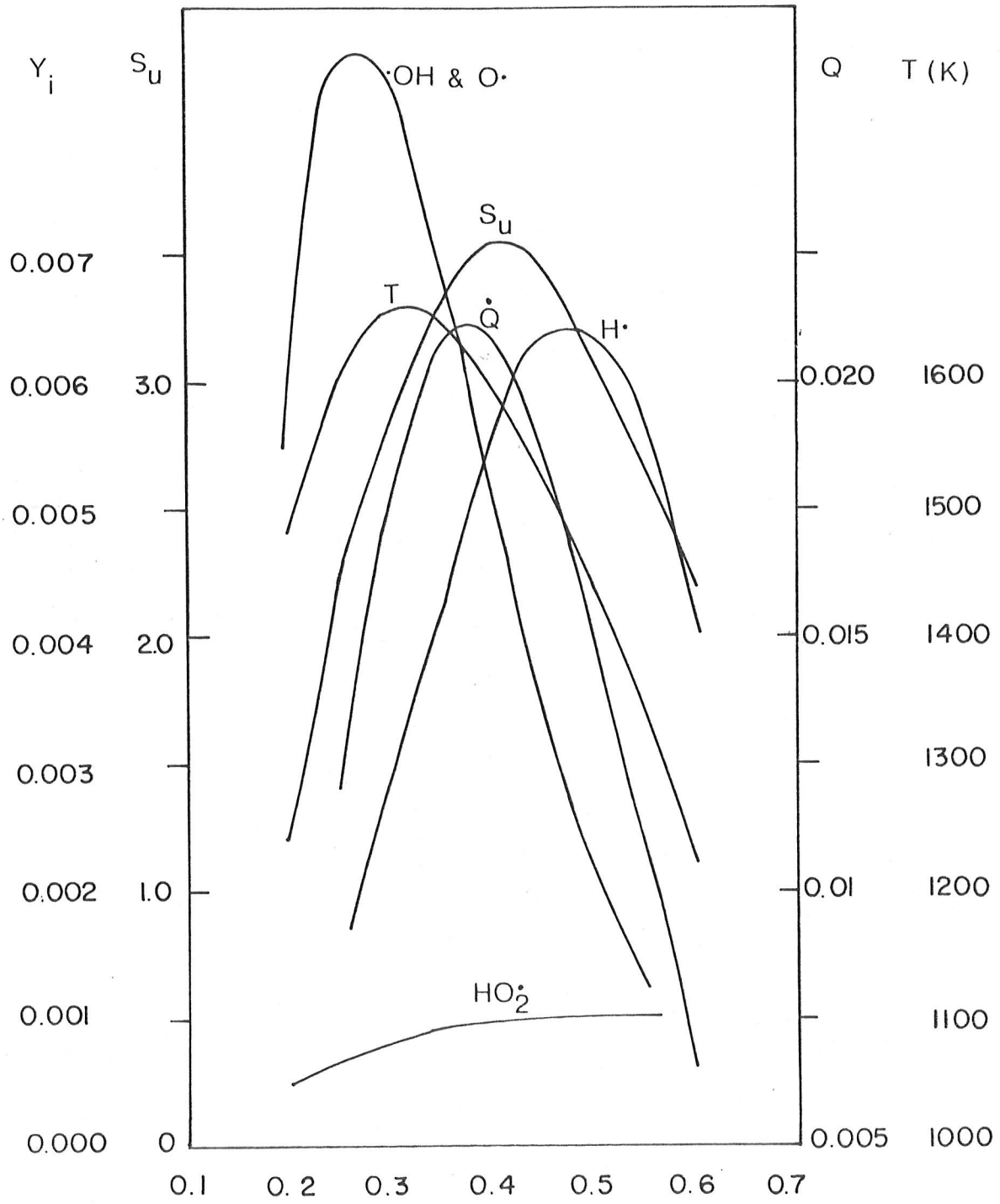

FIGURE 38: Maximum calculated values of key species concentrations and flame properties for H_2-air flames

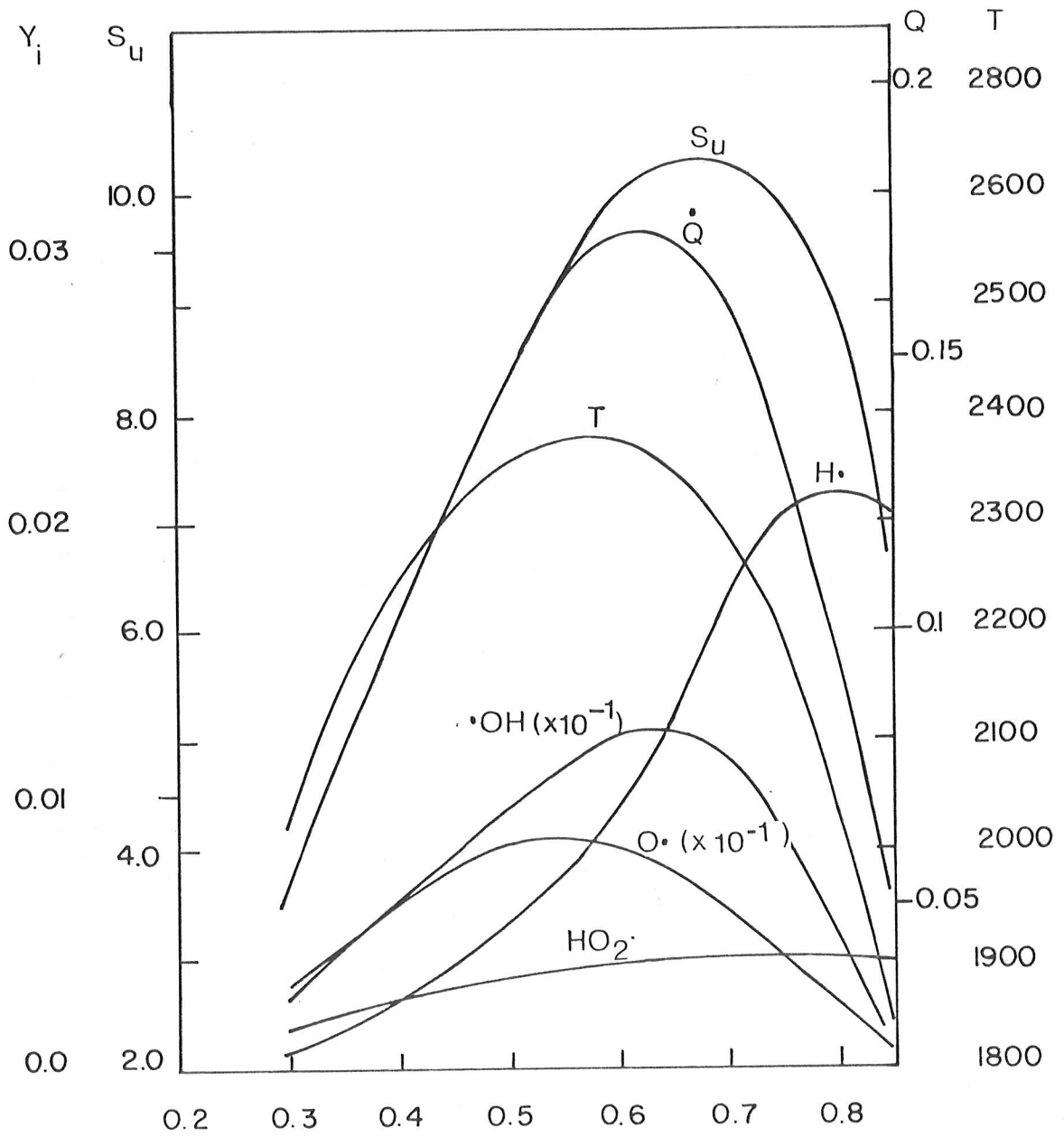

FIGURE 39: Maximum calculated values of key species and flame properties for H_2-O_2 flames

decreased availability of molecular O_2 in rich mixtures. This, however, is offset by the increasing availability of H atoms in the richer flames. The sustained yield of HO_2 in the rich flames is further evidence of the importance of H atoms diffusing to the unburnt gas to release their energy specifically in the formation of HO_2.

Figure 39, for H_2-O_2, shows the same general trend as in Figure 38. The burning velocity in lean to stoichiometric mixtures is driven predominately by increasing thermal gradients and chain branching reactions, and the burning velocity in rich flames is sustained by an increasing contribution from H atom diffusion. The differences from H_2-air in Figure 38 are mainly due to the abundance of O_2, which has replaced the N_2 in air.

To summarize, excess hydrogen influences the burning velocity by two mechanisms, increased thermal diffusivity and increased rates of reactions R1 and R5. The principal product of these reactions is the energetic and highly mobile H atom, which diffuse from the high temperature reaction zone to deposit their energy in the exothermic reaction cycle initiated by reaction R11. This increase in the rate of heat release nearer the unburnt gas accelerates thermal diffusion to the unburnt gas, resulting in a higher burning velocity.

6.9 ISOTOPE EFFECT - DEUTERIUM FLAMES

In Figures 17, 18 and 19, the burning velocities were compared for hydrogen and deuterium mixtures. The ratio $S_u(H_2)/S_u(D_2)$ was about 1.37 and decreased with addition of diluent to about 1.26. This result is interpreted in terms of differences in thermal diffusivity and of differences in reactivity, owing to the lower collision frequency and higher dissociation energy of D_2 relative to H_2.

The thermal diffusivities of the mixtures containing D_2 and H_2 are calculated directly from Equation (7). Since, in Equation (6), burning velocity is proportional to $\alpha^{\frac{1}{2}}$, the ratio $\alpha^{\frac{1}{2}}(H_2)/\alpha^{\frac{1}{2}}(D_2)$ gives the contribution of thermal diffusivity to the observed burning velocity ratio. Table 6 contains the result of this calculation for selected mixtures. The ratios of $\alpha^{\frac{1}{2}}$ for H_2 and D_2 mixtures are less than the ratios of the burning velocities, indicating that additional effects are occurring in the rate term of Equation (6).

The most immediately predictable change to the rate term is due to the lower collision frequency of D_2 and $D^\bullet$ relative to H_2 and $H^\bullet$, and the corresponding decrease in rates of all reactions of these species. The collision frequency is inversely proportional to the mass, so the ratio of H and D collision frequencies will be $\sqrt{2}$. The effect on the ratio of H_2 and D_2 burning velocities will be $2^{\frac{1}{4}}$, or 1.19. This factor is assumed constant with added diluent, as is indicated in Table 6.

TABLE 6

RATIOS OF THERMAL DIFFUSIVITIES, COLLISION FREQUENCIES AND BURNING VELOCITIES FOR SELECTED H_2 AND D_2 FLAMES

Mixture	$(\text{ratio})^{\frac{1}{2}}$ of H_2/D_2 thermal diffusivities	$(\text{ratio})^{\frac{1}{2}}$ of H/D collision freq.	$S_u(H_2)/S_u(D_2)$ predicted by Equation 18	$S_u(H_2)/S_u(D_2)$ measured
stoichiometric	1.15	1.19	1.37	1.36
stoich. + 50% He	1.07	1.19	1.27	1.32
stoich. + 50% N_2	1.10	1.19	1.30	1.27

The product of the thermal diffusivity ratios and the collision frequency ratios (corresponding to the transport term and the rate term of Equation (6)) gives nearly the observed ratio of burning velocities for mixtures of H_2 and D_2. Furthermore it correctly indicates the observed decrease in burning velocity ratio with added diluent. The decreased thermal diffusivity ratios with added diluent simply reflects the decreasing

fraction of H_2 or D_2 in the total mixture. But even for highly dilute mixtures, the burning velocity ratios will always be greater than 1.19, because of the constant effect of the collision frequency in the rate term.

Based on these considerations, the burning velocities of D_2 can be predicted to within 5% from the burning velocity of corresponding mixtures containing H_2 by the expression,

$$\frac{S_u(H_2)}{S_u(D_2)} = \left(\frac{\alpha_{H_2}}{\alpha_{D_2}}\right)^{\frac{1}{2}} 1.19 \qquad (18)$$

where α_{H_2} and α_{D_2} are the thermal diffusivities of the mixtures containing H_2 and D_2, respectively and 1.19 is a constant.

In Equation (18), it is important to note that the experimentally observed isotope effect is explained for stoichiometric flames without attributing any effect to the difference of 8.4 kJ/mol in dissociation energies of H_2 and D_2 [56]. Calculations indicate that if H_2 dissociation were an important factor in flame propagation (rate limiting) the ratio $S_u(H_2)/S_u(D_2)$ could be as high as 1.9 at 3000 K. From our results we can conclude that H_2 dissociation is of minor importance in determining the rate of flame propagation, particularly for stoichiometric flames. For lean flames, $S_u(H_2)/S_u(D_2)$ slightly exceeds the prediction based only on diffusivity and collision frequency. It is thus possible that H_2 dissociation assumes some importance in lean flames. However, due to the polyhedral flames observed for lean mixtures, burning velocities cannot be measured with sufficient precision to resolve this.

7. CONCLUSIONS

The burning velocities of H_2-O_2 flames containing the diluents He, Ar, N_2, CO_2 and steam have been measured by the nozzle burner/schlieren cone angle method, with particle tracking by Laser Doppler Anemometry. Further, H_2 and O_2 were added as diluents to stoichiometric flames, and lean and rich flames were thus studied as diluted systems. New data are given for the H_2-air-steam mixtures containing up to 50% steam.

(1) The diluents studied reduce the burning velocity in the order $CO_2 > N_2 > Ar > steam > O_2 > He > H_2$ up to 50% diluent and, at diluent fractions > 50%, $CO_2 > steam > N_2 > Ar > O_2 > He > H_2$.

(2) An equation based on physical properties of the gas mixture and flammability limits successfully predicts the burning velocities of mixtures containing inert diluents He, Ar and N_2.

(3) Departures from the prediction of the ideal diluent equation for steam and O_2 diluent have been quantitatively linked to changes in the rates of individual reaction steps.

Steam diluent accelerates the burning velocity by 27% to counteract its effect on flame cooling and heat transport, by catalysing the heat-releasing oxidation pathway in the preheat zone of the flame.

$$H + O_2 + M \rightarrow HO_2 + M \qquad R11$$

O_2 in excess of stoichiometric increases the burning velocity by increasing the rates of both the bimolecular and termolecular reactions of O_2 with H atoms about equally.

$$H + O_2 \rightarrow OH + O \qquad R3$$

$$H + O_2 + M \rightarrow HO_2 + M \qquad R11$$

(4) H_2, in excess of stoichiometric, increases the rate of reactions producing H atoms. H-atoms diffuse upstream to release their energy, almost exclusively, in the exothermic HO_2 pathway in the preheat zone of the flame, to increase the burning velocity.

(5) CO_2 diluent provides the greatest suppression of burning velocities, primarily as a result of its increased heat capacity at elevated temperatures and the resulting flame cooling.

(6) Deuterium flames have a lower burning velocity than hydrogen flames due to a lower thermal diffusivity and collision frequency. Bond cleavage of H_2(or D_2) is not a significant factor in the overall rate of reaction. Burning velocities for mixtures with deuterium can be predicted from data for hydrogen mixtures from the expression

$$\frac{S_u(H_2)}{S_u(D_2)} = \frac{\alpha^{\frac{1}{2}}(H_2)}{\alpha^{\frac{1}{2}}(D_2)} \cdot 1.19$$

REFERENCES

1. Warnatz, J.; "Calculation of the Structure of Laminar Flat Flames II: Flame Velocity and Structure of Freely Propagating Hydrogen-Oxygen and Hydrogen-air Flames;" Ber. Bunsenges. Phys. Chem. 82, 643-649 (1978).

2. Rallis, C.J. and Garforth, A.M.; "The Determination of Laminar Burning Velocity;" Prog. Energ Combust. Sci.; 6, p. 303-329 (1980).

3. Takahashi, F., Mizomoto, M., and Ikai, S.; "Laminar Burning Velocities of Hydrogen/Oxygen/Inert Gas Mixtures;" Third Miami International Conf. on Alt. Ener. Sources; Proc. (1982) p. 272-284.

4. Yamane, Kimitaka; Ueno, Zene; Morita, Akiri; Nagoaka, Tadahiko; Iwaki, Shigeo; pp. 6, "Burning Rate Control in Hydrogen Fuel Combustor;" (Nissan Motor Co. Ltd.) Brit. 1, 517, 799 (Cl.F23R1/02), 1978 July 12, Appl. 75/41, 398, 1975 October 09.

5. Liu, D.D.S., Harrison, W.C., Tamm, H., MacFarlane, R. and Clegg, L.J.; "Canadian Hydrogen Combustion Studies Related to Nuclear Reactor Safety Assessment;" Atomic Energy of Canada Limited Report, AECL-6994 (1980).

6. Glassman, Irvine; Combustion; Academic Press Inc. (1977).

7. Gaydon, A.G. and Wolfhard, H.G.,; Flames: Their Structure, Radiation and Temperature, 3rd Ed; Chapman and Hall Ltd., 11 New Fetter Lane, London (1970).

8. Andrews, G.E. and Bradley, D.; "Determination of Burning Velocities - A Critical Review;" Comb. and Flame; 18, 133-153 (1972).

9. Lewis, B. and Von Elbe, G.; Combustion, Flames and Explosions of Gases; 2nd Ed; Academic Press Inc., N.Y. and London (1961).

10. Dixon-Lewis, G.; "Kinetic Mechanism Structure and Properties of Premixed Flames in Hydrogen-Oxygen-Nitrogen Mixtures;" Phil. Trans. Roy. Soc. A 292, 45-99 (1979).

11. Stephenson, P.L. and Taylor, R.G.; "Laminar Flame Propagation in Hydrogen, Oxygen, Nitrogen Mixtures;" Comb. and Flame; 20; 231-244 (1973).

12. Mulpuru, S.R.; "Numerical Solution of One-Dimensional Equations;" Whiteshell Nuclear Research Establishment, Unpublished (1985).

13. Bradley, J.N.; Flame and Combustion Phenomena; Methuen's Monographs on Chemical Subjects, Methuen & Co. Ltd., London (1969).

14. Bahn, G.S.; Reaction Rate Compilation for the H-O-N System; PYRODYNAMICS, 5, 1967.

15. Baulch, D.L., Drysdale, Horne, D.G. and Lloyd, A.C.; Evaluated Kinetic Data for High Temperature Rections; V. 1; Butterworths, London (1972).

16. Baulch, D.L., Drysdale, D.D., and Horne, D.G.; Evaluated Kinetic Data for High Temperature Reactions; V. 2; Butterworths, London (1973).

17. Baulch, D.L.; Drysdale, D.D.; Duxbury, J., and Grant, S.J.; Evaluated Kinetic Data for High Temperature Reactions; V. 3; Butterworths, London (1976).

18. Warnatz, J.; "Concentration-, Pressure-, and Temperature-Dependence of the Flame Velocity in Hydrogen-Oxygen-Nitrogen Mixtures;" Comb. Sci. and Tech.; 26, 203-213 (1981).

19. Walsh, A.D.; "Efficiencies of Third Bodies in the Reaction: $H + O_2 + M \rightarrow HO_2 + M$;" Fuel 33, 247 (1954).

20. Baldwin, R.R., Moyes, R.B., Rossiter, B.N., and Walker, R.W.; "The Third Body Coefficients of H_2O and D_2O in the $H_2 + O_2$ and $D_2 + O_2$ Reaction;" Comb. and Flame; 14, 181 (1970).

21. Jahn, G.; "Zer Zundvorgang in Gasgemischen" Oldenbourg, Berlin (1934), as summarized in Lewis and Von Elbe [9].

22. Friedman, Raymond; "The Quenching of Laminar Oxyhydrogen Flames by Solid Surfaces;" Third Symposium (Int'l) on Combustion; pp. 110-120 (1951).

23. Mellish, C.E. and Linnett, J.W.; "The Influence of Inert Gases on Some Flame Phenomena." Fourth Symp. (Int'l) on Comb.; p. 407-420 (1953).

24. Morgan, G.H. and Kane, W.R.; "Some Effects of inert Diluents on Flame Speeds and Temperatures;" Fourth Symp. (Int'l) Comb.; p. 313 (1953).

25. France, D.H. and Pritchard, R.; "Burning Velocity Measurements of Multicomponent Fuel Gas Mixtures with Inert Gas Additions;" Gaz Wärme International; Bd. 26, Nr. 12, (1977).

26. David, W.T. and Mann, J.; "Influence of Water Vapor on Flame Gas Temperatures;" Nature; 150, 521-522 (1942).

27. Kuehl, D.K.; "Effects of Water on the Burning Velocity of Hydrogen-Air Flames;" A.R.S.J. 32, 1724-1726 (1962).

28. Levy, A.; "Effects of Water on Hydrogen Flames;" AIAA J. 1, 1239 (1963).

29. Dixon-Lewis, G. and Williams, A.; "Effects of Nitrogen, Excess Hydrogen, and Water Vapor on Hydrogen-Air Flames;" AIAA Journal; 1 (10) p. 2416 (1963).

30. Liu, D.D.S. and MacFarlane, R.; "Laminar Burning Velocities of Hydrogen-Air and Hydrogen-Air-Steam Flames;" Comb. and Flame; 49, 59-71 (1983).

31. Müller-Dethlefs, K. and Schlader, A.F.; "The Effect of Steam on Flame Temperature, Burning Velocity and Carbon Formation in Hydrocarbon Flames," Comb. and Flame 27, 205-215 (1976).

32. Dryer, F.L.; "Water Addition to Practical Combustion Systems - Concepts and Applications;" Sixteenth Symposium (Int'l) on Combustion, The Combustion Institute, Pittsburgh, PA (1976).

33. Westgate, R.; "Mix Gas with Water for More mpg?" Popular Science, 108, (1974) July.

34. Rao, V.K. and Bardon, M.F.; "The Effect of Water on Gas Phase Soot Formation in Laminar Diffusion Flames;" Comb. and Flame 55, 73-78 (1984).

35. Miyauchi, T., Mori, Y., and Yamaguchi, T.; "Effect of Steam Addition on NO Formation;" Eighteenth Symp. (Int'l) on Comb.; The Combustion Institute (1981) p. 43-51.

36. Shaw, H.; "Reduction of Nitrogen Oxide Emissions from a Gas Turbine Combustor by Fuel Modifications;" Trans. ASME, J. Eng. Power; Oct. (1972) p. 271-278.

37. Behrens, H.; Z.p.C., 195, 24 (1950);
Z.p.C., 195, 225 (1950);
Z.p.C., 195, 329 (1950);
Z.p.C., 196, 78 (1050);
from Gaydon and Wolfhard [7].

38. Van Berlo, J.; Memo to P.J. Allen, file 29-32000-220-001 (1982 July 13) Report on Moderator Cover Gas Deuterium after a Moderator Accident.

39. Gray, P. and Smith, D.B.; "Isotope Effects on Flame Speeds for Hydrogen and Deuterium;" Chem. Commun. (1967) 146-148.

40. Fristrom, R.M., Avery, W.H., Prescott, R., and Mattuck, A.; "Flame Zone Studies by the Particle Track Technique. I. Apparatus and Technique;" J. Chem. Phys. 22(1), 106 (1954).

41. Yeh, Y. and Cummins, H.Z.; Applied Phys. Letters; 4, 176-178 (1964).

42. Durst, F., Melling, A. and Whitelaw, J.H.; Principles and Practice of Laser Doppler Anemometry, 2nd Ed. Academic Press (1981).

43. France, D.H. and Pritchard, R.; "Laminar Burning Velocity Measurements Using a Laser Doppler Anemometer;" J. Inst. Fuel, 49, 79 (1976).

44. Rudd, M.J.; "A New Theoretical Model for the Laser Doppler Meter;" J. Sci. Instr. (J. of Phys. E.) Series 2 Volume 2 (1969).

45. Durst, F. and Stevenson, W.H.; "Visual Modelling of Laser Doppler Anemometer Signals by Moiré Fringes;" Appl. Opt. 15 (1), 137-144 (1976).

46. Edmondson, H. and Heap, M.P.; "The Burning Velocity of Hydrogen-Air Flames;" Comb. and Flame; 16, 161-165 (1971).

47. Andrews, G.E. and Bradley, D.; "Determination of Burning Velocity by Double Ignition in a Closed Vessel;" Comb. and Flame; 20, 77-89 (1973).

48. Garside, J.E. and Jackson, B.; "The Formation and some Properties of Polyhedral Burner Flames;" Fourth Symposium (Int'l) on Combustion (1953).

49. Kumar, R.K. and Hollinger, T.; "Determination of Flammability Limits of Hydrogen-Oxygen-Diluent Systems;" Whiteshell Nuclear Research Establishment, Unpublished Data (1984). (Accepted for publication in J. Fire Science).

50. Mason, E.A., and Saxena, S.C.; The Physics of Fluids; 1, 361-369 (1958) from, Bird, R.B., Stewart, W.E., and Lightfoot, E.N.; Transport Phenomena; John Wiley and Sons Inc. (1960) N.Y. and London.

51. Keenan, J.H. and Kaye, J.; Gas Tables - "Thermodynamic Properties of Air Products of Combustion and Component Gases;" John Wiley and Sons, Inc. (1948).

52. Gordon, S. and McBride, B.; National Aeronautics and Space Administration Report, NASA SP-273 (1971).

53. Kaskan, W.E.; "Abnormal Excitation of OH in $H_2/O_2/N_2$ Flames;" J. Chem. Phys. 31, 944-956 (1959).

54. Tien, C.L. and Lee, S.C.; "Flame Radiation;" Prog. Energy Comb. Sci., 8, 41-59 (1982).

55. Padley, P.J. and Sugden, T.M.; "Chemilumunescence and Radical Recombination in Hydrogen Flames;" Seventh Symp. (Int'l) on Combustion; Butterworths, London (1959) pp. 235-244.

56. Laidler, K.J.; Reaction Kinetics V.1: Homogeneous Gas Reactions; Pergamon Press; Oxford, London, New York, Paris (1963).

APPENDIX I

ONE DIMENSIONAL FLAME MODEL

Burning velocities, heat release, temperature and species profiles in laminar hydrogen-oxygen flames are calculated by solving the one-dimensional conservation equations for overall continuity, individual specie continuity and energy. The model was developed at WNRE by Dr. S.R. Mulpuru. The numerical method departs from that of earlier workers [1,11] by employing the Eulerian (lab) coordinate. Temperature-dependance of transport properties and rate constants are included in the calculation. The following is a brief description of the numerical method, in particular the means by which the interactions of convection, diffusion and the non-linear rate equations are resolved.

The calculation begins with arbitrary profiles of species mass fractions and temperature at time zero. With a suitable grid-point system the differential quotients are replaced by finite difference expressions. The grid Pecklet number, $|U| \cdot \Delta_x/D$, is kept less than 2 to resolve the interactions of convection and diffusion. Here, U is the flow velocity, Δx is the grid interval and D is a diffusion constant. Since the ratio $|U|/D$ decreases in the direction of the burnt gases, the grid interval can increase in the direction of the burnt gas, while satisfying the Pecklet number restriction. The space derivatives are discretized on this non-uniform grid, using central differencing. The time derivative is discretized by first-order backward differencing.

The non-linear reaction rate terms are linearized using a Taylor expansion and the resulting matrix of linear equations is solved to advance the solution by a time step.

The stiffness of the kinetic system is overcome by a variable time step obtained by the criterion $|J|\ \Delta_t \leq 1$, where $|J|$ is a parameter that represents a time constant for the changing species concentrations, energy and temperature. This criteria insures that Δt is varied to resolve the fastest chemical timescale.

Thus the solution is 'marched' forward, step by step, in time until a steadily propagating flame structure is obtained. The flame, which moves in time, is kept within the computational domain by entraining mass from the burnt side boundary. Integration of the species and temperature profiles yields the burning velocity, which approaches a constant value as the flame structure stabilizes (6000 to 15 000 time steps, depending on the mixture).

While the detailed species and temperature profiles cannot be directly verified to the same resolution offered by the computation, they can be verified indirectly by comparing with experiment the burning velocities obtained by integration of these quantities. Such a comparison was made (see Figures 9, 10). The good agreement of measured and calculated burning velocities provides reasonable confidence in the validity of the calculated flame structures.

APPENDIX B

CALCULATED THERMAL DIFFUSIVITIES, α FOR MIXTURES OF H_2-O_2 CONTAINING DILUENTS

The thermal diffusivities are listed as $\alpha^{\frac{1}{2}}$ for use in the correlation equation for predicting laminar burning velocities.

$$\left(\frac{\alpha_o}{\alpha}\right)^{\frac{1}{2}} S_u = S_{u_o} - X_{dil} \left(\frac{S_{u_o}}{X_L}\right) \qquad (17)$$

$\alpha_o^{\frac{1}{2}}$ is the value of $\alpha^{\frac{1}{2}}$ in the tables corresponding to $X_{dil} = 0.0$

S_{u_o} is the experimentally measured burning velocity corresponding to $X_{dil} = 0.0$

X_{dil} is the mole fraction of diluent gas

X_L is the mole fraction of diluent gas at the flammability limit for downward propagation. (Given in Appendix C).

TABLE B-1

CALCULATED THERMAL DIFFUSIVITIES FOR H_2-O_2 MIXTURES CONTAINING DILUENTS

H_2-O_2 ratio	Su_o ($m \cdot s^{-1}$)	X_{H_2}	X_{O_2}	X_{dil}	$\alpha_o^{\frac{1}{2}}$ ($m^2 \cdot s^{-1}$)	$\alpha^{\frac{1}{2}}$ ($m^2 \cdot s^{-1}$)					
						He	Ar	N_2	H_2O	CO_2	H_2
0.5:1	4.5	0.33	0.67	0.00	0.692	0.692	0.692	0.692	0.692	0.692	
		0.30	0.60	0.10		0.728	0.672	0.668	0.658	0.644	
		0.27	0.53	0.20		0.768	0.651	0.644	0.624	0.600	
		0.23	0.47	0.30		0.811	0.630	0.620	0.590	0.559	
		0.20	0.40	0.40		0.858	0.608	0.596	0.556	0.519	
		0.17	0.33	0.50		0.910	0.585	0.572	0.523	0.482	
		0.13	0.27	0.60		0.967	0.560	0.548	0.489	0.446	
		0.10	0.20	0.70		1.032	0.533	0.523	0.454	0.412	
		0.067	0.133	0.80		1.104	0.504	0.499	0.420	0.380	
		0.033	0.067	0.90		1.185	0.473	0.474	0.384	0.348	
1:1	8.1	0.50	0.50	0.00	0.812	0.812	0.812	0.812	0.812	0.812	
		0.45	0.45	0.10		0.842	0.781	0.775	0.763	0.747	
		0.40	0.40	0.20		0.874	0.750	0.739	0.716	0.687	
		0.35	0.35	0.30		0.909	0.718	0.703	0.670	0.632	
		0.30	0.30	0.40		0.947	0.685	0.667	0.624	0.580	
		0.25	0.25	0.50		0.989	0.651	0.632	0.579	0.532	
		0.20	0.20	0.60		1.035	0.615	0.596	0.534	0.486	
		0.15	0.15	0.70		1.086	0.576	0.560	0.489	0.442	
		0.10	0.10	0.80		1.143	0.534	0.523	0.443	0.400	
		0.05	0.05	0.90		1.206	0.489	0.486	0.396	0.358	
2:1	10.9	0.67	0.33	0.00	0.937	0.937	0.937	0.937	0.937	0.937	0.937
		0.60	0.30	0.10		0.960	0.893	0.885	0.872	0.852	0.962
		0.53	0.27	0.20		0.985	0.850	0.835	0.810	0.775	0.989
		0.47	0.23	0.30		1.011	0.806	0.786	0.750	0.705	1.016
		0.40	0.20	0.40		1.040	0.761	0.738	0.691	0.641	1.043
		0.33	0.17	0.50		1.071	0.716	0.690	0.635	0.581	1.070
		0.27	0.13	0.60		1.105	0.669	0.642	0.578	0.525	1.098
		0.20	0.10	0.70		1.142	0.618	0.595	0.522	0.471	1.126
		0.133	0.067	0.80		1.183	0.565	0.547	0.466	0.419	1.155
		0.067	0.033	0.90		1.228	0.505	0.498	0.408	0.368	1.183

H_2–O_2 ratio	Su_o ($m \cdot s^{-1}$)	X_{H_2}	X_{O_2}	X_{dil}	$\alpha_o^{1/2}$ ($m^2 \cdot s^{-1}$)	$\alpha^{1/2}$ ($m^2 \cdot s^{-1}$)				
						He	Ar	N_2	H_2O	CO_2	H_2
5:1	8.6	0.83	0.167	0.00	1.070	1.070	1.070	1.070	1.070	1.070	
		0.75	0.15	0.10		1.086	1.011	1.002	0.962	0.962	
		0.67	0.13	0.20		1.102	0.953	0.936	0.866	0.866	
		0.58	0.117	0.30		1.119	0.896	0.872	0.780	0.780	
		0.50	0.10	0.40		1.138	0.839	0.810	0.702	0.702	
		0.42	0.083	0.50		1.157	0.781	0.750	0.630	0.620	
		0.33	0.067	0.60		1.178	0.722	0.690	0.562	0.562	
		0.25	0.05	0.70		1.200	0.660	0.631	0.499	0.499	
		0.167	0.033	0.80		1.224	0.594	0.571	0.437	0.438	
		0.083	0.017	0.90		1.250	0.521	0.511	0.377	0.378	
9:1	3.4	0.90	0.10	0.00	1.126	1.126	1.126	1.126	1.126	1.126	
		0.81	0.09	0.10		1.138	1.060	1.050	1.008	1.008	
		0.72	0.08	0.20		1.151	0.996	0.977	0.904	0.904	
		0.63	0.07	0.30		1.164	0.933	0.907	0.810	0.810	
		0.54	0.06	0.40		1.178	0.870	0.839	0.726	0.726	
		0.45	0.05	0.50		1.193	0.807	0.773	0.649	0.649	
		0.36	0.04	0.60		1.208	0.743	0.708	0.578	0.578	

APPENDIX C

INERTING DILUENT FRACTIONS, X_L, FOR H_2-O_2 MIXTURES [49]

(DOWNWARD PROPAGATION)

	(298 K)				
H_2/O_2 ratio	He	Ar	N_2	CO_2	steam (373 K)
0.25:1	0.63		0.58	0.48	
0.5:1	0.79		0.74	0.67	
1:1	0.87	0.89	0.81	0.76	
2:1	0.88	0.89	0.85	0.76	0.78
4:1	0.82	0.83	0.76	0.65	
5:1	0.77	0.78	0.70	0.59	
9:1	0.53		0.5	0.35	